GEORGIA INSTITUTE OF TECHNOLOGY — OFFICE OF CONTRACT ADMINISTRATION

PROJECT ADMINISTRATION DATA SHEET

[X] ORIGINAL [ ] REVISION NO. _____

Project No. E-21-678 R6149-0A0 GTRC/GTX DATE 9 / 18 / 86

Project Director: Dr. Paul J. Benkeser School/~~XXX~~ EE

Sponsor: The Whitaker Foundation

Type Agreement: Grant letter dated 6/6/86

Award Period: From 9/15/86 To 9/15/89 (Performance) 11/15/89 (Reports)

Sponsor Amount:	This Change	Total to Date
Estimated: $		$ 136,101
Funded: $		$ 47,127

Cost Sharing Amount: $ _____ Cost Sharing No: _____

Title: Ultrasound Tapered Phased Array Imaging Transducer

ADMINISTRATIVE DATA — OCA Contact E. Faith Gleason X-4820

1) Sponsor Technical Contact:

Mr. Miles J. Gibbons, Jr.
Executive Director
The Whitaker Foundation
875 Poplar Church Road
CampHill, Pennsylvania 17011-2285
717/763-1391

2) Sponsor Admin/Contractual Matters:

Defense Priority Rating: _____ Military Security Classification: _____

(or) Company/Industrial Proprietary: N/A

RESTRICTIONS

See Attached N/A Supplemental Information Sheet for Additional Requirements.

Travel: Foreign travel must have prior approval — Contact OCA in each case. Domestic travel requires sponsor approval where total will exceed greater of $500 or 125% of approved proposal budget category.

Equipment: Title vests with Sponsor

COMMENTS:

Public Announcement of grant requires prior approval from Sponsor

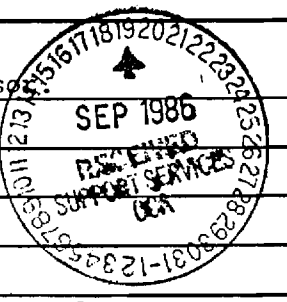

SPONSOR'S I. D. NO. 02.500.057.86.001

COPIES TO:

Project Director
Research Administrative Network
Research Property Management
Accounting
Procurement/GTRI Supply Services
Research Security Services
Reports Coordinator (OCA)
Research Communications (2)
GTRC
Library
Project File
Other A. Jones

12 / 88

GEORGIA INSTITUTE OF TECHNOLOGY
OFFICE OF CONTRACT ADMINISTRATION

NOTICE OF PROJECT CLOSEOUT

Date 10/26/89

Project No. E-21-678 Center No. R6149-0A0

Project Director P. J. Benkeser School/Lab EE

Sponsor Whitaker Foundation

Contract/Grant No. Letter dtd. 6/6/86 GTRC XX GIT ____

Prime Contract No. N/A

Title Ultrasound Tapered Phased Array Imaging Transducer

Effective Completion Date 9/15/89 (Performance) 11/15/89 (Reports)

Closeout Actions Required:

- X None
- ____ Final Invoice or Copy of Last Invoice
- ____ Final Report of Inventions and/or Subcontracts
- ____ Government Property Inventory & Related Certificate
- ____ Classified Material Certificate
- ____ Release and Assignment
- ____ Other ____

Includes Subproject No(s). ____

Subproject Under Main Project No. ____

Continues Project No. ____ Continued by Project No. ____

Distribution:

- X Project Director
- X Administrative Network
- X Accounting
- X Procurement/GTRI Supply Services
- X Research Property Management
- ____ Research Security Services
- X Reports Coordinator (OCA)
- X GTRC
- X Project File
- 2 Contract Support Division (OCA)
- ____ Other ____

E-21-678

GEORGIA INSTITUTE OF TECHNOLOGY
SCHOOL OF ELECTRICAL ENGINEERING
ATLANTA, GEORGIA 30332

TELEPHONE: (404) 894-2912

July 20, 1987

MEMORANDUM

To: Pat Heitmuller

From: P.J. Benkeser

Subject: Progress Report for Whitaker Foundation Grant (Project No. E-21-678)

Enclosed you will find two copies of the annual project report for the subject grant. I am forwarding copies on to the sponsor as directed by the deliverable schedule.

PJB:abp
enclosures

ULTRASOUND TAPERED PHASED ARRAY IMAGING TRANSDUCER

Annual Progress Report #1

July 20, 1987

Submitted to the Whitaker Foundation by

Paul J. Benkeser
Assistant Professor
School of Electrical Engineering
Georgia Institute of Technology
Atlanta, Georgia 30332-0250

INTRODUCTION

This report details the progress made during the first grant year of the project entitled, "Ultrasound Tapered Phased Array Imaging Transducer." The goals for the second year, as well as a revised second year budget, are also included in this report. Copies of two proceedings papers, based upon work accomplished during the first year of the grant, can be found in the Appendix of this report.

CURRENT PROGRESS

The research plan in the grant application called for significant progress to be made in the development of both a theoretical model for the electroacoustic response of elements of the tapered phased array (TPA) and the array controller during the first grant year. Current progress is slightly ahead of the schedule in this plan.

A discrete-time staircase model of the thickness mode piezoelectric transducers is being used to characterize the tapered element. The advantage of this model is its ability to predict the response of the transducer to a variety of arbitrary input functions. This will allow us to study the response of the tapered element to excitation signals that could not easily be implemented with other models. Peter Barthé, a Ph.D. student supported by this grant, has been developing this model and will be presenting this work in a paper entitled, "A Staircase Model of Tapered Piezoelectric Transducers," at the IEEE 1987 Ultrasonics Symposium in October.

A 16-element TPA was fabricated in order to make experimental measurements of the electroacoustic response of its elements. These measurements will be used to verify the aforementioned theoretical model. The fabrication

of this TPA, referred to as TPA #1, was not originally scheduled to begin until the second year.

To facilitate the testing of TPA #1, an array controller is being developed. This controller is microprocessor-based and will regulate both the generating of the pulses that drive the elements and the subsequent processing of the received echo data.

The pulse generator portion of this controller, which employs a programmable pulse generator, has already been developed and tested. Its design is similar to those designed by several other researchers, and therefore, will not be expanded upon here.

The receiver portion of the controller, currently being developed, implements a technique of time expansion which employs a simple microcomputer (IBM PC-XT) control and low-cost A to D converters. The received signals from the TPA elements will be captured at a high rate using CCD (Charge-Coupled Device) delay lines. The signals will then be released at a lower rate, digitized by A to D converters, and subsequently stored in the microcomputer's memory. Digital signal processing techniques will then be used to filter and supply appropriate delays for dynamic focusing of the frequency encoded data in order to form the image. Details of this controller may be found in the second paper in the Appendix.

Perhaps the most important progress made during the past year has been the discovery of a new imaging application of the TPA. The results of comparisons of theoretical (old model) and experimental radiation patterns suggests that when the elements of a TPA are pulsed with the appropriate excitation signals, a linearly aligned group of focused beams, at frequencies corresponding to those contained in the pulsed signals, will be produced.

The advantage of using the TPA in this pulsed "frequency scanning" mode is that it would enable the y-z plane (see Fig. 1 of the first paper in the Appendix) to be scanned, using a single pulse, at a rate much faster than is currently possible with conventional arrays. Fast scanning rates are important for high resolution imaging when viewing dynamic structures such as the heart. This technique, with the addition of beam steering, would also allow a large number of adjacent planes to be rapidly scanned, thereby enabling the formation of a three-dimensional image. The formation of such an image is not currently feasible with conventional ultrasonic imaging instrumentation. For further elaboration on this discovery, see the papers in the Appendix.

GOALS FOR SECOND YEAR

The overall goal of this project remains unchanged: to develop a TPA transducer for medical imaging applications. However, in light of the aforementioned discovery, the scope of the project will be broadened to investigate this new mode of operation.

The specific goals for the second year are:

1. To complete the development of the theoretical model of the electroacoustic response of the TPA.
2. To complete the development of the receiver portion of the array controller and integrate it with the pulse generator.
3. To compare the theoretical and experimental field radiation patterns of TPA #1 when it is driven by the array controller.
4. To design a new type of pulse generator that will produce a properly phased discrete multi-frequency pulse in order to investigate the new mode of operation of the TPA.

BUDGET MODIFICATIONS

An increase in the fringe benefits rate required that minor modifications be made to the budget for the second year of the grant. The total amount of funds requested in this modified budget (see Table 1) is the same as that requested in the budget of the grant application.

TABLE 1. DETAILED BUDGET FOR SECOND YEAR

Personal Services		
Paul J. Benkeser, Assistant Professor 4 months @ $4,420/month		$17,680
Peter G. Barthé, Graduate Research Assistant 12 months @ 1/3 time @ $2,160/month		$ 8,640
Fringe Benefits		
27.6% of Direct Salaries (excluding students)		$ 4,880
Materials and Supplies		
Electronic Components, Materials for Fabricating the TPA and Controller, Publication Costs		$ 4,500
Travel		$ 1,117
	Total Direct Costs	$36,817
	Overhead (20%)	$ 7,363
	Total Funds Requested	$44,180

APPENDIX

TO APPEAR IN THE PROCEEDINGS OF THE 13th NORTHEAST BIOENGINEERING CONFERENCE (Philadelphia, PA, March 12 - 13, 1987).

A PULSE-ECHO ULTRASOUND TAPERED PHASED ARRAY TRANSDUCER

P. J. Benkeser

School of Electrical Engineering
Georgia Institute of Technology
Atlanta, Georgia 30332

ABSTRACT

The tapered phased array (TPA) transducer consists of a linear array of piezoelectric elements that have a tapered thickness. In this paper, a TPA transducer operating in the pulse-echo mode is examined. A model for the radiation pattern of a tapered element employing a distributed network of the equivalent circuit of a lossless piezoelectric transducer is described. Comparisons of the theoretical and experimental radiation patterns of a TPA transducer are shown to be in good agreement. These results indicate that when the transducer is pulsed, it produces a linearly aligned group of focused beams at different frequencies which could be used to provide a two-dimensional phased array capability for a pulse-echo imaging system.

INTRODUCTION

Pulse-echo ultrasonic imaging systems are used in a variety of applications as diverse as flaw detection in metal structures and imaging tissues in the body. These systems operate by generating short, broad-band pulses that propagate through the medium of interest and reflect off of regions of discontinuities. The reflected echo is received and its amplitude and time-of-flight delay are used to generate the image. Two-dimensional images are produced by scanning the pulses through the medium. This scanning can be accomplished either by mechanical movement of the ultrasonic transducer, or by the use of an ultrasonic phased array transducer.

A two-dimensional phased array can generate and position a focused beam in three dimensions by controlling the phases of the signals driving each array element so that constructive interference of the waves is achieved at the desired field point. By readjusting the phase periodically, the focus can be scanned over any three-dimensional path at a rate much faster than that of a mechanically scanned system, which is important in viewing dynamic structures such as the heart. However, a two-dimensional phased array is too costly and complex for most imaging applications due to the large number of elements and associated circuitry that are required. Most conventional phased array transducers are of the linear (one-dimensional) type which allow the focus to be scanned over a two-dimensional path.

A new type of phased array, a tapered phased array has been developed for use in ultrasound hyperthermia [1]. This transducer consists of a linear phased array composed of elements that have a tapered thickness, as illustrated in Fig. 1. The frequency response of these elements, due to their tapered thickness, is inherently broad-band. The region along the length of the element that has a thickness resonant at the frequency of the driving signal will produce the greatest acoustical power output. Thus, different regions along the length of the element can be excited by changing the frequency of the continuous wave (cw) signal driving the element.

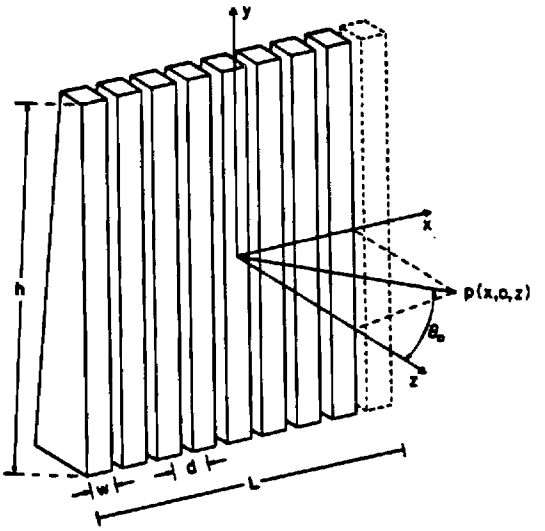

Fig. 1 Tapered array.

The tapered phased array allows the focal region to be swept in two dimensions by controlling the phases of the cw signals, and in the third dimension by controlling the frequency of those signals. The tapered array has the square root of N elements compared with N elements for a two-dimensional array with the same center-to-center spacing of elements.

The purpose of this paper is to theoretically analyze the potential of the tapered phased array in pulse-echo imaging applications.

ANALYSIS OF A PULSE-ECHO TAPERED PHASED ARRAY

The tapered element can be modeled using a parallel network of the simplified Mason's equivalent circuit for a lossless piezoelectric transducer near resonance, as shown in Fig. 2 [2]. This model is accurate for narrow frequency bandwidths where the near resonance approximation holds over the entire length of the tapered element. This model was incorporated into a computer program [3] that implements a rectangular radiator method for calculating the field intensity distribution produced by a cw linear phased array. Figure 3 shows a comparison of the experimental and theoretical field profiles in the y dimension for a cw tapered phased array. This figure illustrates the good agreement that has been obtained between the theoretically predicted fields and the experimental data.

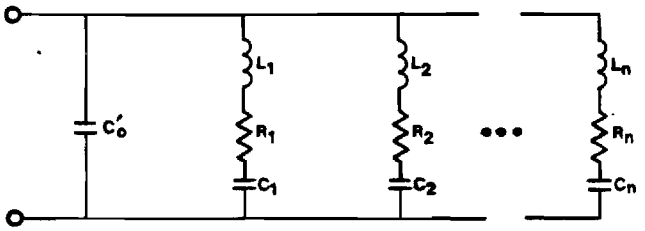

Fig. 2 Equivalent-circuit model for an element with a tapered thickness.

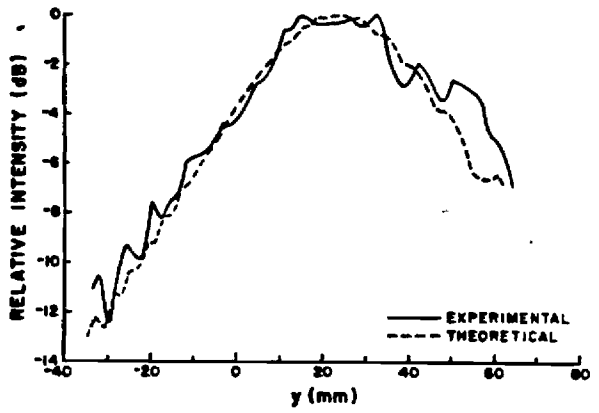

Fig. 3 Comparison of the theoretical and experimental field profiles in the y dimension (x=0, z=100 mm) of a 32-element cw TPA operating at 620 kHz.

Since pulse-echo imaging systems operate by transmitting and receiving short bursts of ultrasound, the spatial response of the tapered phased array should be determined for this broad-band situation. However, the cw analysis can adequately serve as a first-order approximation of the spatial response [4].

If a tapered element of an array was driven by a single broad-band voltage spike, a set of adjoining pulsed beams of different frequencies will be produced along the y dimension of the tapered element, as illustrated in Fig. 4. Discontinuities along the path of each beam will create echoes at corresponding frequencies. The received signal will then consist of a summation of echoes of varying frequency from all of the transmitted beams. Post-reception processing of the received signal could differentiate the position of the echoes in the y dimension through the use of bandpass filtering.

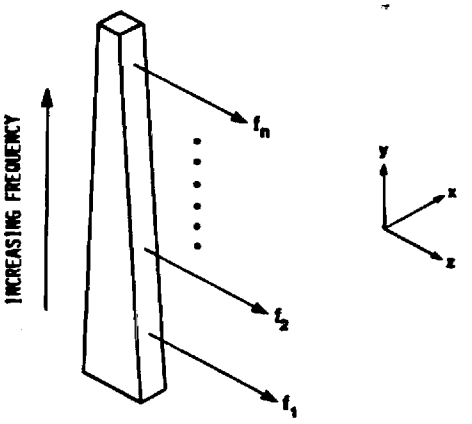

Fig. 4 Spatial frequency response of a tapered element to a broad-band pulsed excitation.

The lateral and axial resolution could be significantly improved in this proposed system if the phase of each transmitted beam were controlled. To focus the beams along a line in the y direction would require the phases (delays) of every frequency component of the signal driving each element to be adjusted so that all of the resulting beams arrive at the desired focal region simultaneously. Figure 5 is a plot of the theoretical spatial response, in the y dimension, of a 64-element tapered phased array driven by a pulse consisting of four frequency components. The four frequency components were phased so that each would be focused at a distance of 5 cm from the array. Each of the peaks in the profile corresponds to one of the four frequency components in the pulsed excitation signal.

DISCUSSION

The obvious advantage of this frequency scanning technique is that it would enable an entire plane (y-z) to be scanned using a single pulse. This would allow a plane to be interrogated at a rate much faster than is currently possible with conventional phased arrays that require multiple pulses to scan a plane. This technique, with the addition of beam steering, would also allow a large number of adjacent planes to be scanned, thereby enabling the formation of a three-dimensional image.

There are several potential limitations to this frequency scanning technique. The characteristics of scattering objects such as reflectivity and attenuation are dependent on the frequency of the

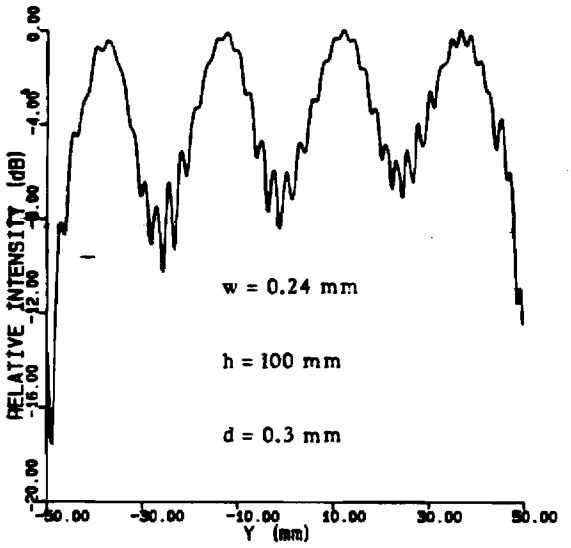

Fig. 5 Theoretical field profile in the y dimension (x=0, z=50 mm) of a 64-element TPA pulsed with an excitation signal with four frequency components (f_1=2.13 MHz, f_2=2.38 MHz, f_3=2.63 MHz, f_4=2.88 MHz).

ultrasonic pulse. Therefore, the amplitudes of the return echoes will be dependent not only on the position and composition of the scatterer, but also the frequency of the incident pulse. These effects can be kept to a minimum if the range of frequencies used is not large.

The resolution in both the lateral and axial dimensions is also a limiting factor. Since the phases of the signals that drive the elements of the array are frequency dependent, a reduction in both the lateral and axial resolution can be expected when using the frequency scanning technique unless each frequency component of the excitation pulse has the proper phase. The resolution in the axial dimension may be reduced if the Q of the tapered element is not low enough to produce the desired acoustical pulse duration.

CONCLUSIONS

A theoretical analysis of a TPA transducer operating in the pulse-echo mode suggests that it is capable of scanning targets at a rate much faster than is possible with conventional phased arrays. In addition, the TPA can provide a 2-D phased array capability that is not yet possible with conventional arrays. Thus, this analysis indicates that pulse-echo TPA transducers warrant further study.

ACKNOWLEDGEMENTS

The author wishes to thank Eugene Goff for his technical assistance. The partial support of this study by The Whitaker Foundation is gratefully ackowledged.

REFERENCES

[1] Benkeser, P. J., L. A. Frizzell, K. B. Ocheltree, and C. A. Cain, "A tapered phased array ultrasound transducer for hyperthermia treatment," IEEE Trans. Ultrasonics, Ferroelectrics, and Frequency Control (in press) 1987.

[2] Benkeser, P. J., "Unfocused multielement and tapered phased array ultrasound transducers for hyperthemia treatment," Ph.D. thesis, Univ. of Illinois at Urbana-Champaign, 1985.

[3] Ocheltree, K. B., P. J. Benkeser, L. A. Frizzell, and C. A. Cain, "An ultrasonic phased array applicator for hyperthermia," IEEE Trans. Son. and Ultrason., Vol. SU-31, pp. 526-531, 1984.

[4] Von Ramm, O. T., and S. W. Smith, "Beam steering with linear arrays," IEEE Trans. Biom. Engr., Vol. BME-30, No. 8, pp. 438-452, 1983.

TO APPEAR IN THE PROCEEDINGS OF THE 1987 ULTRASONICS INTERNATIONAL CONFERENCE (London, UK, July 6 - 9, 1987).

ANALYSIS OF A PULSE-ECHO ULTRASOUND TAPERED PHASED ARRAY TRANSDUCER

P.J. Benkeser, E.F. Goff, and W.O. Rice

School of Electrical Engineering, Georgia Institute of Technology
Atlanta, Georgia, 30332, USA

The tapered phased array (TPA) transducer consists of a linear array of piezoelectric ceramic elements that are inherently broad-band because of their tapered thickness. In this paper, the TPA transducer operating in the pulsed mode will be examined to determine its potential for use in imaging applications. A TPA transducer was constructed in order to verify a theoretical model of its radiation pattern. The results of comparisons of the theoretical and experimental radiation patterns suggest that when the elements are pulsed with the appropriate signals, a linearly aligned group of focused beams at different frequencies will be produced. This group of focused beams can be used to provide a high-resolution two-dimensional phased array capability for a pulse-echo imaging system.

INTRODUCTION

A two-dimensional phased array can generate and position a focused beam in three dimensions by controlling the phases of the signals driving each array element so that constructive interference of the waves is achieved at the desired field point. However, a two-dimensional phased array is too costly and complex for most imaging applications due to the large number of elements and associated circuitry that are required. Most conventional phased array transducers are of the linear (one-dimensional) type which allow the focus to be scanned over a two-dimensional path.

A new type of phased array, a tapered phased array (TPA) has been recently developed for use in ultrasound hyperthermia [1]. This transducer consists of a linear phased array composed of elements that have a tapered thickness, as illustrated in Fig. 1. The frequency response of these elements, due to their tapered thickness, is inherently broad-band. The region along the length of the element that has a thickness resonant at the frequency of the driving signal will produce the greatest acoustical power output. Therefore, the TPA can sweep the focal region in three dimensions by controlling the phases and frequency of the continuous wave (cw) signals driving each element. This array has the square root of N elements compared with N elements for a two-dimensional array with the same center-to-center spacing of elements.

The purpose of this paper is to report on some initial results of the development of a TPA transducer for pulse-echo imaging applications. The design of the transmit and receive circuitry required by the TPA transducer will also be discussed.

THEORY

The tapered element can be modeled using a parallel network of the simplified Mason's equivalent circuit for a lossless piezoelectric transducer near resonance [1]. This model is accurate for narrow frequency bandwidths where the near resonance approximation holds over the entire length of the tapered element. This model was incorporated into a computer program [2] to calculate the field intensity distribution produced by a TPA.

If a tapered element of an array was driven by a single broad-band voltage pulse, like those used to drive elements of conventional linear arrays, a set of adjoining pulsed beams of different

frequencies will be produced along the y dimension of the tapered element, as illustrated in Fig. 2. Discontinuities along the path of each beam will create echoes at corresponding frequencies. The received signal will then consist of a summation of echoes of varying frequency from all of the transmitted beams. The frequency of the received echoes can be used to discern the y-position of the reflector(s).

However, in order to achieve the best possible lateral and axial resolution in a TPA, the phases (delays) of all frequency components of the signals driving each element would have to be controlled so that all of the resulting beams arrive at the desired focal region simultaneously.

METHODS AND RESULTS

In order to experimentally verify the theoretical performance of a TPA transducer, a 16-element TPA was constructed. The piezoelectric ceramic elements were 101.6 mm in length, 2.1 mm in width, and had a tapered thickness ranging from 2.3 mm to 4.1 mm. These element dimensions were chosen to simplify the fabrication of the transducer for this pilot study and do not necessarily represent optimal dimensions for imaging applications. The elements were mounted in an anodized aluminum housing and were air-backed. A thin mylar sheet covered the front faces of the elements and served to keep the housing water-proof.

All acoustical field measurements were made in an ultrasonic beam observation tank (Medsonics Model ME104) using a 1 mm diameter PVDF hydrophone probe. These measurements were plotted as relative intensity (in dB) versus position.

Figures 3 and 4 compare the theoretical and experimental field profiles of an element of the TPA, in the y dimension, when driven by a 450 kHz and a 500 kHz cw signal, respectively. These figures are typical of the good agreement obtained between the experimental results and theoretical predictions.

Figure 5 illustrates the theoretical field profile of the TPA when driven by a pulse consisting of the two properly phased frequency components used in Figs. 3 and 4. Each of the peaks in this figure corresponds to one of the two frequency components in the pulsed excitation signal. Such phasing of the individual frequency components of the pulses will be required for high resolution imaging.

DISCUSSION

An advantage of using the TPA in this pulsed "frequency scanning" mode is that it would enable the y-z plane to be scanned using a single pulse at a rate much faster than is currently possible with conventional phased arrays. This technique, with the addition of beam steering, would also allow a large number of adjacent planes to be scanned, thereby enabling the formation of a three-dimensional image.

There are several potential limitations to this approach. The characteristics of scattering objects such as reflectivity and attenuation are dependent on the frequency of the ultrasonic pulse. Therefore, the amplitudes of the return echoes will be dependent not only on the position and composition of the scatterer, but also the frequency of the incident pulse. These effects can be kept to a minimum if the range of frequencies used is not large.

Figure 6 is a block diagram of the hardware currently being developed to control the TPA. The transmit portion of the controller will employ fast D to A converters and broad-band pulse drivers to produce the desired excitation signals. The receiver portion of the controller will implement a technique of time expansion which employs simple microcomputer control and low-cost A to D converters [3]. The received signals from the array elements will be captured at a high rate using CCD delay lines. The signals will then be released at a lower rate, digitized by A to D converters, and subsequently stored in the microcomputer's memory. Digital signal processing techniques will then be used to bandpass filter and supply appropriate delays for dynamic focusing of the frequency encoded data in order to form the image.

CONCLUSIONS

An analysis of a TPA transducer operating in the pulse-echo mode suggests that it can provide a 2-D phased array capability that is not yet possible with conventional arrays. Further work is required in the development of the transmit and receive hardware for the TPA before a complete assessment of its potential can be made.

ACKNOWLEDGEMENTS

The partial support of this study by the Whitaker Foundation is gratefully acknowledged.

REFERENCES

1 Benkeser, P.J., L.A. Frizzell, K.B. Ocheltree, and C.A. Cain, "A tapered phased array ultrasound transducer for hyperthermia treatment," IEEE Trans. Ultrason. Ferroelect., and Freq. Cont., vol. UFFC-34, no. 4, 1987 (in press).

2 Ocheltree, K.B., P.J. Benkeser, L.A. Frizzell, and C.A. Cain, "An ultrasonic phased array applicator for hyperthermia," IEEE Trans. Son. and Ultrason., vol. SU-31, no. 5, pp. 526-531, 1984..

3 Campbell, M.A., G. Hayward, and A. McNab, "A novel approach to ultrasonic data acquisition," Proc. 1985 Ultrasonics International Conf., pp. 523-527, 1985.

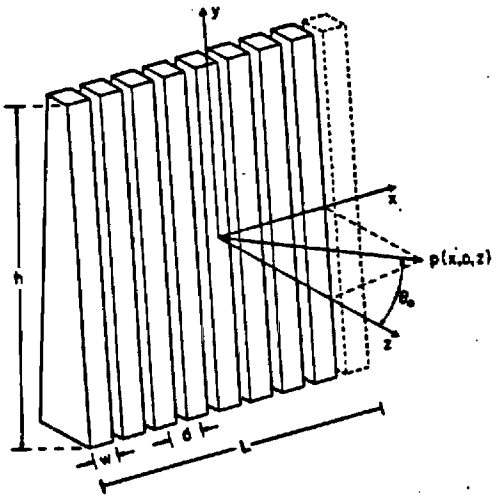

Fig. 1 Tapered Phased Array (TPA)

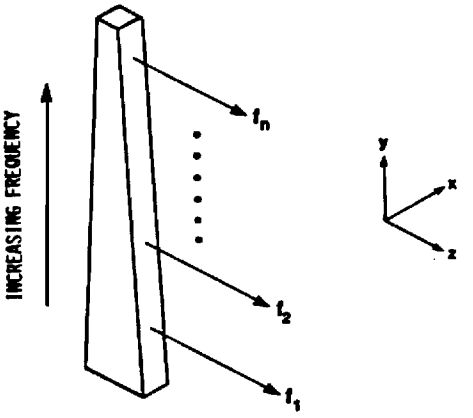

Fig. 2 Spatial frequency response of a tapered element to a broad-band pulsed excitation

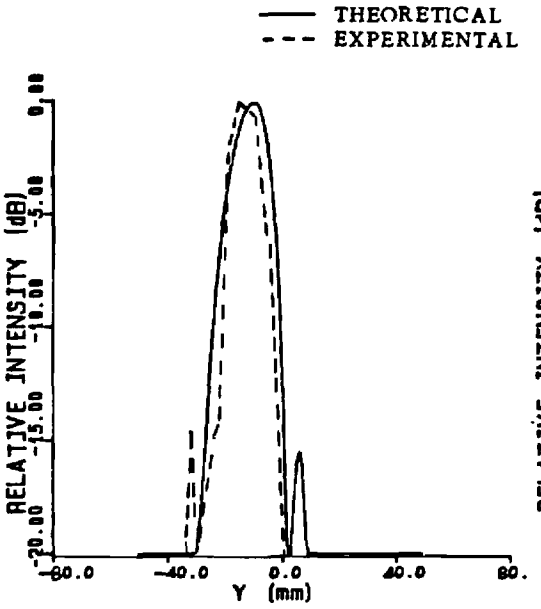

Fig. 3 Field profile of a tapered element (x = 0, z = 50 mm, f = 450 kHz)

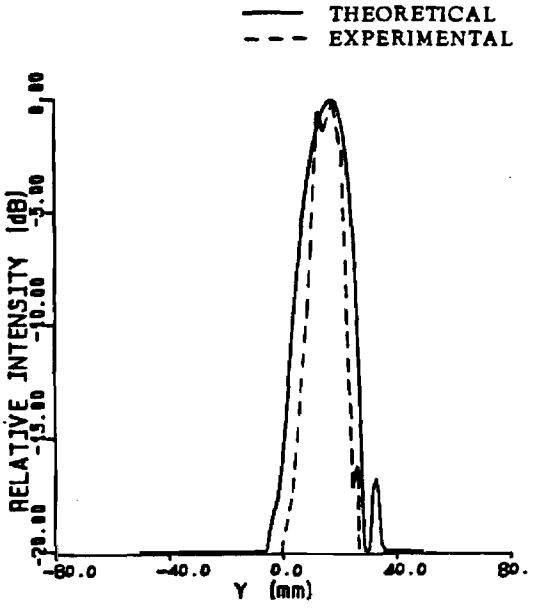

Fig. 4 Field profile of a tapered element (x = 0, z = 50 mm, f = 500 kHz)

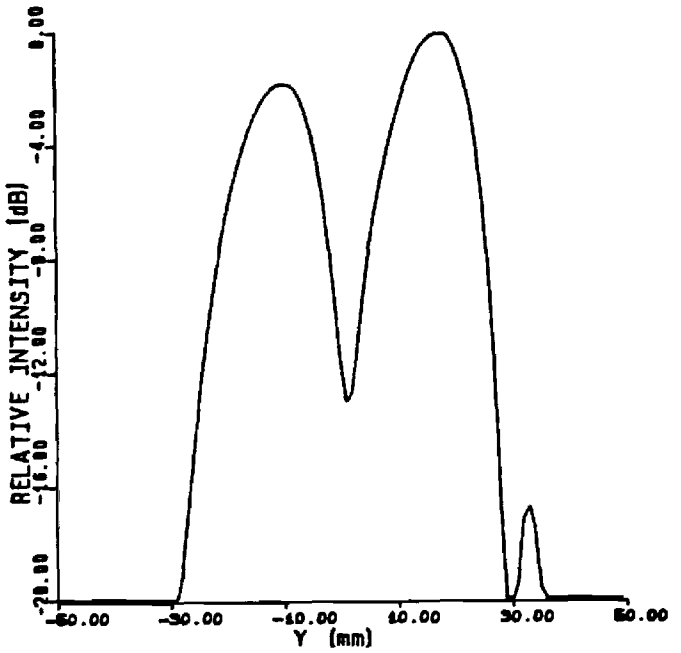

Fig. 5 Theoretical field profile of the TPA pulsed with an excitation signal with two frequency components (f_1 = 450 kHz, f_2 = 500 kHz)

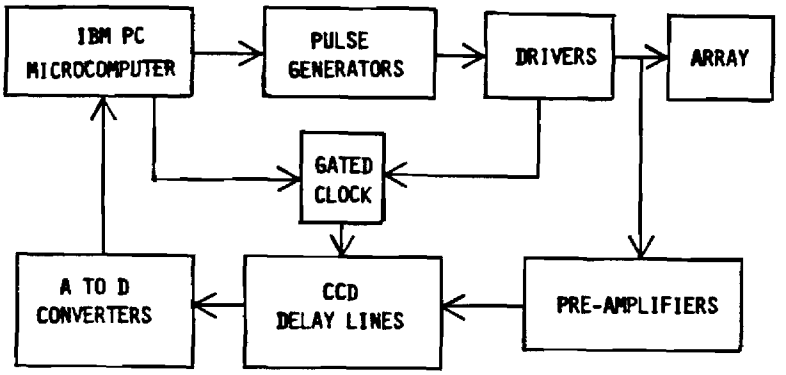

Fig. 6 TPA controller block diagram

ULTRASOUND TAPERED PHASED ARRAY IMAGING TRANSDUCER

Annual Progress Report #2

July 15, 1988

Submitted to the Whitaker Foundation by

Paul J. Benkeser
Assistant Professor
School of Electrical Engineering
Georgia Institute of Technology
Atlanta, Georgia 30332-0250

INTRODUCTION

This report details the progress made during the second grant year of the project entitled, "Ultrasound Tapered Phased Array Imaging Transducer." The goals for the third year, as well as a revised third year budget, are also included in this report. Copies of a proceedings paper, based upon work accomplished during the second year of the grant, can be found in the Appendix of this report.

CURRENT PROGRESS

The research plan in the grant application called for the completion of the development of both a theoretical model for the electroacoustic response of elements of the tapered phased array (TPA) and the array controller by the end of the second grant year. Current progress on schedule with this plan.

A staircase model of the thickness mode piezoelectric transducers is being used to characterize the tapered element. The advantage of this model is its ability to predict the response of the transducer to a variety of arbitrary input functions. This will allow us to study the response of the tapered element to excitation signals that could not easily be implemented with other models.

A 16-element TPA, TPA #1, was fabricated in order to make experimental measurements of the electroacoustic response of its elements. These measurements were used to verify the aforementioned theoretical model. Peter Barthé, a Ph.D. student previously supported by this grant, presented this work in a paper entitled, "A Staircase Model of Tapered Piezoelectric Transducers," at the IEEE 1987 Ultrasonics Symposium (see Appendix).

The results of comparisons of theoretical and experimental radiation patterns suggest that when the elements of a TPA are pulsed with the appropriate excitation signals, a linearly aligned group of focused beams, at frequencies corresponding to those contained in the pulsed signals, will be produced.

The advantage of using the TPA in this pulsed "frequency scanning" mode is that it would enable an entire plane to be scanned, using a single pulse, at a rate much faster than is currently possible with conventional arrays. Fast scanning rates are important for high resolution imaging when viewing dynamic structures such as the heart. This technique, with the addition of beam steering, would also allow a large number of adjacent planes to be rapidly scanned, thereby enabling the formation of a three-dimensional image. Two new graduate research assistants are currently investigating the feasibility of implementing this technique.

To facilitate future testing of TPA #1, an array controller has been designed and is currently being tested. This controller is microprocessor-based and will regulate both the generating of the pulses that drive the elements and the subsequent processing of the received echo data.

The receiver portion of the controller implements a technique of time expansion which employs a simple microcomputer (IBM PC-XT) control and low-cost A to D converters. The received signals from the TPA elements will be captured at a high rate using CCD (Charge-Coupled Device) delay lines. The signals will then be released at a lower rate, digitized by A to D converters, and subsequently stored in the microcomputer's memory. Digital signal processing beam-forming techniques will then be used to implement dynamic focusing of the frequency encoded data in order to form the image.

GOALS FOR THIRD YEAR

The overall goal of this project remains unchanged: to develop a TPA transducer for medical imaging applications. The specific goals for the third year are:

1. To complete the testing of the array controller.
2. To compare the theoretical and experimental field radiation patterns of TPA #1 when it is driven by the array controller.
3. To test the imaging capabilities of the TPA.
4. To continue to investigate the feasibility of the new mode of operation of the TPA.

BUDGET MODIFICATIONS

A decrease in the fringe benefits rate and the addition of new graduate research assistants required that minor modifications be made to the budget for the third year of the grant. The total amount of funds requested in this modified budget (see Table 1) is the same as that requested in the budget of the grant application.

TABLE 1. DETAILED BUDGET FOR THIRD YEAR

Personal Services	
Paul J. Benkeser, Assistant Professor 2.5 months @ $4,680/month	$11,700
Tsang-Long Pao, Graduate Research Assistant 9 months @ 1/3 time @ $2,160/month	$ 6,480
Intaek Kim, Graduate Research Assistant 9 months @ 1/3 time @ $1,860/month	$ 5,580
Chankil Lee, Graduate Research Assistant 9 months @ 1/3 time @ $1,860/month	$ 5,580
Fringe Benefits	
25.5% of Direct Salaries (excluding students)	$ 2,984
Materials and Supplies	
Electronic Components, Materials for Fabricating another TPA, Publication Costs	$ 4,000
Travel	$ 1,004
Total Direct Costs	$37,328
Overhead (20%)	$ 7,466
Total Funds Requested	$44,794

APPENDIX

A STAIRCASE MODEL OF TAPERED PIEZOELECTRIC TRANSDUCERS*

P. G. Barthé and P. J. Benkeser
School of Electrical Engineering
Georgia Institute of Technology
Atlanta, Georgia 30332-0250

ABSTRACT

A classic trade-off in the design of thickness mode piezoelectric transducers for pulse-echo imaging has been increased bandwidth at the cost of decreased sensitivity through the use of backing materials. However, a multiple resonance, tapered-thickness piezoelectric ceramic does not require a backing material to make it broadband. A new model is presented for the analysis of tapered ceramics where the thickness gradient is represented as a series of discrete steps. Each step is, in turn, represented by an appropriate model which contributes to the net transducer response. The theoretical results obtained using this staircase model will be presented and shown to agree well with experimentally obtained data from a tapered piezoelectric ceramic transducer.

I. Introduction

A piezoelectric ceramic with a linearly tapered thickness has been shown to exhibit an inherently broadband frequency response [1-4]. Several investigators have examined the potential of using such tapered ceramics in pulse-echo imaging transducers [5,6,7]. They found that transducers using tapered ceramics do not require lossy backing materials to achieve the desired bandwidth and are thus simpler to fabricate. However, no simple theoretical model exists which adequately describes the response of such a transducer.

Vibrations of piezoelectric crystals with contoured dimensions were first studied during development of ultrasonic delay lines [1,2]. In general, this research employed mathematical solutions of the elasticity equations with boundary conditions to describe coupled-mode vibrations in quartz. Applications were limited because of the focus and complexity of analysis and because results were not in a form suitable for modeling pure-mode devices. The ceramic tapered bar transducer has been examined with a similar approach in longitudinal and shear wave devices [3,4].

The theoretical modeling of the tapered bar transducer was also approached as a study of response errors induced by an uneven device thickness [8]. A novel approach was used in which a single model was obtained by integrating over a transducer surface area composed of smaller models. This is similar to the new model developed herein except that the results from several model steps are combined rather than combining models to obtain a result. Hence, no integration is necessary.

In this paper, the thickness gradient of a tapered piezoelectric transducer is represented as a sequence of discrete steps. Each step is, in turn, represented by an appropriate model which contributes to the net response. The staircase approach is detailed along with input impedance and convergence considerations. The theory is verified through comparisons with experimental results obtained from a tapered bar transducer.

II. THEORY

A. Staircase Model Approach

A description of devices in the form of the staircase model is presented in this section. A tapered bar transducer is shown in Fig. 1. The thickness varies linearly from L_{min} to L_{max} in the poling or z-direction. The device has a length T in the x-direction, and a width W in the y-direction.

Consider the device divided into N equal sections along the x-axis. Each element located at position x_i, for $i = 1,2,\ldots,N$, can be modeled as a separate transducer. The position x_i may be described as

$$x_i = \left(i - \frac{1}{2}\right)\Delta x , \qquad (1)$$

where

$$\Delta x = \frac{T}{N}$$

is the length of each section. The width of each element remains W, while the thickness of each section is represented by its average thickness which is simply the thickness of the transducer at $x = x_i$. Hence, the thickness of the i-th section, L_i, may be expressed as

$$L_i = L_{min} + x_i \tan\theta \qquad (2)$$

where

$$\tan\theta = \frac{L_{max} - L_{min}}{T} ,$$

and θ is the angle the sloped transducer face makes with the x-axis. Since the region of stress generation is along the thickness center of the

*This work was supported by The Whitaker Foundation.

tapered bar, the generated waves will be at an angle of θ with the x-axis.

The power of this approach is that models which are well defined in the literature may now be used to represent the individual steps.

B. Electric Input Impedance

The electric input impedance of an electromechanical transducer is of fundamental importance in the analysis and design of transducers and their associated systems. The input impedance for a thickness-mode device may be expressed as [9]

$$Z_{IN} = \frac{1}{j\omega C_o}\left[1 + K_T^2 \frac{j(Z_1+Z_2)Z_c \sin\phi - 2Z_c^2(1-\cos\phi)}{\phi\left[(Z_c^2+Z_1Z_2)\sin\phi - j(Z_1+Z_2)Z_c\cos\phi\right]}\right] \quad (3)$$

where Z_1, Z_c, and Z_2 are the front (flat) surface acoustic impedance, the ceramic characteristic acoustic impedance, and the back (tapered) surface acoustic impedance, respectively; C_o is the clamped capacitance of the transducer; K_T is the clamped electromechanical coupling factor; ω is the angular input frequency; and ϕ is a frequency-dependent phase angle.

For a tapered transducer in the staircase form, the input impedance can be expressed in terms of the input admittance Y_{IN} such that

$$Y_{IN} = \sum_{i=1}^{N} Y_i \quad (4)$$

where for each $Y_i = 1/Z_i$ we have

$$C_{o_i} = \frac{WT\varepsilon^s}{NL_i} \quad (5)$$

and

$$\phi_i = \frac{\omega}{\overline{V}_a} L_i \,. \quad (6)$$

In the last two equations, ε^s is the clamped permittivity of the ceramic and $\overline{V}_a$ is its piezoelectrically stiffened acoustic wave velocity. Calculating the input impedance of a tapered device therefore reduces to obtaining the input admittance of each element, summing, and inverting the final result. Obviously, these calculations are well suited for a computer. However, a value of N must be chosen to assure negligible error. Above N steps little will be gained in terms of accuracy and computation time would only increase.

C. Number of Steps and Convergence

Guidelines for choosing a sufficient number of steps for a transducer configuration may be obtained from further analysis of device admittance.

The following relationship can be used to determine the number of steps required to minimize the error:

$$\lim_{i \to N_{min}} \frac{\partial Y_{IN}}{\partial i} \to 0 \quad (7)$$

where N_{min} represents the lowest acceptable N. This can be further simplified by noting that

$$\frac{\partial Y_{IN}}{\partial i} = \frac{\partial Y_{IN}}{\partial L_i} \cdot \frac{\partial L_i}{\partial i} \,. \quad (8)$$

Equations (1)-(8) provide the solution to (7) based on the transducer configuration embedded in $\partial Y_{IN}/\partial L_i$.

The relative deviation between using a large N and small n may be quantified with the percent root mean square deviation, Δ. The error is evaluated between the frequencies of interest, f_{min} and f_{max}, and may be expressed for impedance magnitude as

$$\Delta = \left[\frac{1}{N}\sum_{f=f_{min}}^{f_{max}}\left[\frac{Z_{IN(N)} - Z_{IN(n)}}{Z_{IN(N)}}\right]^2\right]^{\frac{1}{2}} \,. \quad (9)$$

III. EXPERIMENTAL RESULTS

Experimental measurements were made on a tapered bar transducer using a vector impedance meter. The transducer's dimensions were W = 2.01 mm wide, L = 101.3 mm long, and L_{min} = 2.79 mm to L_{max} = 4.07 mm thickness. A quasi-longitudinal mode model was chosen for the N steps since the thickness of the device was comparable to its width. Under these conditions, the device does not operate in a pure thickness mode. This requires the use of effective constants in the thickness-mode model [10,11]. The device was composed of Channel C5800 material, with an unstiffened acoustic wave velocity V_a = 3100 m/s, dielectric constant $\varepsilon^s/\varepsilon_o$ = 1100, density ρ = 7550 kg/m^3, and parallel longitudinal mode coupling factor of $K_{33}^2 = K_{33} = 0.67$. The effective coupling coefficient, K_{eff}, was chosen as 0.63 for the transducer dimensions. The effective dielectric permittivity was then $\varepsilon^s_{eff} = 1100(1-K^2_{eff})\varepsilon_o = 663\,\varepsilon_o$. The effective acoustic impedance was Z^o = 29.8 MRayl. This data was used to simulate the input impedance and convergence with N of the impedance magnitude.

A computed simulation in Fig. 2 shows that the approximation error does approach zero for increasing N. The errors are large because this is the total error over an entire frequency band (400-800 KHz in this example). Since the curve leveled at N = 512, a value of N = 500 was used in the following input impedance simulations.

Figures 3 and 4 compare the theoretical and experimental plots of the transducer's input impedance magnitude and phase in air, respectively. These plots indicate multiple resonances between 400 to 580 KHz. At approximately 625 KHz, the transducer is resonant at its narrow thickness, L_{min}. Above this frequency, the device passes out of a region of stiffness control and is no longer resonant.

Figures 5 and 6 compare the theoretical and experimental plots of the input impedance magnitude and phase, respectively, with air backing and a water load. These figures demonstrate that the transducer is inherently broadband in nature. The linear phase characteristic in Fig. 6 implies a distortionless time or impulse response.

IV. CONCLUSION

A new staircase model has been developed to characterize tapered transducers. The input impedance of tapered devices has been discussed along with model convergence considerations. The theoretical approach agrees well with empirically obtained data from an tapered transducer.

REFERENCES

[1] J.L. Bleustein, "Thickness-Twist and Face-Shear Vibrations of a Contoured Crystal Plate," Inter. Jour. Sol. Struct., vol. 2, 1966, pp. 351-360.

[2] C.B. Loutzenheiser and W.J. Denkmann, "Thickness/Twist Vibrations of a Truncated, Linearly Tapered, Crystal Strip," Jour. Acou. Soc. Am., vol. 41, pt. 2, no. 4, 1967, pp. 962-968.

[3] B.N. Alekseev, D.B. Dianov, and S.P. Karuzo, "Tapered-Bar Transducer," in Proceedings of the Eighth All-Union Acoustics Conference [in Russian], Moscow, 1973.

[4] B.N. Alekseev, D.B. Dianov, and S.P. Karuzo, "Tapered Piezoelectric Bar Transducer with Transverse Polarization of the Piezoceramic," Sov. Phys. Acou., vol. 23, no. 1, 1977, pp. 1-4.

[5] T. Kobayashi, "Wedged Ultrasonic Transducers Having Thickness Extensional Vibration," Jour. Acou. Soc. Jpn. [in Japanese], vol. 38, no. 10-12, 1982, p. 748.

[6] Y. Tomikawa, H. Yamada, and M. Onoe, "Wide Band Ultrasonic Transducer Using Tapered Piezoelectric Ceramics for Non-Destructive Inspection," Jpn. Jour. Appl. Phys., vol. 23, suppl. 23-1, 1984, pp. 113-115.

[7] P.J. Benkeser, "A Pulse-Echo Ultrasound Tapered Phased Array Transducer," Proc. 13th NE Bioengineering Conf., pp. 286-288, 1987.

[8] Y. Jayet, M. Perdrix, and R. Goutte, "Effects on the Damping of Ultrasonic Transducers Due to a Lack of Parallelism in the Piezoelectric Element," Ultrasonics, vol. 21, no. 4, 1983, pp. 179-183.

[9] G. S. Kino, Acoustic Waves, Devices, Imaging, and Analog Signal Processing, New York: Prentice Hall, 1987, p. 32.

[10] R.H. Coursant, C. Méquio, and P. Pesqué, "Simulation of the Acousto-Electric Response of Ultrasonic Narrow Strip Transducers with Mechanical Losses," Ultrasonics International 83, Conference Proceedings, Halifax, Canada, July 12-14, 1983, pp. 414-419.

[11] J. Sato, M. Kawabuchi, and A. Fukumoto, "Dependence of the Electromechanical Coupling Coefficient on the Width-to-Thickness Ratio of Plank-Shaped Piezoelectric Transducers used for Electronically Scanned Ultrasound Diagnostic Systems," Jour. Acoust. Soc. Am., vol. 66, no. 6, 1979, pp. 1609-1611.

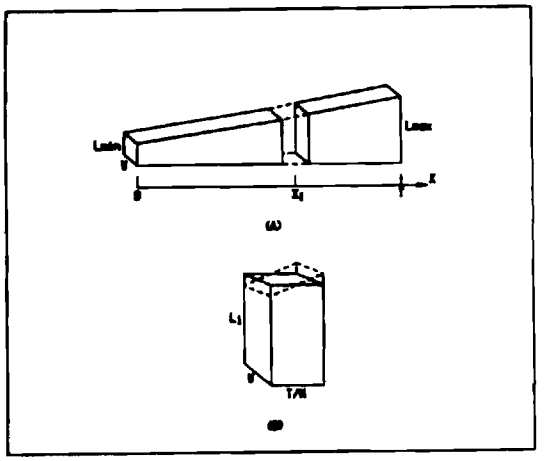

Fig. 1. Staircase model approximation of a tapered bar transducer (a) with close-up of the i-th step (b).

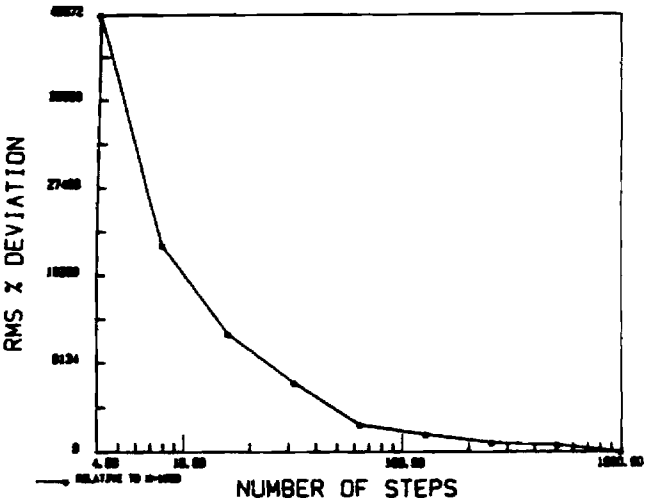

Fig. 2. Convergence of impedance magnitude with increasing number of steps relative to N=1000.

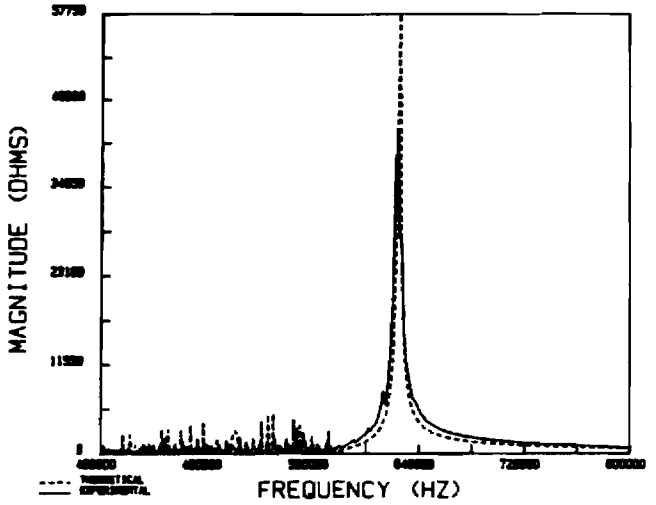

Fig. 3. Comparison of simulated and measured input impedance magnitude in air.

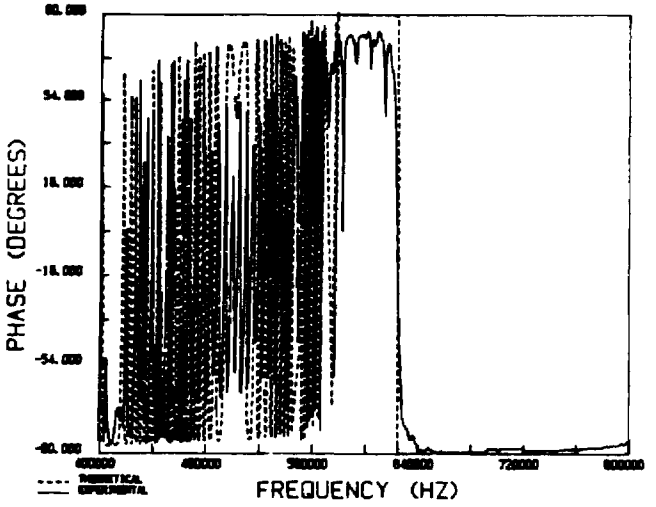

Fig. 4. Comparison of simulated and measured input impedance phase in air.

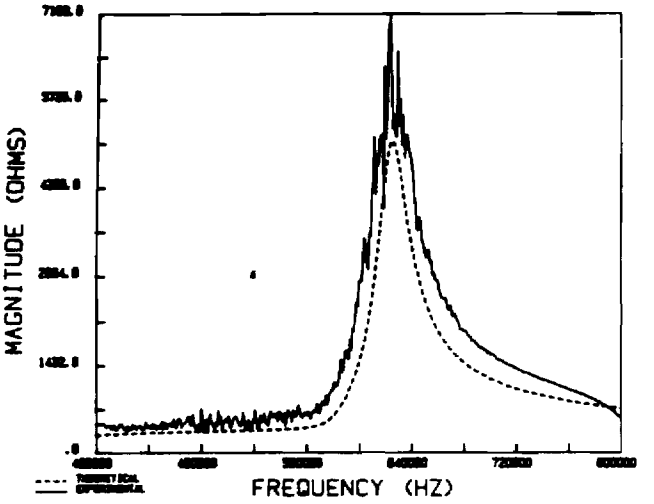

Fig. 5. Comparison of simulated and measured input impedance magnitude with Z_1(flat face)=water, and Z_2=air.

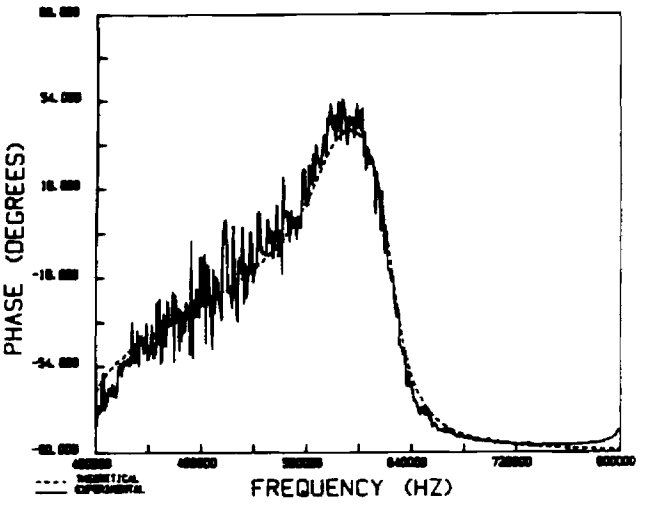

Fig. 6. Comparison of simulated and measured input impedance phase with Z_1(flat face)=water, and Z_2=air.

GEORGIA INSTITUTE OF TECHNOLOGY
SCHOOL OF ELECTRICAL ENGINEERING
ATLANTA, GEORGIA 30332

TELEPHONE: (404) 894-

October 23, 1989

Miles J. Gibbons, Jr.
Executive Director
The Whitaker Foundation
4718 Old Gettysburg Road
Suite 405
Mechanicsburg, PA 17055-4325

Dear Mr. Gibbons:

Enclosed you will find two copies of the final report for my grant from The Whitaker Foundation.

I have not been successful to date in securing any grant support to continue my research in this particular area. However, I have identified several "spin-off" research topics which I am hoping will be funded in the near future.

I am grateful to The Whitaker Foundation for assisting me in beginning my medical research career.

Sincerely,

Paul J. Benkeser
Assistant Professor

ULTRASOUND TAPERED PHASED ARRAY IMAGING TRANSDUCER

Final Report

October 23, 1989

Submitted to The Whitaker Foundation by

Paul J. Benkeser
Assistant Professor
School of Electrical Engineering
Georgia Institute of Technology
Atlanta, GA 30332-0250

Introduction

This report details the progress made during the course of the project entitled "Ultrasound Tapered Phased Array Imaging Transducer." The main body of the report is a general overview of the progress made. The more specific technical discussions of this research can be found in the Appendix, where all publications based upon research supported by The Whitaker Foundation appear.

Progress

The research plan of the grant application called for the completion of both the theoretical and experimental analysis of the electroacoustic response of an element of a tapered phased array (TPA) by the end of the grant period. These tasks have been successfully completed. In addition, the experimental testing of the imaging capabilities of the TPA (see Fig. 1) was also to be completed by the end of the grant period. However, delays in the construction of the electronics necessary to control the TPA have prevented the completion of this task to date. It is anticipated that these experimental measurements will be completed within the next six months.

A critical part of this project was the development of a theoretical model of the electroacoustic response of a tapered

piezoelectric element. A staircase model was derived which allowed the performance of the TPA in imaging applications to be theoretically analyzed [1-3]. Using this model, it was discovered that when the elements of the TPA are pulsed with the appropriately phased excitation signals, a linearly aligned group of focused beams, at frequencies corresponding to those contained in the pulsed signals, will be produced as shown in Fig. 2 [4]. The advantages of using the TPA in this pulsed "frequency scanning" mode is that it would enable an entire plane to be scanned, using a single pulse, at a rate much faster than is currently possible with conventional arrays [5]. Fast scanning rates are important for imaging dynamic structures such as the heart. This technique, with the addition of beam steering, would also allow a large number of adjacent planes to be rapidly scanned, thereby enabling the formation of a three-dimensional image.

The electronic circuitry necessary to detect and process the received echo signals from the array was designed, fabricated, and tested (see Fig. 3). It consists of a microcomputer controller (IBM PC-XT) and a low-cost analog-to-digital (A to D) converter. The received signals from the TPA elements are captured at a high sampling rate using a charge-coupled device (CCD) delay line. The captured signals are then released from the CCD at a lower rate and digitized by the A to D converters, and subsequently stored in the microcomputer's memory. Dynamic signal processing beam-forming techniques are then used to implement the dynamic focusing of the frequency encoded data in order to form the image.

While no problems were encountered in developing the receiver electronics, the same did not apply to the transmitting electronics. In order to implement the frequency scanning technique, a high speed digital to analog (D to A) converter is required. This device is required to generate the transmitted signal consisting of the proper frequency spectrum. There are commercially available instruments capable of generating this type of signal. However the cost of such an instrument was prohibitively expensive for the budget of this grant. Alternate schemes for generating these signals were pursued, including designing our own D to A, without success. It was finally decided that a less than optimal scheme must be employed. This consisted of employing a conventional broadband pulser to serve as the transmitter. The drawback of using this conventional pulser is that the transmitting pulse cannot be "tailor made" for the TPA. Its frequency spectrum will not yield a uniform excitation along the height of the elements and thus will have to be compensated for.

Currently, the transmitting circuitry is being constructed and interfaced with the receiver electronics. Once this is completed the experimental testing of the TPA will commence. The frequency scanning technique will be evaluated in the light of the less than optimal transmitting electronics. Should the results of the test prove promising, additional grant support for the complete development of this imaging system will be pursued.

References

[1] P.G. Barthe and P.J. Benkeser, " A Staircase Model of Tapered Piezoelectric Transducers," Proc. 1987 IEEE Ultrasonics Symp., pp. 697-700, 1987.

[2] P.G. Barthe and P.J. Benkeser, "Analysis of the Mechanically-Uncoupled Electric Resonance in Tapered-Thickness Piezoelectric Transducers," Proc. 1988 IEEE Ultrasonic Symp., pp. 717-720, 1988.

[3] P.G. Barthe and P.J. Benkeser, "A Staircase Model of Tapered-Thickness Piezoelectric Ceramics," J. Acoustical Soc. Amer., (accepted for publication).

[4] P.J. Benkeser, "A Pulse-Echo Ultrasound Tapered Phased Array Transducer," Proc. 13th Northeast Bioengr. Conf., pp.286-288, 1987.

[5] P.J. Benkeser, E.F. Goff, and W.O. Rice, "Analysis of a Pulse-Echo Ultrasound Tapered Phased Array Transducer," Proc. Ultrason. International Conf., pp. 697-700, 1987.

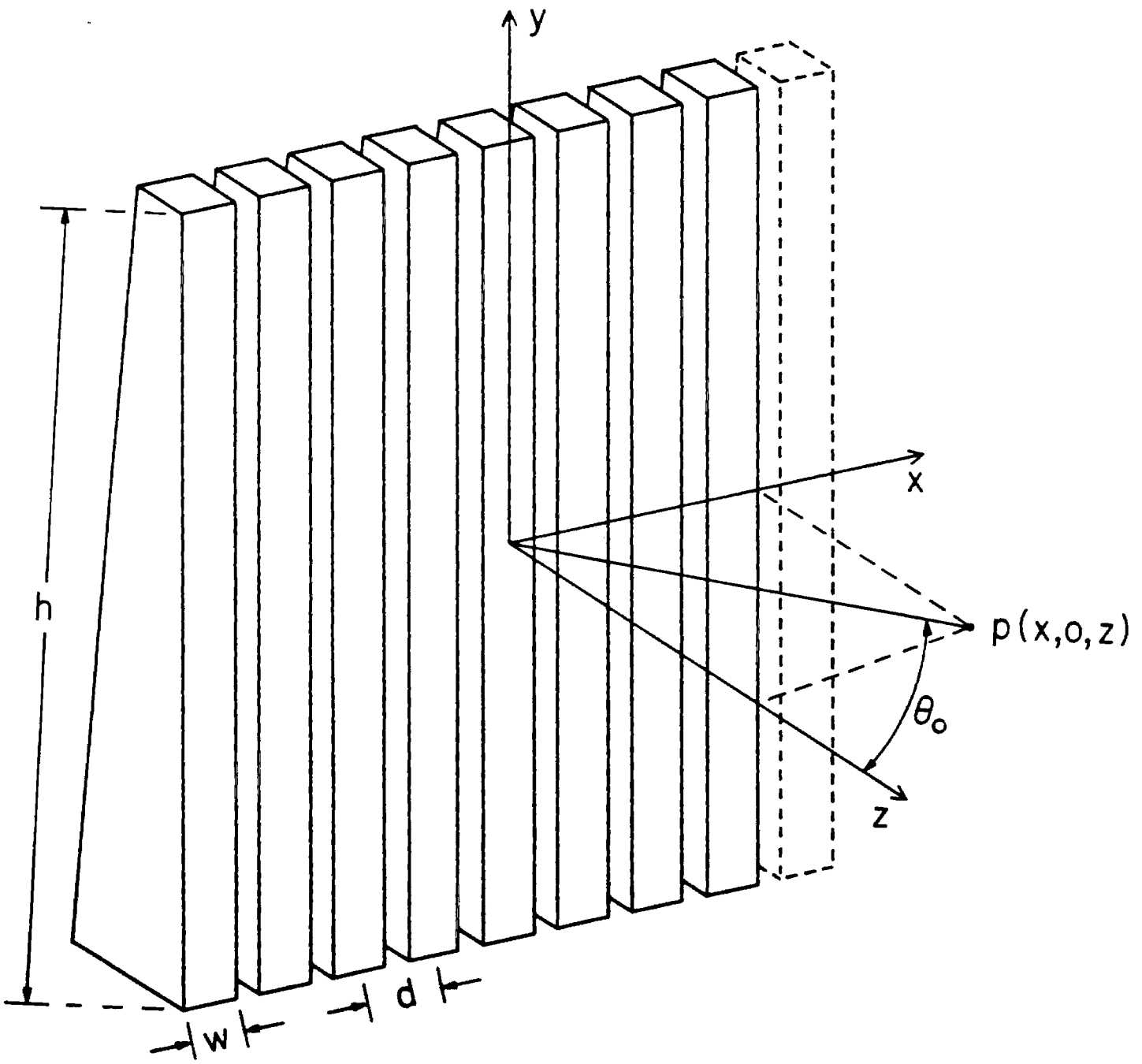

Figure 1. Tapered phased array.

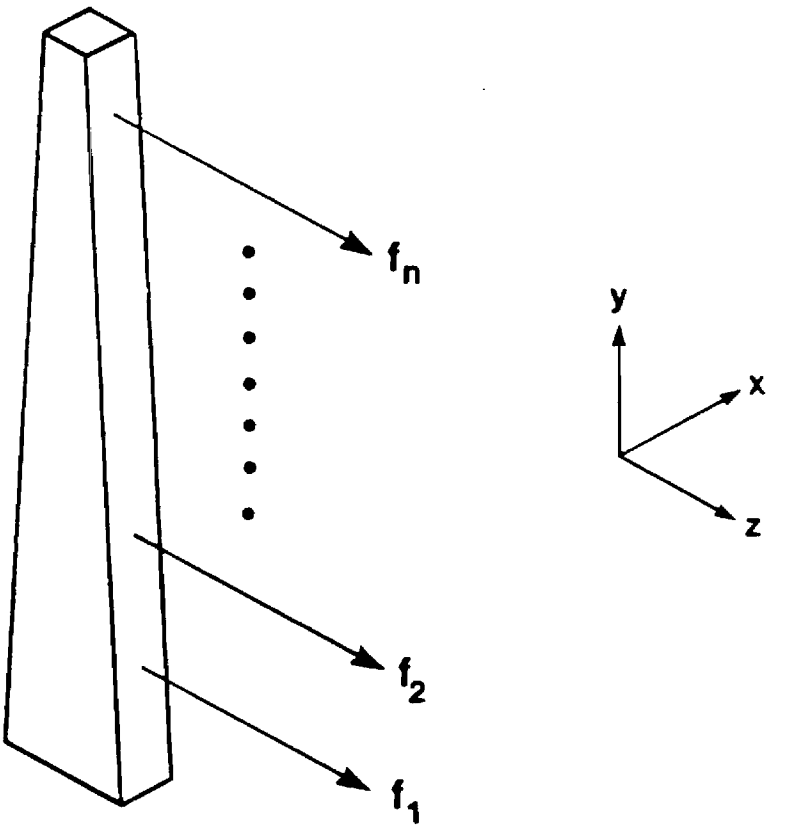

Figure 2. Frequency response of a tapered element to a broadband pulse excitation.

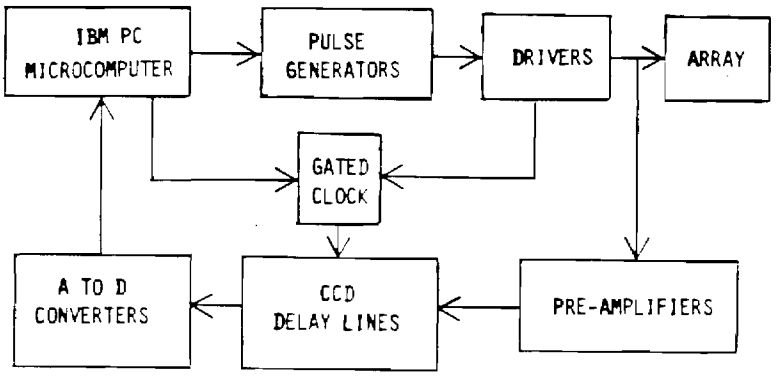

Figure 3. Block diagram of the tapered phased array controller.

APPENDIX

A PULSE-ECHO ULTRASOUND TAPERED PHASED ARRAY TRANSDUCER

P. J. Benkeser

School of Electrical Engineering
Georgia Institute of Technology
Atlanta, Georgia 30332

ABSTRACT

The tapered phased array (TPA) transducer consists of a linear array of piezoelectric elements that have a tapered thickness. In this paper, a TPA transducer operating in the pulse-echo mode is examined. A model for the radiation pattern of a tapered element employing a distributed network of the equivalent circuit of a lossless piezoelectric transducer is described. Comparisons of the theoretical and experimental radiation patterns of a TPA transducer are shown to be in good agreement. These results indicate that when the transducer is pulsed, it produces a linearly aligned group of focused beams at different frequencies which could be used to provide a two-dimensional phased array capability for a pulse-echo imaging system.

INTRODUCTION

Pulse-echo ultrasonic imaging systems are used in a variety of applications as diverse as flaw detection in metal structures and imaging tissues in the body. These systems operate by generating short, broad-band pulses that propagate through the medium of interest and reflect off of regions of discontinuities. The reflected echo is received and its amplitude and time-of-flight delay are used to generate the image. Two-dimensional images are produced by scanning the pulses through the medium. This scanning can be accomplished either by mechanical movement of the ultrasonic transducer, or by the use of an ultrasonic phased array transducer.

A two-dimensional phased array can generate and position a focused beam in three dimensions by controlling the phases of the signals driving each array element so that constructive interference of the waves is achieved at the desired field point. By readjusting the phase periodically, the focus can be scanned over any three-dimensional path at a rate much faster than that of a mechanically scanned system, which is important in viewing dynamic structures such as the heart. However, a two-dimensional phased array is too costly and complex for most imaging applications due to the large number of elements and associated circuitry that are required. Most conventional phased array transducers are of the linear (one-dimensional) type which allow the focus to be scanned over a two-dimensional path.

A new type of phased array, a tapered phased array has been developed for use in ultrasound hyperthermia [1]. This transducer consists of a linear phased array composed of elements that have a tapered thickness, as illustrated in Fig. 1. The frequency response of these elements, due to their tapered thickness, is inherently broad-band. The region along the length of the element that has a thickness resonant at the frequency of the driving signal will produce the greatest acoustical power output. Thus, different regions along the length of the element can be excited by changing the frequency of the continuous wave (cw) signal driving the element.

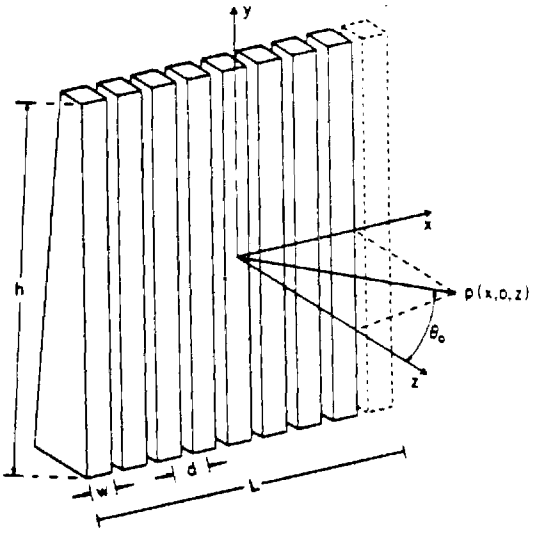

Fig. 1 Tapered array.

The tapered phased array allows the focal region to be swept in two dimensions by controlling the phases of the cw signals, and in the third dimension by controlling the frequency of those signals. The tapered array has the square root of N elements compared with N elements for a two-dimensional array with the same center-to-center spacing of elements.

The purpose of this paper is to theoretically analyze the potential of the tapered phased array in pulse-echo imaging applications.

CH2436-4/87/0000-0286 $1.00 © 1987 IEEE

ANALYSIS OF A PULSE-ECHO TAPERED PHASED ARRAY

The tapered element can be modeled using a parallel network of the simplified Mason's equivalent circuit for a lossless piezoelectric transducer near resonance, as shown in Fig. 2 [2]. This model is accurate for narrow frequency bandwidths where the near resonance approximation holds over the entire length of the tapered element. This model was incorporated into a computer program [3] that implements a rectangular radiator method for calculating the field intensity distribution produced by a cw linear phased array. Figure 3 shows a comparison of the experimental and theoretical field profiles in the y dimension for a cw tapered phased array. This figure illustrates the good agreement that has been obtained between the theoretically predicted fields and the experimental data.

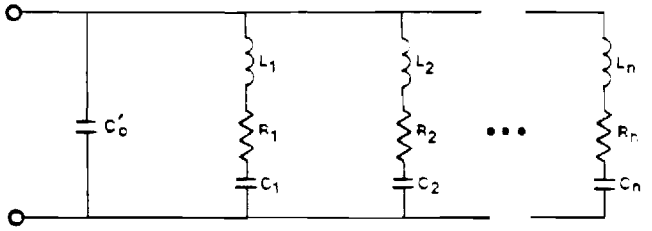

Fig. 2 Equivalent-circuit model for an element with a tapered thickness.

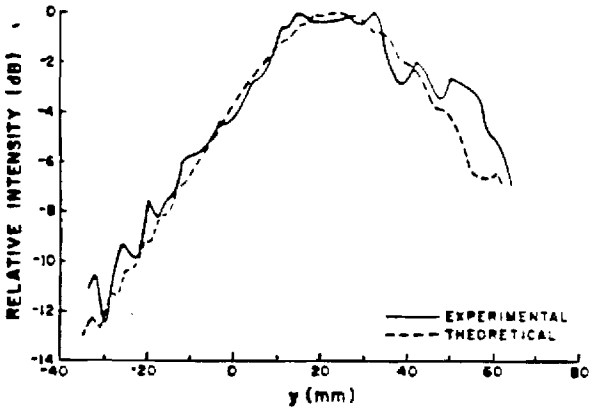

Fig. 3 Comparison of the theoretical and experimental field profiles in the y dimension (x=0, z=100 mm) of a 32-element cw TPA operating at 620 kHz.

Since pulse-echo imaging systems operate by transmitting and receiving short bursts of ultrasound, the spatial response of the tapered phased array should be determined for this broad-band situation. However, the cw analysis can adequately serve as a first-order approximation of the spatial response [4].

If a tapered element of an array was driven by a single broad-band voltage spike, a set of adjoining pulsed beams of different frequencies will be produced along the y dimension of the tapered element, as illustrated in Fig. 4. Discontinuities along the path of each beam will create echoes at corresponding frequencies. The received signal will then consist of a summation of echoes of varying frequency from all of the transmitted beams. Post-reception processing of the received signal could differentiate the position of the echoes in the y dimension through the use of bandpass filtering.

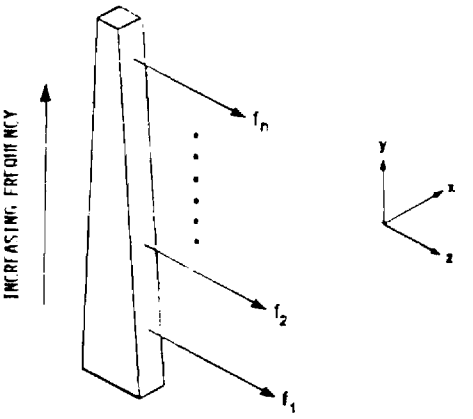

Fig. 4 Spatial frequency response of a tapered element to a broad-band pulsed excitation.

The lateral and axial resolution could be significantly improved in this proposed system if the phase of each transmitted beam were controlled. To focus the beams along a line in the y direction would require the phases (delays) of every frequency component of the signal driving each element to be adjusted so that all of the resulting beams arrive at the desired focal region simultaneously. Figure 5 is a plot of the theoretical spatial response, in the y dimension, of a 64-element tapered phased array driven by a pulse consisting of four frequency components. The four frequency components were phased so that each would be focused at a distance of 5 cm from the array. Each of the peaks in the profile corresponds to one of the four frequency components in the pulsed excitation signal.

DISCUSSION

The obvious advantage of this frequency scanning technique is that it would enable an entire plane (y-z) to be scanned using a single pulse. This would allow a plane to be interrogated at a rate much faster than is currently possible with conventional phased arrays that require multiple pulses to scan a plane. This technique, with the addition of beam steering, would also allow a large number of adjacent planes to be scanned, thereby enabling the formation of a three-dimensional image.

There are several potential limitations to this frequency scanning technique. The characteristics of scattering objects such as reflectivity and attenuation are dependent on the frequency of the

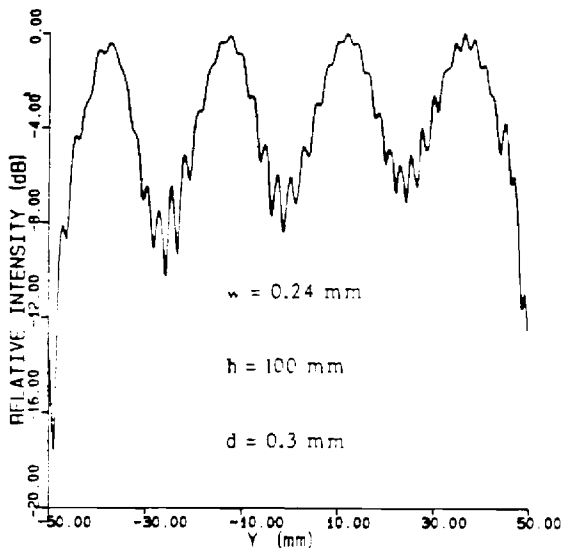

Fig. 5 Theoretical field profile in the y dimension (x=0, z=50 mm) of a 64-element TPA pulsed with an excitation signal with four frequency components (f_1=2.13 MHz, f_2=2.38 MHz, f_3=2.63 MHz, f_4=2.88 MHz).

ultrasonic pulse. Therefore, the amplitudes of the return echoes will be dependent not only on the position and composition of the scatterer, but also the frequency of the incident pulse. These effects can be kept to a minimum if the range of frequencies used is not large.

The resolution in both the lateral and axial dimensions is also a limiting factor. Since the phases of the signals that drive the elements of the array are frequency dependent, a reduction in both the lateral and axial resolution can be expected when using the frequency scanning technique unless each frequency component of the excitation pulse has the proper phase. The resolution in the axial dimension may be reduced if the Q of the tapered element is not low enough to produce the desired acoustical pulse duration.

CONCLUSIONS

A theoretical analysis of a TPA transducer operating in the pulse-echo mode suggests that it is capable of scanning targets at a rate much faster than is possible with conventional phased arrays. In addition, the TPA can provide a 2-D phased array capability that is not yet possible with conventional arrays. Thus, this analysis indicates that pulse-echo TPA transducers warrant further study.

ACKNOWLEDGEMENTS

The author wishes to thank Eugene Goff for his technical assistance. The partial support of this study by The Whitaker Foundation is gratefully ackowledged.

REFERENCES

[1] Benkeser, P. J., L. A. Frizzell, K. B. Ocheltree, and C. A. Cain, "A tapered phased array ultrasound transducer for hyperthermia treatment," IEEE Trans. Ultrasonics, Ferroelectrics, and Frequency Control (in press) 1987.

[2] Benkeser, P. J., "Unfocused multielement and tapered phased array ultrasound transducers for hyperthemia treatment," Ph.D. thesis, Univ. of Illinois at Urbana-Champaign, 1985.

[3] Ocheltree, K. B., P. J. Benkeser, L. A. Frizzell, and C. A. Cain, "An ultrasonic phased array applicator for hyperthermia," IEEE Trans. Son. and Ultrason., Vol. SU-31, pp. 526-531, 1984.

[4] Von Ramm, O. T., and S. W. Smith, "Beam steering with linear arrays," IEEE Trans. Biom. Engr., Vol. BME-30, No. 8, pp. 438-452, 1983.

ANALYSIS OF A PULSE-ECHO ULTRASOUND TAPERED PHASED ARRAY TRANSDUCER

P.J. Benkeser, E.F. Goff, and W.O. Rice

School of Electrical Engineering, Georgia Institute of Technology
Atlanta, Georgia, 30332, USA

The tapered phased array (TPA) transducer consists of a linear array of piezoelectric ceramic elements that are inherently broad-band because of their tapered thickness. In this paper, the TPA transducer operating in the pulsed mode will be examined to determine its potential for use in imaging applications. A TPA transducer was constructed in order to verify a theoretical model of its radiation pattern. The results of comparisons of the theoretical and experimental radiation patterns suggest that when the elements are pulsed with the appropriate signals, a linearly aligned group of focused beams at different frequencies will be produced. This group of focused beams can be used to provide a high-resolution two-dimensional phased array capability for a pulse-echo imaging system.

INTRODUCTION

A two-dimensional phased array can generate and position a focused beam in three dimensions by controlling the phases of the signals driving each array element so that constructive interference of the waves is achieved at the desired field point. However, a two-dimensional phased array is too costly and complex for most imaging applications due to the large number of elements and associated circuitry that are required. Most conventional phased array transducers are of the linear (one-dimensional) type which allow the focus to be scanned over a two-dimensional path.

A new type of phased array, a tapered phased array (TPA) has been recently developed for use in ultrasound hyperthermia [1]. This transducer consists of a linear phased array composed of elements that have a tapered thickness, as illustrated in Fig. 1. The frequency response of these elements, due to their tapered thickness, is inherently broad-band. The region along the length of the element that has a thickness resonant at the frequency of the driving signal will produce the greatest acoustical power output. Therefore, the TPA can sweep the focal region in three dimensions by controlling the phases and frequency of the continuous wave (cw) signals driving each element. This array has the square root of N elements compared with N elements for a two-dimensional array with the same center-to-center spacing of elements.

The purpose of this paper is to report on some initial results of the development of a TPA transducer for pulse-echo imaging applications. The design of the transmit and receive circuitry required by the TPA transducer will also be discussed.

THEORY

The tapered element can be modeled using a parallel network of the simplified Mason's equivalent circuit for a lossless piezoelectric transducer near resonance [1]. This model is accurate for narrow frequency bandwidths where the near resonance approximation holds over the entire length of the tapered element. This model was incorporated into a computer program [2] to calculate the field intensity distribution produced by a TPA.

If a tapered element of an array was driven by a single broad-band voltage pulse, like those used to drive elements of conventional linear arrays, a set of adjoining pulsed beams of different

frequencies will be produced along the y dimension of the tapered element, as illustrated in Fig. 2. Discontinuities along the path of each beam will create echoes at corresponding frequencies. The received signal will then consist of a summation of echoes of varying frequency from all of the transmitted beams. The frequency of the received echoes can be used to discern the y-position of the reflector(s).

However, in order to achieve the best possible lateral and axial resolution in a TPA, the phases (delays) of all frequency components of the signals driving each element would have to be controlled so that all of the resulting beams arrive at the desired focal region simultaneously.

METHODS AND RESULTS

In order to experimentally verify the theoretical performance of a TPA transducer, a 16-element TPA was constructed. The piezoelectric ceramic elements were 101.6 mm in length, 2.1 mm in width, and had a tapered thickness ranging from 2.3 mm to 4.1 mm. These element dimensions were chosen to simplify the fabrication of the transducer for this pilot study and do not necessarily represent optimal dimensions for imaging applications. The elements were mounted in an anodized aluminum housing and were air-backed. A thin mylar sheet covered the front faces of the elements and served to keep the housing water-proof.

All acoustical field measurements were made in an ultrasonic beam observation tank (Medsonics Model ME104) using a 1 mm diameter PVDF hydrophone probe. These measurements were plotted as relative intensity (in dB) versus position.

Figures 3 and 4 compare the theoretical and experimental field profiles of an element of the TPA, in the y dimension, when driven by a 450 kHz and a 500 kHz cw signal, respectively. These figures are typical of the good agreement obtained between the experimental results and theoretical predictions.

Figure 5 illustrates the theoretical field profile of the TPA when driven by a pulse consisting of the two properly phased frequency components used in Figs. 3 and 4. Each of the peaks in this figure corresponds to one of the two frequency components in the pulsed excitation signal. Such phasing of the individual frequency components of the pulses will be required for high resolution imaging.

DISCUSSION

An advantage of using the TPA in this pulsed "frequency scanning" mode is that it would enable the y-z plane to be scanned using a single pulse at a rate much faster than is currently possible with conventional phased arrays. This technique, with the addition of beam steering, would also allow a large number of adjacent planes to be scanned, thereby enabling the formation of a three-dimensional image.

There are several potential limitations to this approach. The characteristics of scattering objects such as reflectivity and attenuation are dependent on the frequency of the ultrasonic pulse. Therefore, the amplitudes of the return echoes will be dependent not only on the position and composition of the scatterer, but also the frequency of the incident pulse. These effects can be kept to a minimum if the range of frequencies used is not large.

Figure 6 is a block diagram of the hardware currently being developed to control the TPA. The transmit portion of the controller will employ fast D to A converters and broad-band pulse drivers to produce the desired excitation signals. The receiver portion of the controller will implement a technique of time expansion which employs simple microcomputer control and low-cost A to D converters [3]. The received signals from the array elements will be captured at a high rate using CCD delay lines. The signals will then be released at a lower rate, digitized by A to D converters, and subsequently stored in the microcomputer's memory. Digital signal processing techniques will then be used to bandpass filter and supply appropriate delays for dynamic focusing of the frequency encoded data in order to form the image.

CONCLUSIONS

An analysis of a TPA transducer operating in the pulse-echo mode suggests that it can provide a 2-D phased array capability that is not yet possible with conventional arrays. Further work is required in the development of the transmit and receive hardware for the TPA before a complete assessment of its potential can be made.

ACKNOWLEDGEMENTS

The partial support of this study by the Whitaker Foundation is gratefully acknowledged.

REFERENCES

1 Benkeser, P.J., L.A. Frizzell, K.B. Ocheltree, and C.A. Cain, "A tapered phased array ultrasound transducer for hyperthermia treatment," IEEE Trans. Ultrason. Ferroelect., and Freq. Cont., vol. UFFC-34, no. 4, 1987 (in press).

2 Ocheltree, K.B., P.J. Benkeser, L.A. Frizzell, and C.A. Cain, "An ultrasonic phased array applicator for hyperthermia," IEEE Trans. Son. and Ultrason., vol. SU-31, no. 5, pp. 526-531, 1984.

3 Campbell, M.A., G. Hayward, and A. McNab, "A novel approach to ultrasonic data acquisition," Proc. 1985 Ultrasonics International Conf., pp. 523-527, 1985.

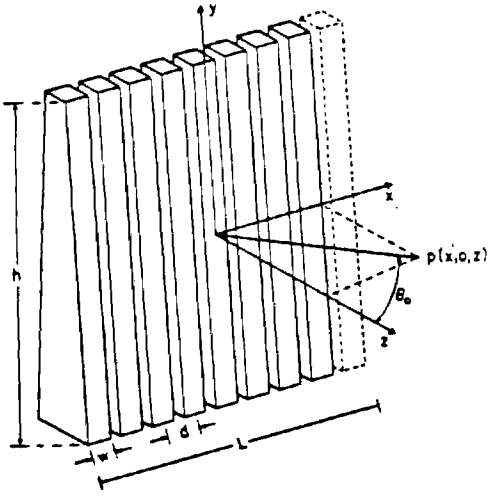

Fig. 1 Tapered Phased Array (TPA)

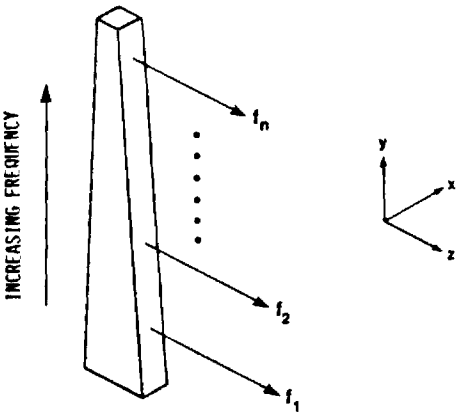

Fig. 2 Spatial frequency response of a tapered element to a broad-band pulsed excitation

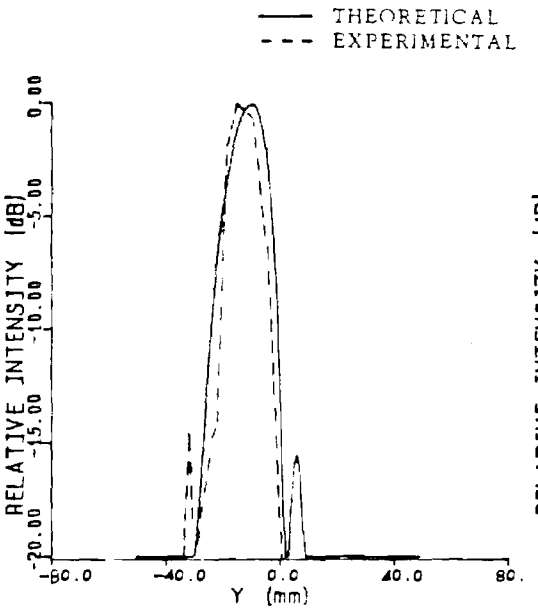

Fig. 3 Field profile of a tapered element (x = 0, z = 50 mm, f = 450 kHz)

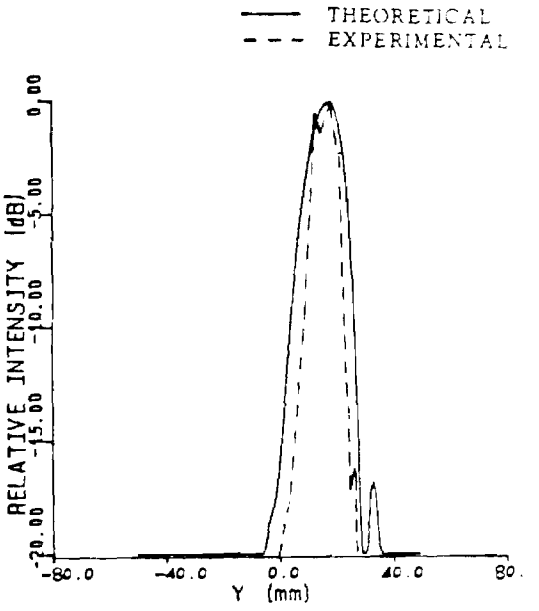

Fig. 4 Field profile of a tapered element (x = 0, z = 50 mm, f = 500 kHz)

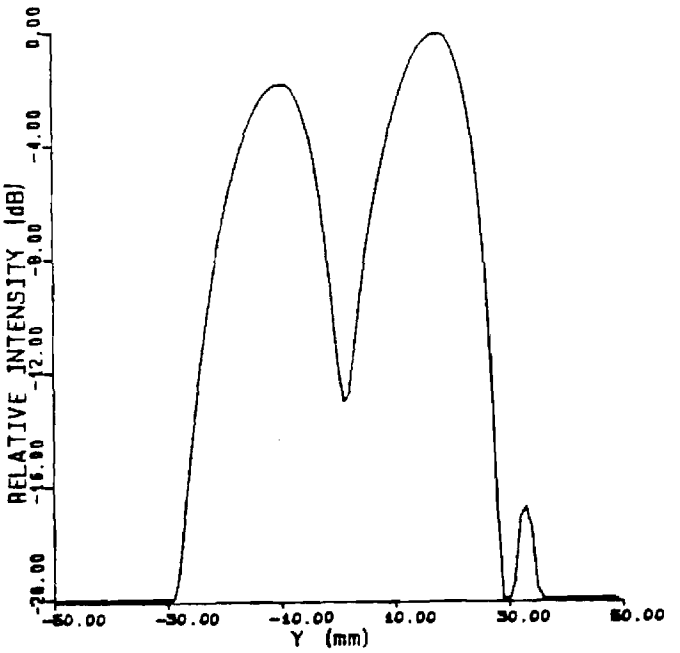

Fig. 5 Theoretical field profile of the TPA pulsed with an excitation signal with two frequency components (f_1 = 450 kHz, f_2 = 500 kHz)

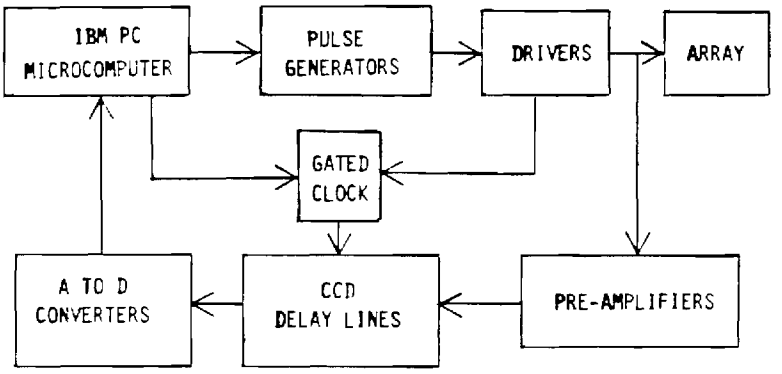

Fig. 6 TPA controller block diagram

A STAIRCASE MODEL OF TAPERED PIEZOELECTRIC TRANSDUCERS*

P. G. Barthé and P. J. Benkeser
School of Electrical Engineering
Georgia Institute of Technology
Atlanta, Georgia 30332-0250

ABSTRACT

A classic trade-off in the design of thickness mode piezoelectric transducers for pulse-echo imaging has been increased bandwidth at the cost of decreased sensitivity through the use of backing materials. However, a multiple resonance, tapered-thickness piezoelectric ceramic does not require a backing material to make it broadband. A new model is presented for the analysis of tapered ceramics where the thickness gradient is represented as a series of discrete steps. Each step is, in turn, represented by an appropriate model which contributes to the net transducer response. The theoretical results obtained using this staircase model will be presented and shown to agree well with experimentally obtained data from a tapered piezoelectric ceramic transducer.

I. Introduction

A piezoelectric ceramic with a linearly tapered thickness has been shown to exhibit an inherently broadband frequency response [1-4]. Several investigators have examined the potential of using such tapered ceramics in pulse-echo imaging transducers [5,6,7]. They found that transducers using tapered ceramics do not require lossy backing materials to achieve the desired bandwidth and are thus simpler to fabricate. However, no simple theoretical model exists which adequately describes the response of such a transducer.

Vibrations of piezoelectric crystals with contoured dimensions were first studied during development of ultrasonic delay lines [1,2]. In general, this research employed mathematical solutions of the elasticity equations with boundary conditions to describe coupled-mode vibrations in quartz. Applications were limited because of the focus and complexity of analysis and because results were not in a form suitable for modeling pure-mode devices. The ceramic tapered bar transducer has been examined with a similar approach in longitudinal and shear wave devices [3,4].

The theoretical modeling of the tapered bar transducer was also approached as a study of response errors induced by an uneven device thickness [8]. A novel approach was used in which a single model was obtained by integrating over a transducer surface area composed of smaller models. This is similar to the new model developed herein except that the results from several model steps are combined rather than combining models to obtain a result. Hence, no integration is necessary.

In this paper, the thickness gradient of a tapered piezoelectric transducer is represented as a sequence of discrete steps. Each step is, in turn, represented by an appropriate model which contributes to the net response. The staircase approach is detailed along with input impedance and convergence considerations. The theory is verified through comparisons with experimental results obtained from a tapered bar transducer.

II. THEORY

A. Staircase Model Approach

A description of devices in the form of the staircase model is presented in this section. A tapered bar transducer is shown in Fig. 1. The thickness varies linearly from L_{min} to L_{max} in the poling or z-direction. The device has a length T in the x-direction, and a width W in the y-direction.

Consider the device divided into N equal sections along the x-axis. Each element located at position x_i, for $i = 1,2,\ldots,N$, can be modeled as a separate transducer. The position x_i may be described as

$$x_i = \left(i - \frac{1}{2}\right)\Delta x \,, \qquad (1)$$

where

$$\Delta x = \frac{T}{N}$$

is the length of each section. The width of each element remains W, while the thickness of each section is represented by its average thickness which is simply the thickness of the transducer at $x = x_i$. Hence, the thickness of the i-th section, L_i, may be expressed as

$$L_i = L_{min} + x_i \tan\theta \qquad (2)$$

where

$$\tan\theta = \frac{L_{max} - L_{min}}{T} \,,$$

and θ is the angle the sloped transducer face makes with the x-axis. Since the region of stress generation is along the thickness center of the

*This work was supported by The Whitaker Foundation.

0090-5607/87/0000-0697 $1.00 © 1987 IEEE

tapered bar, the generated waves will be at an angle of θ with the x-axis.

The power of this approach is that models which are well defined in the literature may now be used to represent the individual steps.

B. Electric Input Impedance

The electric input impedance of an electromechanical transducer is of fundamental importance in the analysis and design of transducers and their associated systems. The input impedance for a thickness-mode device may be expresaed as [9]

$$Z_{IN} = \frac{1}{j\omega C_o}\left[1 + K_T^2 \frac{j(Z_1+Z_2)Z_c \sin\phi - 2Z_c^2(1-\cos\phi)}{\phi[(Z_c^2+Z_1Z_2)\sin\phi - j(Z_1+Z_2)Z_c\cos\phi]}\right] \quad (3)$$

where Z_1, Z_c, and Z_2 are the front (flat) surface acoustic impedance, the ceramic characteristic acoustic impedance, and the back (tapered) surface acoustic impedance, respectively; C_o is the clamped capacitance of the transducer; K_T is the clamped electromechanical coupling factor; ω is the angular input frequency; and ϕ is a frequency-dependent phase angle.

For a tapered transducer in the staircase form, the input impedance can be expressed in terms of the input admittance Y_{IN} such that

$$Y_{IN} = \sum_{i=1}^{N} Y_i \quad (4)$$

where for each $Y_i = 1/Z_i$ we have

$$C_{o_i} = \frac{WT\varepsilon^s}{NL_i} \quad (5)$$

and

$$\phi_i = \frac{\omega}{\overline{V}_a} L_i \,. \quad (6)$$

In the last two equations, ε^s is the clamped permittivity of the ceramic and $\overline{V}_a$ is its piezoelectrically stiffened acoustic wave velocity. Calculating the input impedance of a tapered device therefore reduces to obtaining the input admittance of each element, summing, and inverting the final result. Obviously, these calculations are well suited for a computer. However, a value of N must be chosen to assure negligible error. Above N steps little will be gained in terms of accuracy and computation time would only increase.

C. Number of Steps and Convergence

Guidelines for choosing a sufficient number of steps for a transducer configuration may be obtained from further analysis of device admittance.

The following relationship can be used to determine the number of steps required to minimize the error:

$$\lim_{i \to N_{min}} \frac{\partial Y_{IN}}{\partial i} \to 0 \quad (7)$$

where N_{min} represents the lowest acceptable N. This can be further simplified by noting that

$$\frac{\partial Y_{IN}}{\partial i} = \frac{\partial Y_{IN}}{\partial L_i} \cdot \frac{\partial L_i}{\partial i} \,. \quad (8)$$

Equations (1)-(8) provide the solution to (7) based on the tranaducer configuration embedded in $\partial Y_{IN}/\partial L_i$.

The relative deviation between using a large N and small n may be quantified with the percent root mean square deviation, Δ. The error is evaluated between the frequencies of interest, f_{min} and f_{max}, and may be expressed for impedance magnitude as

$$\Delta = \left[\frac{1}{N}\sum_{f=f_{min}}^{f_{max}}\left[\frac{Z_{IN(N)} - Z_{IN(n)}}{Z_{IN(N)}}\right]^2\right]^{\frac{1}{2}} \,. \quad (9)$$

III. EXPERIMENTAL RESULTS

Experimental measurements were made on a tapered bar transducer using a vector impedance meter. The transducer's dimensions were W = 2.01 mm wide, L = 101.3 mm long, and L_{min} = 2.79 mm to L_{max} = 4.07 mm thickness. A quasi-longitudinal mode model was chosen for the N steps since the thickness of the device was comparable to its width. Under these conditions, the device does not operate in a pure thickness mode. This requires the use of effective constants in the thickness-mode model [10,11]. The device was composed of Channel C5800 material, with an unstiffened acoustic wave velocity V_a = 3100 m/s, dielectric constant $\varepsilon^s/\varepsilon_o$ = 1100, density ρ = 7550 kg/m^3, and parallel longitudinal mode coupling factor of $K_p = K_{33}$ = 0.67. The effective coupling coefficient, K_{eff}, was chosen as 0.63 for the transducer dimensions. The effective dielectric permittivity was then $\varepsilon^s_{eff} = 1100(1-K^2_{eff})\varepsilon_o$ = 663 ε_o. The effective acoustic impedance was Z^o = 29.8 MRayl. This data was used to simulate the input impedance and convergence with N of the impedance magnitude.

A computed simulation in Fig. 2 shows that the approximation error does approach zero for increasing N. The errors are large because this is the total error over an entire frequency band (400-800 KHz in this example). Since the curve leveled at N = 512, a value of N = 500 was used in the following input impedance simulations.

Figures 3 and 4 compare the theoretical and experimental plots of the transducer's input impedance magnitude and phase in air, respectively. These plots indicate multiple resonances between 400 to 580 KHz. At approximately 625 KHz, the transducer is resonant at its narrow thickness, L_{min}. Above this frequency, the device passes out of a region of stiffness control and is no longer resonant.

Figures 5 and 6 compare the theoretical and experimental plots of the input impedance magnitude and phase, respectively, with air backing and a water load. These figures demonstrate that the transducer is inherently broadband in nature. The linear phase characteristic in Fig. 6 implies a distortionless time or impulse response.

IV. CONCLUSION

A new staircase model has been developed to characterize tapered transducers. The input impedance of tapered devices has been discussed along with model convergence considerations. The theoretical approach agrees well with empirically obtained data from an tapered transducer.

REFERENCES

[1] J.L. Bleustein, "Thickness-Twist and Face-Shear Vibrations of a Contoured Crystal Plate," Inter. Jour. Sol. Struct., vol. 2, 1966, pp. 351-360.

[2] C.B. Loutzenheiser and W.J. Denkmann, "Thickness/Twist Vibrations of a Truncated, Linearly Tapered, Crystal Strip," Jour. Acou. Soc. Am., vol. 41, pt. 2, no. 4, 1967, pp. 962-966.

[3] B.N. Alekseev, D.B. Dianov, and S.P. Karuzo, "Tapered-Bar Transducer," in Proceedings of the Eighth All-Union Acoustics Conference [in Russian], Moscow, 1973.

[4] B.N. Alekseev, D.B. Dianov, and S.P. Karuzo, "Tapered Piezoelectric Bar Transducer with Transverse Polarization of the Piezoceramic," Sov. Phys. Acou., vol. 23, no. 1, 1977, pp. 1-4.

[5] T. Kobayashi, "Wedged Ultrasonic Transducers Having Thickness Extensional Vibration," Jour. Acou. Soc. Jpn. [in Japanese], vol. 38, no. 10-12, 1982, p. 748.

[6] Y. Tomikawa, H. Yamada, and M. Onoe, "Wide Band Ultrasonic Transducer Using Tapered Piezoelectric Ceramics for Non-Destructive Inspection," Jpn. Jour. Appl. Phys., vol. 23, suppl. 23-1, 1984, pp. 113-115.

[7] P.J. Benkeser, "A Pulse-Echo Ultrasound Tapered Phased Array Transducer," Proc. 13th NE Bioengineering Conf., pp. 286-288, 1987.

[8] Y. Jayet, M. Perdrix, and R. Goutte, "Effects on the Damping of Ultrasonic Transducers Due to a Lack of Parallelism in the Piezoelectric Element," Ultrasonics, vol. 21, no. 4, 1983, pp. 179-183.

[9] G. S. Kino, Acoustic Waves, Devices, Imaging, and Analog Signal Processing, New York: Prentice Hall, 1987, p. 32.

[10] R.B. Coursant, C. Méquio, and P. Pesqué, "Simulation of the Acousto-Electric Response of Ultrasonic Narrow Strip Transducers with Mechanical Losses," Ultrasonics International 83, Conference Proceedings, Halifax, Canada, July 12-14, 1983, pp. 414-419.

[11] J. Sato, M. Kawabuchi, and A. Fukumoto, "Dependence of the Electromechanical Coupling Coefficient on the Width-to-Thickness Ratio of Plank-Shaped Piezoelectric Transducers used for Electronically Scanned Ultrasound Diagnostic Systems," Jour. Acoust. Soc. Am., vol. 66, no. 6, 1979, pp. 1609-1611.

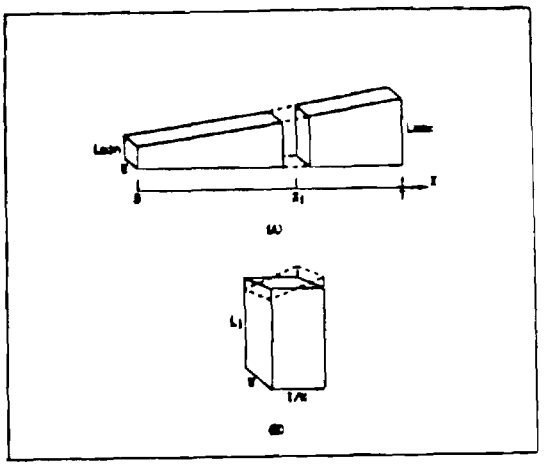

Fig. 1. Staircase model approximation of a tapered bar transducer (a) with close-up of the i-th step (b).

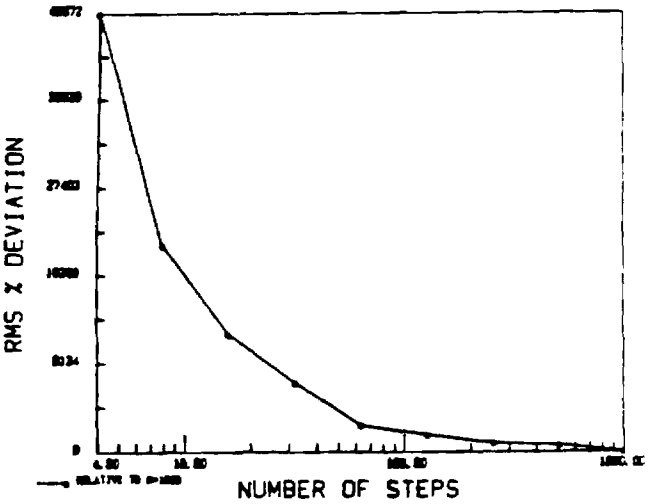

Fig. 2. Convergence of impedance magnitude with increasing number of steps relative to N=1000.

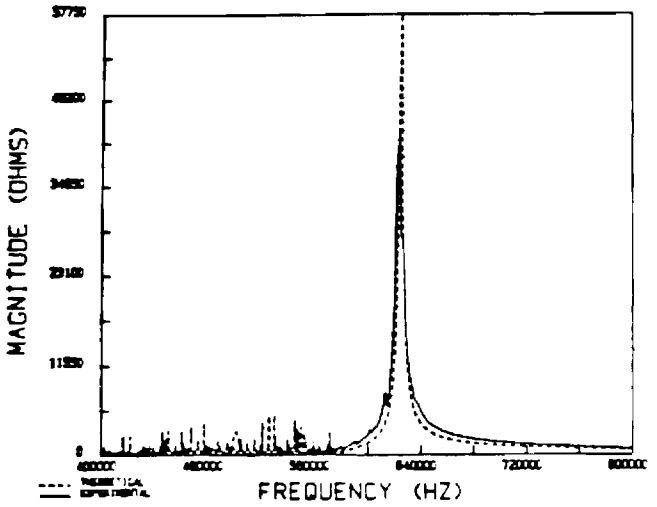

Fig. 3. Comparison of simulated and measured input impedance magnitude in air.

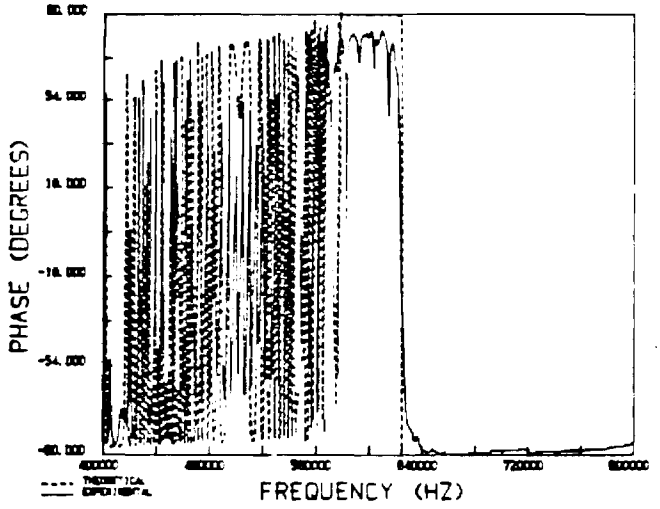

Fig. 4. Comparison of simulated and measured input impedance phase in air.

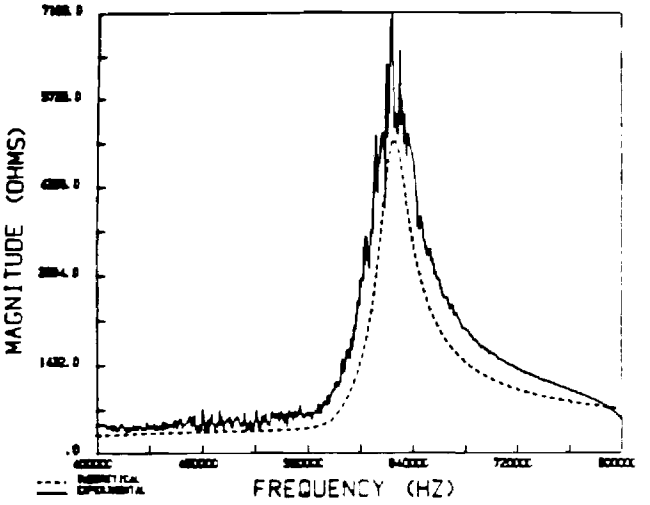

Fig. 5. Comparison of simulated and measured input impedance magnitude with Z_1(flat face)=water, and Z_2=air.

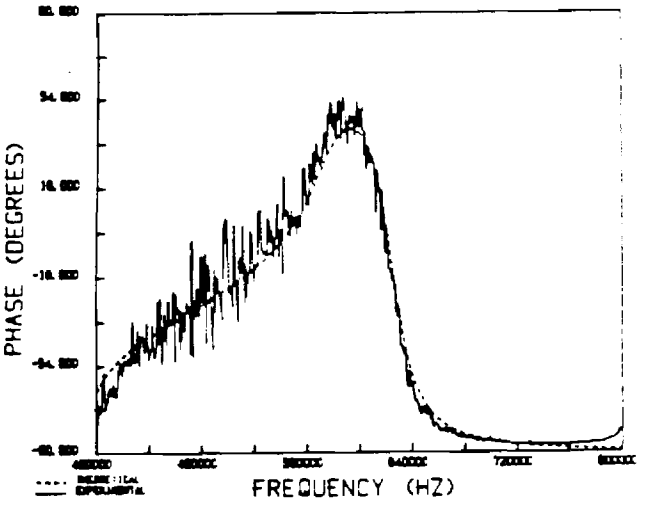

Fig. 6. Comparison of simulated and measured input impedance phase with Z_1(flat face)=water, and Z_2=air.

ANALYSIS OF THE MECHANICALLY-UNCOUPLED ELECTRIC RESONANCE IN TAPERED-THICKNESS PIEZOELECTRIC TRANSDUCERS*

P.G. Barthé and P.J. Benkeser
School of Electrical Engineering
Georgia Institute of Technology
Atlanta, Georgia 30332-0250

ABSTRACT

Tapered-thickness piezoelectrics have been studied for use in novel devices and imaging techniques, such as wideband transducers and frequency-controlled beam-translation. These tapered devices exhibit a resonance peak in the electric input impedance, but no corresponding peak in the transmit response of the device. In this paper, a previously developed staircase model of tapered piezoelectrics will be used to show that unlike conventional transducers, which are either mass-controlled below resonance or stiffness-controlled above resonance, thickness tapering produces periodically alternating regions of mass-control and stiffness-control along the length of a device. Interaction between these mass and stiffness regions contribute to a resonance peak in the electric input impedance which is shown not to be coupled to the distributed half-wavelength resonances of the device. The theoretical pulse response obtained with the model is shown to be in close agreement with the measured wideband, uniform amplitude pressure profile of a tapered piezoelectric transducer.

I. INTRODUCTION

Tapered-thickness piezoelectrics have been studied to characterize their performance in novel devices and imaging techniques. A survey of these studies appears in [1]. In conventional constant-thickness piezoelectrics, a sharp impedance resonance implies a relatively narrow-band transmit response. However, tapered devices exhibit a resonance peak in the electric input impedance [1], [3], yet possess a broadband, uniform-amplitude transmit response [2], [3]. In this paper a staircase model representation of a tapered piezoelectric will be used to characterize this effect. Using undamped equivalent circuit models for each step (section) along the device, and canonical electroacoustic impedance and admittance representations, it is shown that different portions of a tapered piezoelectric may be under mass or stiffness control. This is unlike the case for constant thickness device. The operation of a tapered device may be described as several local resonances acting alone, and a resonance peak which results from their union. The location of the resonance peak is found from the shunt motional and blocked admittances of the tapered device. This theory gives physical insight into the electrical and mechanical dynamics of tapered transducer operation. Experimental verification of this theory is provided. The impedance concepts are verified, and the pulse response of a tapered ceramic transducer is simulated with the staircase model. The results are shown to be in close agreement with the measured broadband, uniform amplitude pressure profile.

*This work was supported by The Whitaker Foundation.

II. THEORY

A. Conventional Transducer Electrical and Mechanical Characteristics

The theoretical development is facilitated with the use of Mason's model [4] of a lossless, thickness-mode piezoelectric transducer under no external damping, as shown in Fig.1(a). Parameters are $C_0 = \epsilon^s A/\ell$, $f_0 = \bar{V}_a/2\ell$, and $Z = A\rho\bar{V}_a$. The constants ϵ^s, $\bar{V}_a = V^D$, ρ, and h are standard piezoelectric material values; the transducer area is A and thickness, ℓ.

The condition of no external damping is strictly met in vacuum, but effectively satisfied when the ratio of load impedance (such as air) to piezoelectric impedance is close to zero. The equivalent circuit in Fig.1(b) may be obtained by combining impedances on the secondary side of the ideal transformer and reflecting the impedance to the primary circuit. The result is the standard, or canonical form of a transducer's admittance.

The canonical impedance representation of Fig.1(c), and admittance representation of Fig.1(d) are defined by [5]

$$Z_{ee} = Z_e + Z_{\text{mot}} \tag{1}$$

and

$$Y_{ee} = Y_e + Y_{\text{mot}} \tag{2}$$

where

$$Y_{ee} \equiv \frac{1}{Z_{ee}}, \text{ and } Y_e \equiv \frac{1}{Z_e}. \tag{3}$$

It is imperative to note that once the definitions in Eq.(3) are employed $Y_{\text{mot}} \neq 1/Z_{\text{mot}}$ in general, but in fact

$$Y_{\text{mot}} = \frac{-1}{Z_e + \frac{Z_e^2}{Z_{\text{mot}}}}, \tag{4}$$

as a result of combining Eqs.(1)-(3). In the equations above, the electric input impedance, or total impedance is represented by Z_{ee} the blocked impedance by Z_e and motional impedance by Z_{mot}. Corresponding admittances are defined in the same manner. If the surface motion of a transducer is supressed (or negligible, as is the case well below resonance) the electric impedance measured at its terminals is the blocked impedance, Z_e. Therefore Z_e represents the

0090-5607/88/0000-0717 $1.00 © 1988 IEEE

purely electric aspect of a transducer. In a lossless dielectric medium such as a piezoelectric the blocked impedance is represented by the clamped capacitance, C_0 of Mason's model,

$$Z_e = 1/j\omega\, C_0\ . \tag{5}$$

Conversely, the motional impedance represents the mechanical dynamics of a transducer. It is an electric quantity by virtue of electromechanical transduction factors introduced by the piezoelectric effect. For the lossless, unloaded transducer model described above, the motional impedance simplifies to

$$Z_{\text{mot}} = \frac{-k_T^2}{j\omega C_0}\ \frac{\tan\left(\frac{\pi f}{2f_0}\right)}{\left(\frac{\pi f}{2f_0}\right)}\ , \tag{6}$$

where k_T is the thickness-mode electromechanical coupling factor. The motional impedance is purely imaginary in this case because no acoustic radiation occurs in the unloaded condition.

The sign (+, -, or zero) of the $\tan(\pi f/2f_0)$ factor in Eq. (6) determines the physical character of the motional impedance. When $0 < f < f_0$, Z_{mot} is a $+j$ quantity. Using the inductance-mass, capacitance-reciprocal stiffness analogy [6] it is evident that the transducer is mass-controlled below resonance. Over the region $f_0 < f < 2f_0$ the transducer is stiffness-controlled. As the resonant frequency is approached, that is $f \rightarrow f_0$ or odd-multiples thereof, $Z_{\text{mot}} \rightarrow \pm j\infty$. This is the case of mechanical resonance characterized by an impedance maximum in $|Z_{ee}|$. Because of the odd-harmonic resonances present in the piezoelectric transducer, the mass-control/stiffness-control regions are also periodic with f.

In a compact description, the regions are

Mass control:

$$mf_0 < f < (m+1)f_0\ ,\ \text{for } m = 0, 2, 4, \ldots \tag{7a}$$

Stiffness Control:

$$(m+1)f_0 < f < (m+2)f_0\ ,\ \text{for } m = 0, 2, 4, \ldots \tag{7b}$$

These impedance/admittance and mass/stiffness representations may be extended to tapered transducers to obtain physical insight about their operation.

B. Tapered-Thickness Transducer Electrical and Mechanical Characteristics

A tapered piezoelectric transducer may be accurately represented by a staircase composed of N steps of discrete-thickness transducers [1]. Because each step may be represented with Mason's model, and each step is electrically in parallel, the equivalent circuit models in Fig.2(a) and (b) may be obtained. The local mechanical resonant frequencies of each step, f_{oi}, $i = 1 \ldots, N$ of a tapered device will extend from $f_{oN}(f_{\min})$ at the transducer's thick end, $(L_{\max})$, to $f_{01}(f_{\max})$ at the transducer's thin end, $(L_{\min})$. At some frequency f, where $f_{\min} < f < f_{\max}$, portions of the transducer will be above resonance, and others below resonance. If $L_{\max}/L_{\min} \leq 2$ the situation reduces mass-control at the narrow end below resonance, and stiffness-control at the thick end above resonance. In the admittance domain of Fig. 2(b), the values of $Y_{\text{mot (i)}}$ are given directly by Eq (4) and are not, in general, inductive or capacitive susceptances. When the net shunt motional admittance, $\sum_{i=1}^{N} Y_{\text{mot (i)}}$ is inductive, a parallel resonance with C_0 will occur creating an impedance maximum at some frequency, henceforth called f_0. However, this resonance is not a conventional mechanical resonance in that portions of the transducer remain partitioned under both mass and stiffness control. The series impedance of $Z_{e(i)}$ and $Z_{\text{mot (i)}}$ for $i = 1, \ldots, N$ that determines a local mechanical resonance f_{oi} is unaffected or in other words, mechanically-uncoupled to the macroscopic resonance effect created by shunting several devices. The local resonances do not create the impedance maximum because at any frequency within the passband of the device, $Z_{ee(i)}$ is in shunt with non-resonant, low-impedance transducer sections.

In summary, for an unloaded transducer the local mechanical resonances are related by $f_{\max}/f_{\min} = L_{\max}/L_{\min}$, and for the thickness ℓ_i, $f_{oi} = \bar{V}_a/2\ell_i$. The major resonance occurs when the net Y_{mot} resonates with Y_e.

C. Location of Electric Impedance Maximum

The location of the impedance maximum at f_0 is found by evaluating Y_{mot} and Y_e. This may be accomplished by direct integration, or by using the staircase formulation. Proceeding with the former, Fig. 3 represents the boundary conditions for a general, linear-tapered piezoelectric with angle θ, length T, width W and thickness $L_{\min}$ to $L_{\max}$, and $\tan(\theta) = (L_{\max} - L_{\min})/T$. Using Eqs. (4)-(6), the motional admittance at constant ω for the tapered piezoelectric along x between ℓ_a and ℓ_b (corresponding to x_a and x_b) can be shown to be

$$Y_{\text{mot}} = \frac{j\omega\varepsilon' W}{\tan\theta}\ \int_{u_a}^{u_b} \left[\frac{1}{\frac{u}{k_T^2}\cot u - 1}\right]\frac{du}{u} \tag{8}$$

using the substitution of variable,

$$u \equiv \frac{\omega x}{2\bar{V}_a}\tan\theta \tag{9}$$

The blocked admittance can be found, using Eq. (9), to be

$$Y_e = \frac{j\omega\varepsilon' W}{\tan\theta}\ \int_{u_a}^{u_b}\frac{du}{u}\ =\ \frac{j\omega T_{ab}\varepsilon' W}{(\ell_a - \ell_b)}\ \ln\left(\frac{\ell_b}{\ell_a}\right) \tag{10}$$

where T_{ab} represents the length of the transducer between x_a and x_b. The alternative to using numerical integration in Eq. (8) is to use the staircase approach with N discrete transducer steps, and adding the motional admittances of each step. The model in Fig. 1(b) or Eqs. (4)-(6) give Y_{mot} per step. The shunt admittance resonance represents $Y_{\text{mot}} + Y_e \rightarrow 0$. The analysis so far has indicated if f_0 is in the passband of the tapered transducer, that is, $f_{\min} < f_0 < f_{\max}$, it should not interfere with the local resonances.

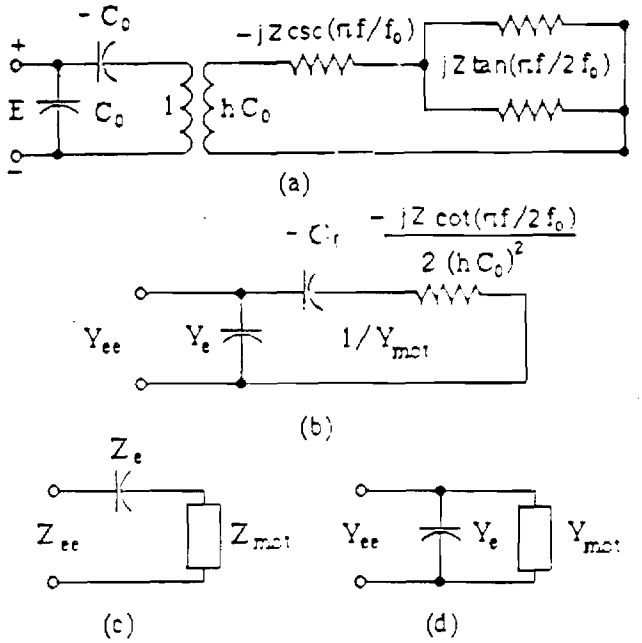

Fig. 1. (a) Undamped Mason's model, (b) transformed equivalent circuit, (c) canonical impedance and (d) admittance representation.

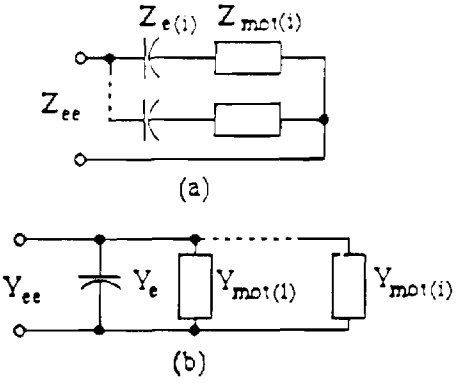

Fig. 2. (a) Canonical impedance representation of N-step staircase model, and (b) admittance representation.

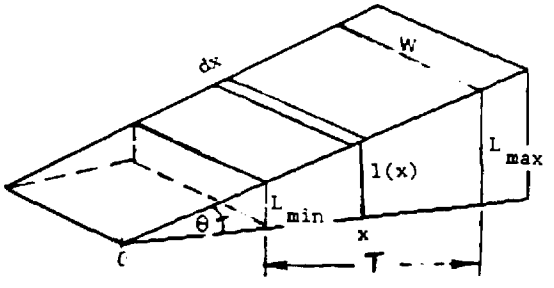

Fig. 3. Boundary conditions for general, linear-tapered piezoelectric used for admittance calculations.

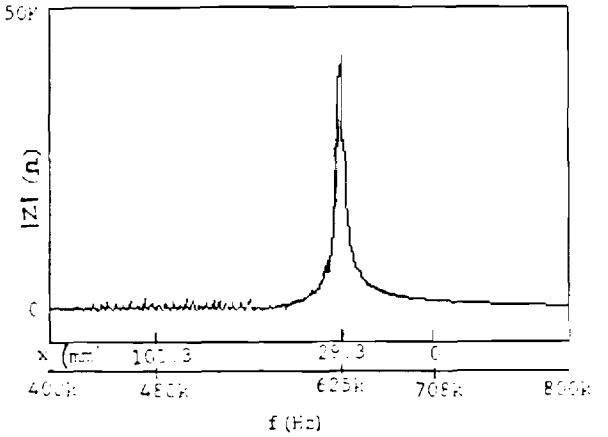

Fig. 4. Measured input impedance of tapered piezoelectric bar showing local resonant regions, and major resonance at 625KHz.

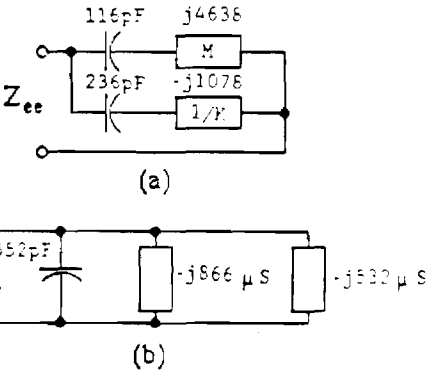

Fig. 5. (a) Impedance representation of tapered bar at 625KHz showing equivalent mass and stiffness regions, and (b) admittance formulation.

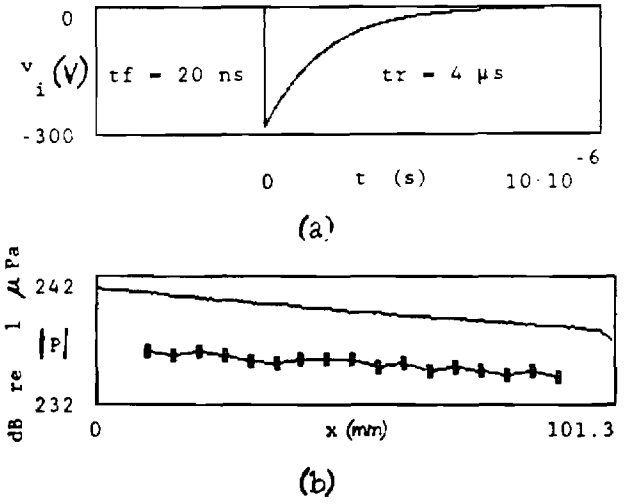

Fig. 6. (a) Broadband input pulse voltage. (b) Staircase model simulated, and measured (marked curve) pressure profiles.

This can be shown through the pressure output of each step during transmission.

D. Transmit Pressure Profile

The transmit response of a tapered piezoelectric is readily found from the staircase model by representing each step with an appropriate model, and pressure output angle θ. Since the frequency-domain resonances were of interest, an s-domain set of transfer functions [7] was used.

The theory presented above allows for physical understanding of the electric and mechanical processes that distinguish a tapered piezoelectric from a constant thickness device. These concepts were verified by experimental investigations.

III. Experimental Results

A. Electrical Impedance/Admittance

A tapered ceramic bar transducer (Channel C5800) with dimensions W = 2.01 mm, T = 101.3 mm, L_{min} = 2.79 mm and L_{max} = 4.07 mm was used for experimental measurements. This transducer was previously modeled as a quasi-longitudinal device of 500 segments [1]. The device constants used were ρ = 7550 kg/m^3, ϵ^s/ϵ_o = 663, $\bar{V}_a$ = 3950 m/s, k_T = 0.63, and Z/A = 29.8 MRayl. The transducer's input impedance was measured with a Hewlett-Packard 4193A impedance meter and is shown in Fig.4. The position x, where the transducer's local resonance at f occurs is below the frequency axis. Determining where the major resonance f_0 is located requires using the relations of Eqs. (8)-(10) and/or the staircase approach, iteratively, if necessary.

The position of resonance is x_0 = 29.3 mm. This corresponds to the i-th step (out of 500) of 145. Using the staircase model, $Z_{ee} = j2450$ at $f_0 \approx 625$ KHz, for i = 1,... 145. This narrow end is mass-controlled since $f_0 < f_{0i}$. The Z_e for the narrow end can be calculated from Eq. (10) to be $-j2188$. Thus $Z_{mot} = Z_{ee} - Z_e = +j4638$. For the thick end, $Z_e = -j1078$, and Z_{ee} over steps 146 to 500 is $-j2470\Omega$. This yields a $Z_{mot} = -j1392$, and indicates a region stiffness-controlled as expected.

This representation of the tapered device as two sections is shown in Fig.5(a). Figure 5(b) shows the admittance form, with C_0 = 352 pF ($Y_e = +j1289\mu$S), $Y_{mot(m)} = -j866\mu$S, and $Y_{mot(k)} = -j523\mu$S. As noted from (4) Y_{mot} and Z_{mot} are not reciprocals, thus it is possible for both motional admittances to represent inductances that resonate with C_0.

B. Pressure Profile

To determine if the transducer's local pressure output was affected by f_0, the transducer pulse response was simulated with N = 256, Z_P = 1.5 MRayl, Z_B = 427 Rayl and measured with a hydrophone probe. The transducer was enclosed in an air-backed housing, with its front, flat face loaded by water but separated by a 25.4 μm mylar film (V_a = 2540 m/sec, λ = 5 mm @ 500 KHz). A Panametrics 5052UA pulser was used to generate the input pulse (under load) shown in Fig.6(a). The pulse was modeled as a discrete function and a DFT computer routine was used to obtain an s-domain spectrum for input to the staircase simulation. Comparison of the theoretical and empirical pressure profile plots in Fig.6(b) show that over the length of the device there is excellent general agreement, and no pressure peak at the location x_0 where the transducer has its main resonance. The loss of a few dB between the simulated and experimental plot may be attributable to the separation and the material between the piezoelectric and the probe, which was not accounted for in the simulation.

In summary, the experiment data of the electric impedance and admittance, as well as the pressure response, are in good agreement with the theoretical predictions.

IV. CONCLUSION

An analysis of the resonance in tapered-thickness piezoelectrics was presented. Electroacoustic theory and a staircase model was used to show that local resonances are distributed along the device at the half-wavelength resonant frequency. In addition, there is a net response when the blocked and motional admittance resonate, that is mechanically uncoupled to the local response. Experimental data based on impedance and pressure profile measurements are in good agreement with the theory presented.

REFERENCES

[1] P.G. Barthé and P.J. Benkeser, "A Staircase Model of Tapered Piezoelectric Transducers," Proc. IEEE Ultrason. Symp., pp. 697-700, 1987.

[2] Y. Tomikawa, H. Yamada, and M. Onoe, "Wide Band Ultrasonic Transducer Using Tapered Piezoelectric Ceramics for Non-Destructive Inspection," Jpn. J. Appl. Phys., vol. 23, suppl. 23-1, pp. 113-115, 1984,

[3] T. Kobayashi, "Wedged Ultrasonic Transducers Having Thickness Extensional Vibration," J. Acoust. Soc. Jpn., [in Japanese], vol. 38, no. 10-12, pp. 748-754, 1982.

[4] W.P. Mason, *Electromechanical Transducers and Wave Filters*, New York: Van Nostrand, 1948.

[5] F.V. Hunt, *Electroacoustics*, Cambridge: Harvard rpess, pp. 93-136, 1954.

[6] P.M. Morse and K.V. Ingard, *Theoretical Acoustics*, New York: McGraw-Hill, p. 36, 1968.

[7] G. Hayward and M.N. Jackson, "Discrete-Time Modeling of the Thickness Mode Piezoelectric Transducer," IEEE Trans. Sonics Ultrason., vol. SU-31, no. 3, pp. 137-150, 1984.

A staircase model of tapered-thickness piezoelectric ceramics

Peter G. Barthé
and
Paul J. Benkeser

School of Electrical Engineering
Georgia Institute of Technology
Atlanta, GA 30332

Received

ABSTRACT

Tapered-thickness piezoelectric ceramics have been studied for use in novel devices and imaging techniques, such as wideband transducers and frequency-controlled beam-translation. These tapered devices exhibit a resonance peak in the electric input impedance, but no corresponding peak in the transmit response of the device. In this paper, a staircase model of tapered piezoelectrics will be developed to show that unlike conventional transducers, which are either stiffness-controlled below resonance or mass-controlled above resonance, thickness tapering produces periodically alternating regions of mass-control and stiffness-control along the length of the device. Interaction between these mass and stiffness regions contribute to a resonance peak in the electric input impedance which is shown not to be coupled to the distributed half-wavelength resonances of the device. The theoretical electric input impedance, spectral content, pulse and continuous wave pressure profile responses obtained with the model are shown to be in close agreement with the measured response of a tapered piezoelectric transducer.

I. INTRODUCTION

In conventional constant-thickness piezoelectric ceramics, operation near a sharp impedance resonance implies a relatively narrow-band transmit response. However, a piezoelectric ceramic with a linearly tapered thickness has been shown to exhibit a resonance peak in the electric input impedance, yet possess a broadband, uniform-amplitude transmit response.[1,2] Several investigators have attempted to exploit this phenomena by using such tapered ceramics in pulse-echo imaging transducers.[1-3] They found that transducers using tapered ceramics do not require lossy backing materials to achieve the desired bandwidth and are thus simpler to fabricate. However, no simple theoretical model exists which adequately describes the response of such a transducer.

The analysis of constant-thickness piezoelectrics for resonators or transducers has traditionally followed two paths.[4] One approach employs solutions describing field quantity perturbations in piezoelectric plates. These solutions are derived from the equations of linear elasticity, the wave equation, and boundary conditions. The other approach, more suitable for the analysis of transducers, employs equivalent circuits based on these same equations. The alternate approaches are consistent, but only accurate when the physical systems meet the original boundary conditions assumed in the solution or equivalent circuit.

The analysis of tapered-thickness piezoelectrics has similarly developed along two paths with one additional observation. These two approaches may be further subdivided into those which consider tapering an undesired effect, or others which exploit the characteristics derived from thickness tapering. The set of research based on the wave equation approach is described first. The earliest references to tapered-thickness piezoelectrics concerned parasitic effects induced by non-parallelism in resonators.[5] A brief analytic treatment of this problem has been formulated.[6] This research showed that small non-parallelism in one-dimensional resonators introduces inhomogenous broadening in the frequency-domain response and a corresponding damping in the time-domain response. An extension to full three-dimensional wave propagation shows non-parallelism can produce inharmonic or spurious resonances which may interface with harmonic nodes.

Piezoelectrics with contoured dimensions were also studied during development of trapped-energy resonators and delay lines.[7,8] This research employed field equations to describe coupled-mode vibrations in quartz. The ceramic tapered bar transducer has been examined with a similar approach in longitudinal and shear wave devices.[9,10] Applications of this research to pulse-echo imaging were limited because of the complexity of analysis in solving the equations of motion and/or because the emphasis was not on pure-mode transducers.

The second set of research is based on the equivalent circuit formalism. A spheroconcave contoured ceramic transducer has been described.[11] This transducer was modeled as a collection of discrete-thickness, uncoupled concentric rings to obtain a mathematical transmit or receive model. A radially symmetric thickness taper allowed wideband response along one axis. This is in contrast with the tapered bar, which has an output spectrum distributed along its thickness variation. The theoretical modeling of the tapered bar transducer was also approached as a study of response errors induced by an uneven device thickness.[12] A single mathematical transmit or receive model was obtained by integrating over a transducer surface area composed of smaller models. This is similar to the new model developed herein except that the results from several model steps are combined rather than combining models to obtain a result. Hence, no integration is necessary. This is significant because important parameters of tapered piezoelectrics, such as the electric input impedance, have forms which cannot be integrated directly. Furthermore, this method retains the characteristic of varied spectral distribution versus position rather than provide a spatially averaged pressure. The former information is useful for frequency-controlled acoustic wave steering.

In this study, the thickness gradient of a tapered piezoelectric ceramic is represented as a sequence of discrete steps. Each step is, in turn, represented by an equivalent circuit model. This approach allows the results and techniques developed for constant-thickness devices to be readily applied to those with a tapered thickness. The staircase model provides physical insight into the electrical and mechanical dynamics of tapered transducer operation. Verification of this theory is obtained through comparisons of the simulated and experimentally measured electrical input impedance, resonant frequencies versus position,

pulse, and continuous wave response of a tapered ceramic bar.

II. THEORY

A. Conventional Transducer Electrical and Mechanical Characteristics

The theoretical development is facilitated with the use of Mason's model of a lossless, thickness-mode piezoelectric transducer with no external damping, as shown in Fig. 1(a).[13] The parameters of this model are $C_0 = \varepsilon^s A/\ell$, $f_0 = v^D/2\ell$, and $Z = A\rho v^D$, where ε^s is the constant strain dielectric constant, A and ℓ are the area and thickness of the transducer, respectively, v^D is the stiffened acoustic phase velocity in the piezoelectric, ρ is the density, C_0 is the clamped capacitance, f_o is the mechanical resonant frequency, and Z is the mechanical impedance of the transducer.

The condition of no external damping is strictly met in vacuum, but effectively satisfied when the ratio of load impedances (such as air) to piezoelectric impedance is close to zero. The equivalent circuit in Fig. 1(b) may be obtained by combining impedances on the secondary side of the ideal transformer and reflecting the impedance to the primary circuit. The result is the standard, or canonical form of a transducer's admittance.

The canonical impedance representation of Fig. 1(c), and admittance representation of Fig. 1(d) are defined by[14]

$$Z_{ee} = Z_e + Z_{\text{mot}} \tag{1}$$

and

$$Y_{ee} = Y_e + Y_{\text{mot}} \tag{2}$$

where

$$Y_{ee} \equiv \frac{1}{Z_{ee}}, \text{ and } Y_e \equiv \frac{1}{Z_e}. \tag{3}$$

It is important to note that once the definitions in Eq. (3) are employed $Y_{\text{mot}} \neq 1/Z_{\text{mot}}$ in general, but in fact

$$Y_{\text{mot}} = \frac{-1}{Z_e + Z_e^2/Z_{\text{mot}}} , \tag{4}$$

as a result of combining Eqs. (1)-(3). In the equations above, the electric input impedance, or total impedance is represented by Z_{ee}, the blocked impedance by Z_e, and motional impedance by Z_{mot}. Corresponding admittances are defined in the same manner. Another useful relation is that of the complex mechanical impedance of the piezoelectric, $z_m = -Z_{\text{mot}}/T_{em}T_{me}$. T_{em} and T_{me} are reciprocal electromechanical transduction factors, equal in magnitude and sign, hence there is a change in sign between Z_{mot} and z_m. The complex mechanical impedance of a piezoelectric represents damping, mass, and stiffness reactance, yet is distributed rather than lumped. Therefore lumped constant representations are only valid at a given frequency.

If the surface motion of a transducer is supressed the electric impedance measured at its terminals is the blocked impedance, Z_e. Therefore Z_e represents the purely electrical aspect of a transducer. In a lossless dielectric medium, such as a piezoelectric material, the blocked impedance is represented by the clamped capacitance, C_0 of Mason's model,

$$Z_e = 1/j\omega C_0 . \tag{5}$$

Conversely, the motional impedance represents the mechanical dynamics of a transducer. It is an electrical quantity by virtue of electromechanical transduction factors introduced by the piezoelectric effect. For the lossless, unloaded transducer model described above, the motional impedance simplifies to

$$Z_{\text{mot}} = \frac{-k_T^2}{j\omega C_0} \frac{\tan(\pi f/2f_0)}{(\pi f/2f_0)} , \tag{6}$$

where k_T is the thickness-mode electromechanical coupling factor. The motional impedance is purely imaginary in this case because no acoustic radiation occurs in the unloaded condition.

When the transducer is damped by mechanical impedances Z_F at the front face, and Z_B at the rear face the motional impedance becomes[16]

$$Z_{mot} = \frac{k_T^2}{j\omega C_o \phi}\left[\frac{j(Z_F + Z_B)Z\sin\phi - 2Z^2(1-\cos\phi)}{(Z^2 + Z_F Z_B)\sin\phi - j(Z_F + Z_B)Z\cos\phi}\right] \quad (7)$$

where

$$\phi = \pi f / f_o \ .$$

The sign of the $\tan(\pi f/2f_0)$ factor in Eq. (6) determines the physical character of the motional impedance. When $0 < f < f_0$, Z_{mot} is a $+j$ quantity. Using the inductance-mass, capacitance-reciprocal stiffness analogy it is evident that the complex mechanical impedance, z_m, of the transducer is stiffness-controlled below resonance.[15] Over the region $f_0 < f < 2f_0$ the transducer is mass-controlled. As the resonant frequency is approached, or odd-multiples thereof, $Z_{mot} \rightarrow \pm j\infty$. This is the case of mechanical resonance characterized by an impedance maximum in $|Z_{ee}|$. Because of the odd-harmonic resonances present in the piezoelectric transducer, the mass-control/stiffness-control regions are also periodic with f. Therefore we can express these regions in terms of f as

Stiffness control:

$$mf_0 < f < (m+1)f_0 \ , \text{ for } m = 0, 2, 4, \ldots \quad (8a)$$

Mass Control:

$$(m+1)f_0 < f < (m+2)f_0 \ , \text{ for } m = 0, 2, 4, \ldots \quad (8b)$$

In addition to the electrical impedance maximum at the mechanical or parallel resonance, f_0, there is also an impedance minimum at the series resonant frequency, f_1, just below f_0. At the series resonant frequency $Z_{ee} \rightarrow 0$. Thus combining Eqs. (1), (5) and (6) yields

$$\frac{\tan(\pi f_1/2f_0)}{(\pi f_1/2f_0)} = \frac{1}{k_T^2} \ . \quad (9)$$

The second order solution of this equation, accurate for small k_T, is

$$f_1 = f_0\sqrt{1 - 8k_T^2/\pi^2} \ . \tag{10}$$

If a piezoelectric ceramic is air-backed and loaded by water the ratio of load/piezoelectric acoustic impedance is approximately 1/20. Under these boundary conditions the transducer is effectively unloaded and Eq. (9) or the approximation in Eq. (10) may be used to find f_1. The series resonant frequency is important, because a given voltage input will excite the low impedance mode at f_1 with more power than the mode at f_0.

These impedance/admittance and mass/stiffness representations may be extended to tapered transducers to obtain physical insight about their operation.

B. Staircase Model of a Tapered-Thickness Transducer

A tapered bar transducer is shown in Fig. 2(a). The thickness varies linearly from $\ell_{\min}$ to $\ell_{\max}$ in the poling or z-direction. The device has a length T in the x-direction, and a width W in the y-direction.

Consider the device divided into N equal sections (steps) along the x-axis. A minimum value for N is empirically chosen which yields an acceptable error. Each step located at position x_i, for $i = 1, 2, \ldots, N$, can be modeled as a separate transducer as shown in Fig.2(b). The position x_i may be described as

$$x_i = \left(i - \frac{1}{2}\right)\Delta x \ , \tag{11}$$

where

$$\Delta x = \frac{T}{N}$$

is the length of each step. The width of each step remains W, while the thickness of each step is represented by its average thickness, which is simply the thickness of the transducer at $x = x_i$. Hence, the thickness of the i-th section, ℓ_i, may be expressed as

$$\ell_i = \ell_{\min} + x_i \tan\theta \tag{12}$$

where

$$\tan\theta = \frac{\ell_{\max} - \ell_{\min}}{T},$$

and θ is the angle the sloped transducer face makes with the x-axis. Since the region of stress generation is along the thickness center of the tapered bar, the generated waves will internally be at an angle of θ with the x-axis.

Since each step of the model may be represented with Mason's model, and each step is electrically in parallel, the equivalent circuit models in Fig. 3(a) and (b) may be obtained. The local mechanical resonant frequencies of each step, $f_{oi} = v^D/2\ell_i$, $i = 1 \ldots, N$ of a tapered transducer will extend from $f_{oN}(f_{\min})$ at $\ell_{\max}$, to $f_{o1}(f_{\max})$ at $\ell_{\min}$. At some frequency f, where $f_{\min} < f < f_{\max}$, portions of the transducer will be above resonance, and others below resonance. If $\ell_{\max}/\ell_{\min} \leq 2$ the situation reduces to stiffness-control at the narrow end below resonance, and mass-control at the thick end above resonance.

In the admittance domain of Fig. 3(b), the values of $Y_{\text{mot (i)}}$ are given directly by Eq. (4) and are not, in general, inductive or capacitive susceptances. When the net shunt motional admittance, $\sum_{i=1}^{N} Y_{\text{mot (i)}}$ is inductive, a parallel resonance with C_0 will occur creating an impedance maximum at some frequency, henceforth called f_0. However, this resonance is not a conventional mechanical resonance in that portions of the transducer remain partitioned under both mass and stiffness control. The series impedance of $Z_{e(i)}$ and Z_{mot} that determines a local mechanical resonance f_{oi} is unaffected, or in other words, mechanically-uncoupled to the macroscopic resonance effect created by shunting several steps. The local resonances do not create the impedance maximum since at any frequency within the passband of the device, $Z_{ee(i)}$ is in shunt with non-resonant, low-impedance transducer sections.

C. Location of Electrical Impedance Maximum

The location of the electric impedance maximum at f_0 is found by evaluating Y_{mot} and Y_e. This may be attempted by direct integration, or by using the staircase formulation. Proceeding with the former, the boundary conditions are simplified when the point $x = 0$ used in Eq. (11) and Fig. (2) is shifted by $\ell_{min}/\tan\theta$ such that $x = 0$ now describes the

extrapolation of ℓ down to zero. Also, the incremental Δx is replaced with dx, and the discrete function ℓ_i is replaced with $\ell(x)$. Substituting the continuous functions into Eqs. (4)-(6), the motional admittance at constant ω for a section of tapered piezoelectric along x between x_a and $x_b (x_b \leq x_a)$ can be shown to be

$$Y_{\text{mot}}\Big|_{x_a,x_b} = \frac{j\omega\varepsilon' W}{\tan\theta} \int_{u_a}^{u_b} \left[\frac{1}{\frac{u}{k_T^2}\cot u - 1} \right] \frac{du}{u} , \tag{13}$$

using the substitution variable,

$$u \equiv \frac{\omega x}{2v^D} \tan\theta . \tag{14}$$

The blocked admittance, $Y_e = j\omega C_o$, where C_o is a function of ℓ and therefore x, between x_a and x_b is

$$Y_e\Big|_{x_a,x_b} = \frac{j\omega\varepsilon' W}{\tan\theta} \int_{u_a}^{u_b} \frac{du}{u} = \frac{j\omega\varepsilon' W(x_a - x_b)}{(\ell_b - \ell_a)} \ln\left(\frac{\ell_b}{\ell_a}\right) \tag{15}$$

where ℓ_a and ℓ_b correspond to x_a and x_b.

The integral formulation of Y_{mot} in Eq. (13) is only solvable by numerical techniques. Alternatively, Y_{mot} can be calculated using the staircase model with N discrete transducer steps and adding the motional admittances of each step. The model in Fig. 1(b) or Eqs. (4)-(6) gives Y_{mot} per step. The shunt admittance resonance represents $Y_{\text{mot}} + Y_e \rightarrow 0$. The analysis so far has indicated if f_0 is in the passband of the tapered transducer ($f_{\text{min}} < f_0 < f_{\text{max}}$), it should not interfere with the local resonances. This can be shown through the pressure output of each step during transmission.

D. Transmit Pressure Profile

The transmit response of a tapered piezoelectric is readily found from the staircase model by representing each step with an appropriate model characteristic of the dominant mode of the piezoelectric, and pressure output angle θ. Since there is typically a discontinuity in the phase velocity at the piezoelectric to load interface, the acoustic waves will propagate in the load at an angle determined by Snell's law. If θ_L represents the angle the wave makes with the z-axis, and v_L represents the phase velocity in the load then

$$\theta_L = \sin^{-1}\left(v_L \sin\theta / v^D\right) \ . \tag{1}$$

Therefore, in the case of slightly tapered ceramics radiating into water, θ_L will be very small.

The pressure output for each step at position x_i can be obtained from existing models of thickness-mode piezoelectrics. Two models were used for simulation in this study. One is a set of frequency domain transfer functions which provide an ouput force given an input voltage.[17] The other is a powerful equivalent circuit representation, suitable for simulation in the time or frequency domain, with arbitrary terminations at the electrical and mechanical ports.[18] The above models were modified for acoustic pressures with the introduction of a scaling factor $1/A$ to each force, where $A = WT/N$, the area of each step. A pressure profile, $p(x_i, t)$, may be determined by considering each step to be excited by a voltage common to all the steps.

Since the mechanical resonant frequency is a function of position, the approximate relation of Eq. (10) can be written as

$$f_1 = v^D \sqrt{1 - 8k_T^2/\pi^2}/2\left(\ell_{\min} + x\tan\theta\right) \ .$$

Differentiating both sides with respect to x yields the spectral sensitivity of the series resonant frequency with position, that is,

$$\frac{\partial f_1}{\partial x} = -v^D \tan\theta \sqrt{1 - 8k_T^2/\pi^2}/2\left(\ell_{\min} + x\tan\theta\right)^2 \ . \tag{2}$$

The above relations show that at each position x the pressure profile will contain different frequencies, and the rate of change of these frequencies about x also depends on position. The thicker end of the tapered transducer is more sensitive to small changes in f_1 than the narrower end.

The theoretical development was verified by experimental techniques.

III. Methods

A tapered ceramic bar transducer (Channel C5800) with dimensions $W = 2.01$ mm, T

= 101.3 mm, ℓ_{min} = 2.79 mm and ℓ_{max} = 4.07 mm was used for experimental measurements. The device constants used by the staircase model are shown in Table I.

A quasi-longitudinal mode model was chosen for the N steps since the thickness of the bar was comparable to its width. Under these conditions, the device does not operate in a pure thickness mode. This requires the use of effective constants in the thickness-mode model.[19,20] The effective electromechanical coupling coefficient, k_{eff}, varies as a function of the width to thickness ratio. As the width/thickness ratio varies between 0 and ∞, the effective coupling factor varies from the width mode, k'_{33}, to the thickness mode, k_t. For width/thickness ratios about 0.6, the magnitude of k_{eff} is close to k'_{33}, but the motion is nearly unimodal, or quasi-longitudinal with the fundamental mode described by the thickness resonance.

A survey of several piezoelectric ceramics yields an average $k'_{33}/k^{\ell}_{33} = 0.935$ with standard deviation 0.020, where k^{ℓ}_{33} is the pure longitudinal mode. Therefore $k_{eff} \approx 0.935 k'_{33}$. For the C5800 ceramic, $k^{\ell}_{33} = 0.67$, and thus $k_{eff} = 0.63$. This yields the piezoelectrically-stiffened quantities $\varepsilon^{s}_{eff} = \varepsilon^{T}(1 - k^2_{eff})$, and $v^{D} = v^{E}/\sqrt{1 - k^2_{eff}}$ where $\varepsilon^{T} = 1100\varepsilon_o$ is the free dielectric permittivity, and $v^{E} = 3068$ m/s is the unstiffened acoustic phase velocity.

The experimental setup for the continuous wave and pulsed pressure profiles and resonant frequency measurements is shown in Fig. 4. The transducer was enclosed in an air-backed housing, with its front (flat face) loaded by water but separated by a 254 μm mylar film (V_a = 2540 m/sec, λ = 5mm @ 500 KHz). A pulser-receiver (Panametrics 5052UA) was used to generate an input pulse, or alternatively a frequency generator (Wavetek 143) monitored by a frequency counter (Hewlett-Packard 5314A) was configured to generate a sinewave input. A 1mm-diameter PVDF hydrophone probe and preamplifier (Medisonics ME 101) calibrated from 1 to 8 MHz was used to measure the acoustical output of the tapered bar. A digital oscilloscope (Hewlett-Packard 54501A), when strobed, calculated the peak output of the hydrophone preamplifier and transferred the data to a computer.

IV. RESULTS

A. Electrical Impedance/Admittance

The theoretical input impedance of the tapered bar was obtained from Eqs. (3), (7),

(11), and (12) by summing the total admittance of each step. A value of N = 500 steps was used for these simulations. Experimental data was measured with a vector impedance meter (Hewlett-Packard 4193A).

Figure 5(a) shows the theoretical input impedance magnitude in air. The position x where the local resonance at f_{oi} occurs is shown below the frequency axis on this figure. The maximum impedance point occurs at $f_0 = 625$ kHz, which corresponds to an $f_1 = 504$ kHz from the full solution to Eq. (9). The location of the resonance at f_1 is also noticeable in this plot. The spikes in $|Z_{ee}|$ in Fig. 5(a) come from a one-dimensional theoretical simulation, therefore they should not be confused with the inharmonic or spurious modes which may occur due to multi-dimensional wave propagation effects or mode coupling. Experimental data appears in Fig. 5(b). The major resonance is evident precisely where expected but from theoretical considerations, but the location of f_1 is not distinct, as is typically the case. Phase data appears in Fig. 6. These figures illustrate very good agreement. The theoretical and experimental input impedance magnitude for the case of an air-backed transducer loaded by water appears in Fig. 7. Phase data appears in Fig. 8. In Figs. 7 and 8 the experimental data matches the theoretical data very closely, but with the addition of small spike-like perturbations. These perturbations are likely due to wave propagation along x due to reflections between the tapered faces of the piezoelectric. The effect of these perturbations is to add or subtract to the dominant, thickness mode of the device.

The position of f_0, the major resonance, is $x_0 = 29.3$ mm. This corresponds to the i-th step (out of 500) of 145. Using the staircase model, $Z_{ee} = j2450$ at $f_0 \approx 625$ KHz, for $i = 1, \ldots 145$. This narrow end is stiffness-controlled since $f_0 < f_{oi}$. The Z_e for the narrow end can be calculated from Eq. (15) to be $-j2188$. Thus $Z_{\text{mot}} = Z_{ee} - Z_e = +j4638$. For the thick end, $Z_e = -j1078$, and Z_{ee} over steps 146 to 500 is $-j2470\Omega$. This yields a $Z_{\text{mot}} = -j1392$, and indicates a region mass-controlled.

A representation of the tapered device in the admittance form at 625 kHz yields $C_0 = 352$ pF ($Y_e = +j1289\mu$S), $Y_{\text{mot}(k)} = -j866\mu$S, and $Y_{\text{mot}(m)} = -j523\mu$S. As noted from Eq. (4) Y_{mot} and Z_{mot} are not reciprocals, thus it is possible for both motional admittances to represent inductances that resonate with C_0.

B. Pressure Profile

A comparison of the theoretical and experimental series resonant frequencies versus position is shown in Fig. 9. The theoretical values were obtained from the full solution to Eq. (9). Experimental values were obtained by adjusting the input frequency for peak acoustical output. The error varies from 0.5% at ℓ_{min} to 2% at ℓ_{max}. The increase at ℓ_{max} is likely due to an increase in k_{eff} at the thicker end since the width-thickness ratio is decreasing.

To demonstrate if pressure output along the length of the bar was unaffected by f_0, or its associated f_1, the transducer pulse response was simulated with $N = 256$, while $Z_F = 1.5$ MRayl, and $Z_B = 427$ Rayl were the respective front and back face impedances. Fewer steps were used to decrease computation requirements, yet $|Z_{ee}|$ calculated was nearly constant for N > 128.[21] The pulse input had a 10-90% fall time of 20ns to -285V, and a 4μs rise time. It was modeled as a discrete function and a DFT computer routine was used to obtain an s-domain spectrum for input to the staircase model. Comparison of the theoretical and experimental pressure profile plots in Fig. 10 shows that over the length of the device there is excellent general agreement, and no pressure peak at the location x_0 where the transducer has its main resonance; thus the major resonance is uncoupled to distributed half-wavelength resonances of interest.

A continuous wave pressure profile is shown in Fig. 11. The theoretical plot was obtained from the steady-state response of each step implemented with a time domain model. The input was a 29 V pk-pk, 435.6 kHz sinewave. Figure 11 illustrates a 7mm shift in the peak pressure location between theoretical and empirical data. At $x = 70$mm, Eq. (17) gives a spectral sensitivity of -1.5 kHz/mm, thus the 7mm corresponds to a 10.5 kHz (2.4%) shift in f_1. The troughs away from the peak in the continuous wave profile are also likely due to small reflections along the length of bar which add or subtract to the dominant longitudinal vibrations. When the transducer is pulsed, the entire bar is in motion, and these small perturbations are of second order, hence the troughs are less evident.

IV. CONCLUSION

An analysis of tapered-thickness piezoelectrics was presented. A staircase model was

developed using electroacoustics theory and employed to show that local resonances are distributed along the device at the half-wavelength resonant frequency. In addition, there is a net response when the blocked and motional admittances resonate, that is mechanically uncoupled to the local response. The staircase model presented yields physical insight into the electrical and mechanical dynamics of tapered piezoelectrics and allows determination of important electroacoustic parameters for which there are no closed solutions. It also allows direct application of the results and techniques already developed for constant-thickness piezoelectrics. Experimental data based on impedance and pressure profile measurements are in good agreement with the theory presented.

REFERENCES

[1] Y. Tomikawa, H. Yamada, and M. Onoe, "Wide Band Ultrasonic Transducer Using Tapered Piezoelectric Ceramics for Non-Destructive Inspection," Jpn. J. Appl. Phys. Suppl. 1 **23**, 113-115 (1984).

[2] T. Kobayashi, "Wedged Ultrasonic Transducers Having Thickness Extensional Vibration," J. Acoust. Soc. Jpn. **38**, 748-754 (1982).

[3] P.J. Benkeser, "A Pulse-Echo Ultrasound Tapered Phased Array Transducer," *Proc. 13th NE Bioengineering Conf.* (IEEE, New York, 1987) pp. 286-288.

[4] W. Sachse and N.N. Hsu, "Ultrasonic Transducers for Materials Testing and Their Characterization," in *Physical Acoustics*, edited by W.P. Mason and R.N. Thurston (Academic, New York, 1979), Vol. 13, pp. 277-406.

[5] W.G. Cady, Piezoelectricity (Dover, New York, 1964), 2nd ed., Vol. 2, p. 443.

[6] D.I. Bolef and J.G. Miller, "High-Frequency Continuous Wave Ultrasonics," in *Physical Acoustics*, edited by W.P. Mason and R.N. Thurston (Academic, New York, 1971), Vol. 8, pp. 95-201.

[7] J.L. Bleustein, "Thickness-Twist and Face-Shear Vibrations of a Contoured Crystal Plate," Int. J. Solids Struct. **2**, 351-360 (1966).

[8] C.B. Loutzenheiser and W.J. Denkmann, "Thickness/Twist Vibrations of a Truncated, Linearly Tapered, Crystal Strip," J. Acoust. Soc. Am. **41**, 962-968 (1967).

[9] B.M. Alekseev, D.B. Dianov, and S.P. Karuzo, "Tapered-Bar Transducer," in *Proceedings of the Eighth All-Union Acoustics Conference* (Moscow, 1973).

[10] B.N. Alekseev, D.B. Dianov, and S.P. Karuzo, "Tapered Piezoelectric Bar Transducer with Transverse Polarization of the Piezoeceramic," Sov. Phys. Acoust. **23**, 1-4.

[11] A.K. Vopilkin, I.N. Ermolov, V.I. Ivanov, P.Y. Krasinskii, and V.I. Ryzhov-Nokonov, "Theoretical Analysis of Wideband Transducers," Sov. J. Nondestr. Test. **13**, 123-128 (1977).

[12] Y. Jayet, M. Perdrix, and R. Goutte, "Effects on the Damping of Ultrasonic Transducers Due to a Lack of Parallelism in the Piezoelectric Element," Ultrasonics **21**, 179-183 (1983).

[13] W.P. Mason, *Electromechanical Transducers and Wave Filters* (Van Nostrand, New York, 1948), 2nd ed., pp. 358-361.

[14] F.V. Hunt, *Electroacoustics* (Harvard Press, Cambridge, MA, 1954), pp. 93-136.

[15] P.M. Morse and K.U. Ingard, *Theoretical Acoustics* (McGraw-Hill, New York, 1968), pp. 36-49.

[16] G.S. Kino, *Acoustic Waves* (Prentice-Hall, Englewood Cliffs, NJ, 1987), p. 32.

[17] G. Hayward, C.J. MacLeod, T.S. Durrani, "A Systems Model of the Thickness Mode Piezoelectric Transducer," J. Acoust. Soc. Am. **76**, 369-382 (1984).

[18] S.A. Morris and C.G. Hutchens, "Implementation of Mason's Model on Circuit Analysis Programs," IEEE Trans. Ultrason. Ferroelec. Freq. Contr. **UFFC-33**, 295-298 (1986).

[19] R.H. Coursant, C. Méquio, and P. Pesqué, "Simulation of the Acousto-Electric Response of Ultrasonic Narrow Strip Transducers with Mechanical Losses," *Ultrasonics International '83 Conference Proceedings* (Butterworths, London, 1983), pp. 414-419.

[20] J. Sato, M. Kawabuchi, and A. Fukumoto, "Dependence of the Electromechanical Coupling Coefficient on the Width-to-Thickness Ratio of the Plank-Shaped Piezoelectric Transducers used for Electronically Scanned Ultrasound Diagnostic Systems," J. Acoust. Soc. Am. **66**, 1609-1611 (1979).

[21] P.G. Barthé and P.J. Benkeser, "A Staircase Model of Tapered Piezoelectric Transducers," *Proc. IEEE 1987 Ultrason. Symp.* (IEEE, New York, 1987), pp. 697-700, 1987.

Table I. Piezoelectric constants used to model tapered bar

$\rho = 7550\text{kg/m}^3$	$k_T = 0.63$
$\varepsilon^s/\varepsilon_o = 603$	$Z/A = 29.8$ M. Rayl
$v^D = 3950\text{m/s}$	

FIG 1. (a) Undamped Mason's model, (b) transformed equivalent circuit, (c) canonical impedance and (d) admittance representations.

FIG 2. (a) Tapered bar transducer, (b) representation of transducer section with discrete thickness.

FIG 3. (a) Canonical impedance representation of N-step staircase model, and (b) admittance representation.

FIG 4. Experimental setup for continuous and pulsed pressure profiles and resonant frequency measurements.

FIG 5. Electrical input impedance magnitude of the tapered bar in air. (a) Theoretical and (b) experimental. The subaxis in (a) represents the position along the bar where its mechanical resonant frequency is located.

FIG 6. Phase of the electrical input impedance of the tapered bar in air. (a) Theoretical and (b) experimental.

FIG 7. Magnitude of the electrical input impedance of an air-backed tapered bar loaded by water. (a) Theoretical and (b) experimental.

FIG 8. Phase of the electrical input impedance of an air-backed tapered bar loaded by water. (a) Theoretical and (b) experimental.

FIG 9. Comparison of the theoretical (solid line) and experimental resonant frequencies versus position.

FIG 10. Comparison of the theoretical (solid line) and experimental pulsed pressure profiles.

FIG 11. Comparison of the theoretical (dashed line) and experimental (solid line) continuous wave pressure profiles.

Fig. 1.

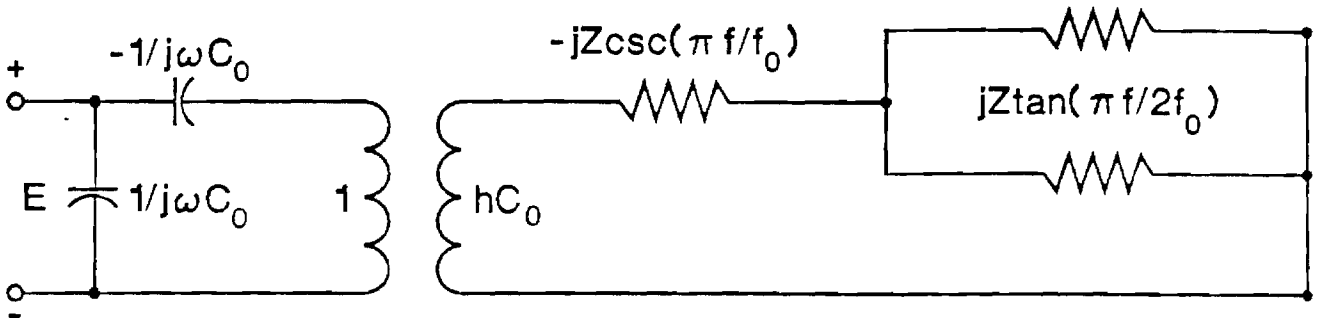
+
-1/jωC0
E
1/jωC0
1
hC0
-jZcsc(π f/f0)
jZtan(π f/2f0)
-

(a)

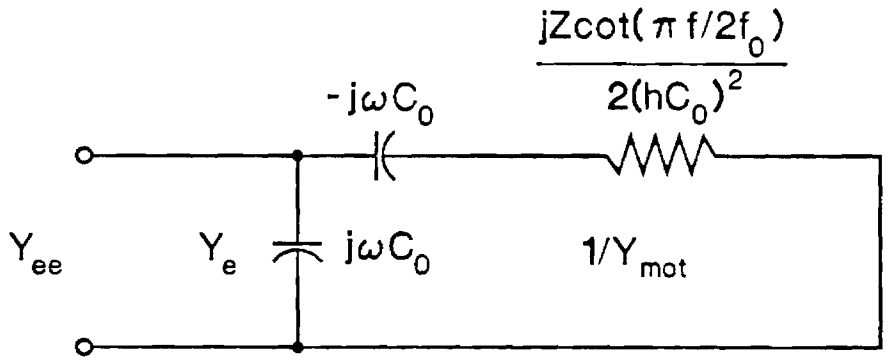
jZcot(π f/2f0)
2(hC0)2
-jωC0
Yee
Ye
jωC0
1/Ymot

(b)

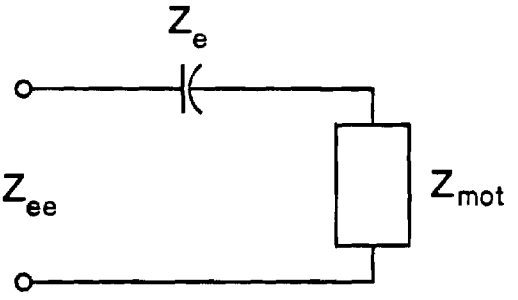
Ze
Zee
Zmot

(c)

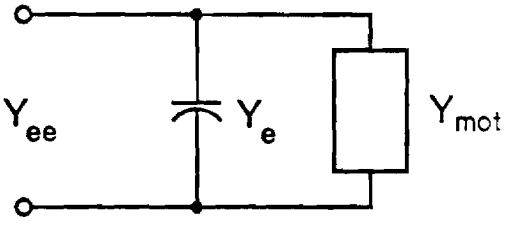
Yee
Ye
Ymot

(d)

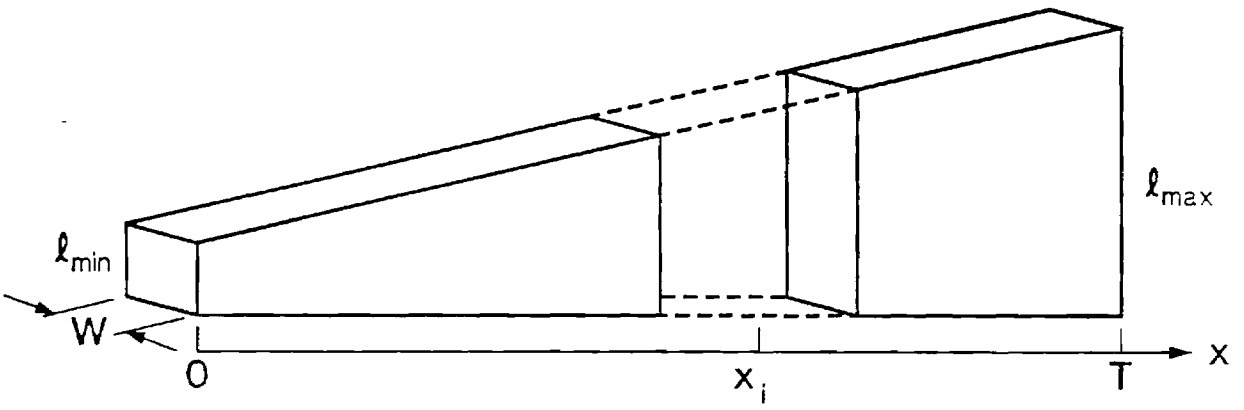

(a)

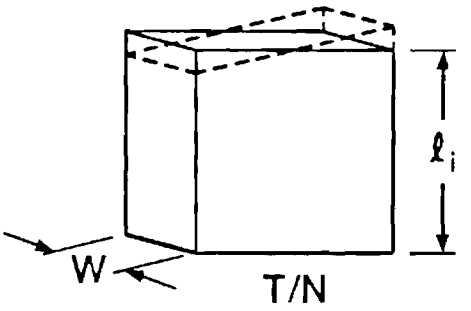

(b)

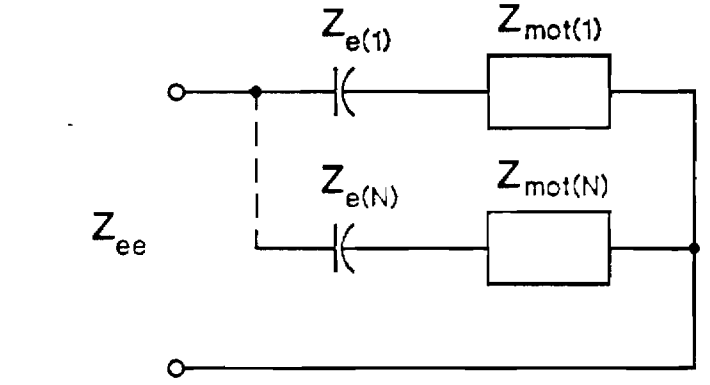

(a)

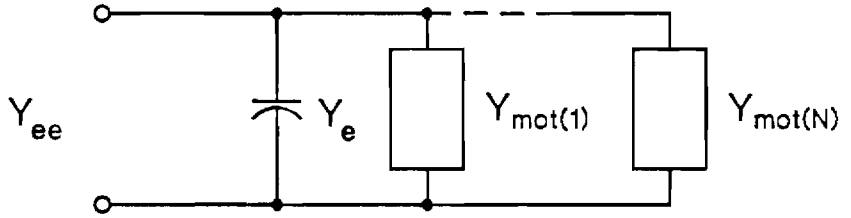

(b)

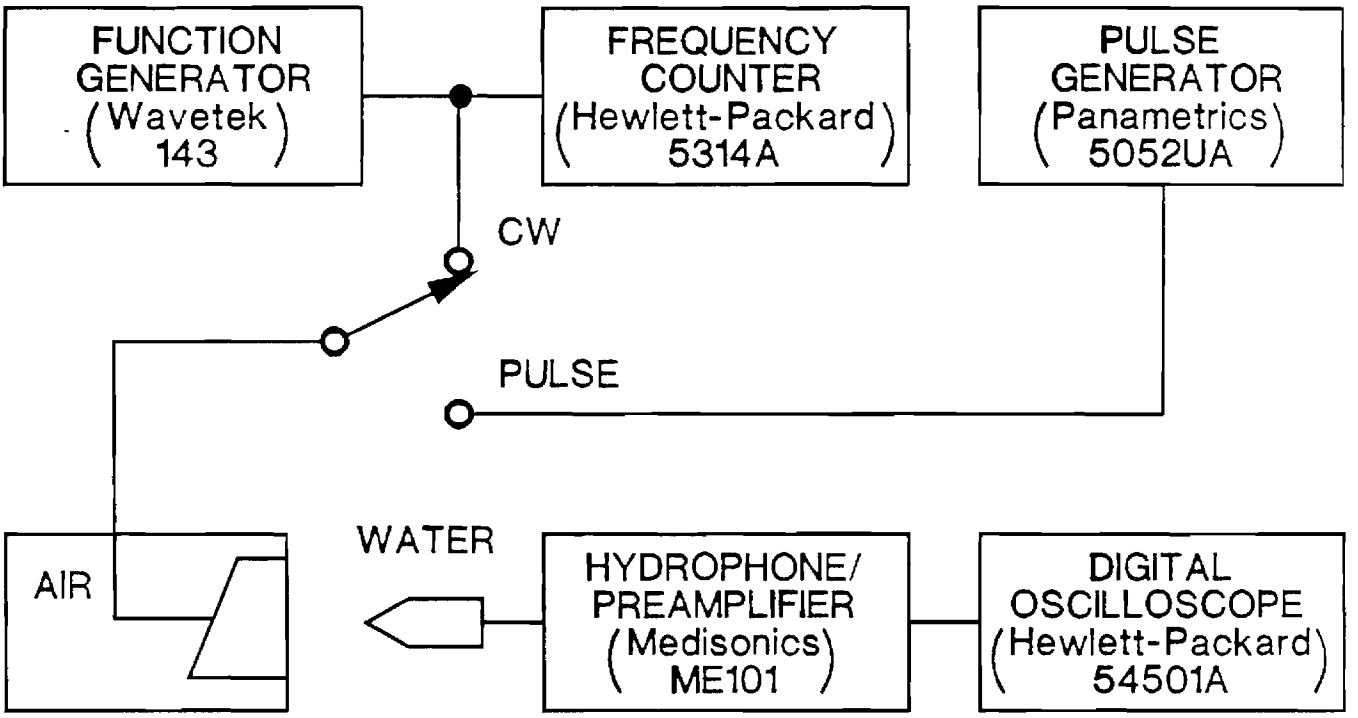
FUNCTION GENERATOR (Wavetek) 143
FREQUENCY COUNTER (Hewlett-Packard) 5314A
PULSE GENERATOR (Panametrics) 5052UA
CW
PULSE
AIR
WATER
HYDROPHONE/ PREAMPLIFIER (Medisonics) ME101
DIGITAL OSCILLOSCOPE (Hewlett-Packard) 54501A

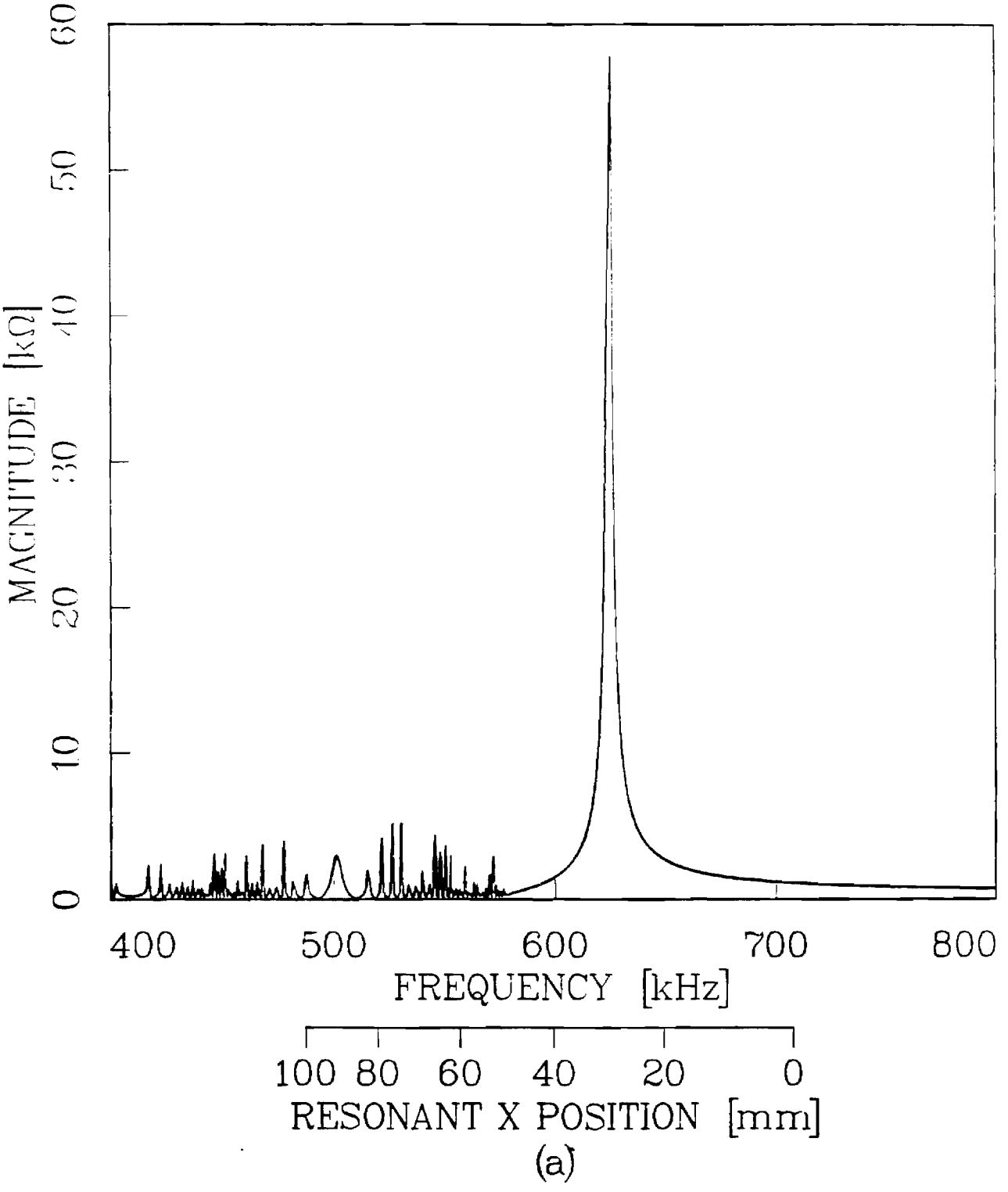
MAGNITUDE [kΩ]
0
10
20
30
40
50
60
400
500
600
700
800
FREQUENCY [kHz]
100 80 60 40 20 0
RESONANT X POSITION [mm]

(a)

FIG. 5(b).

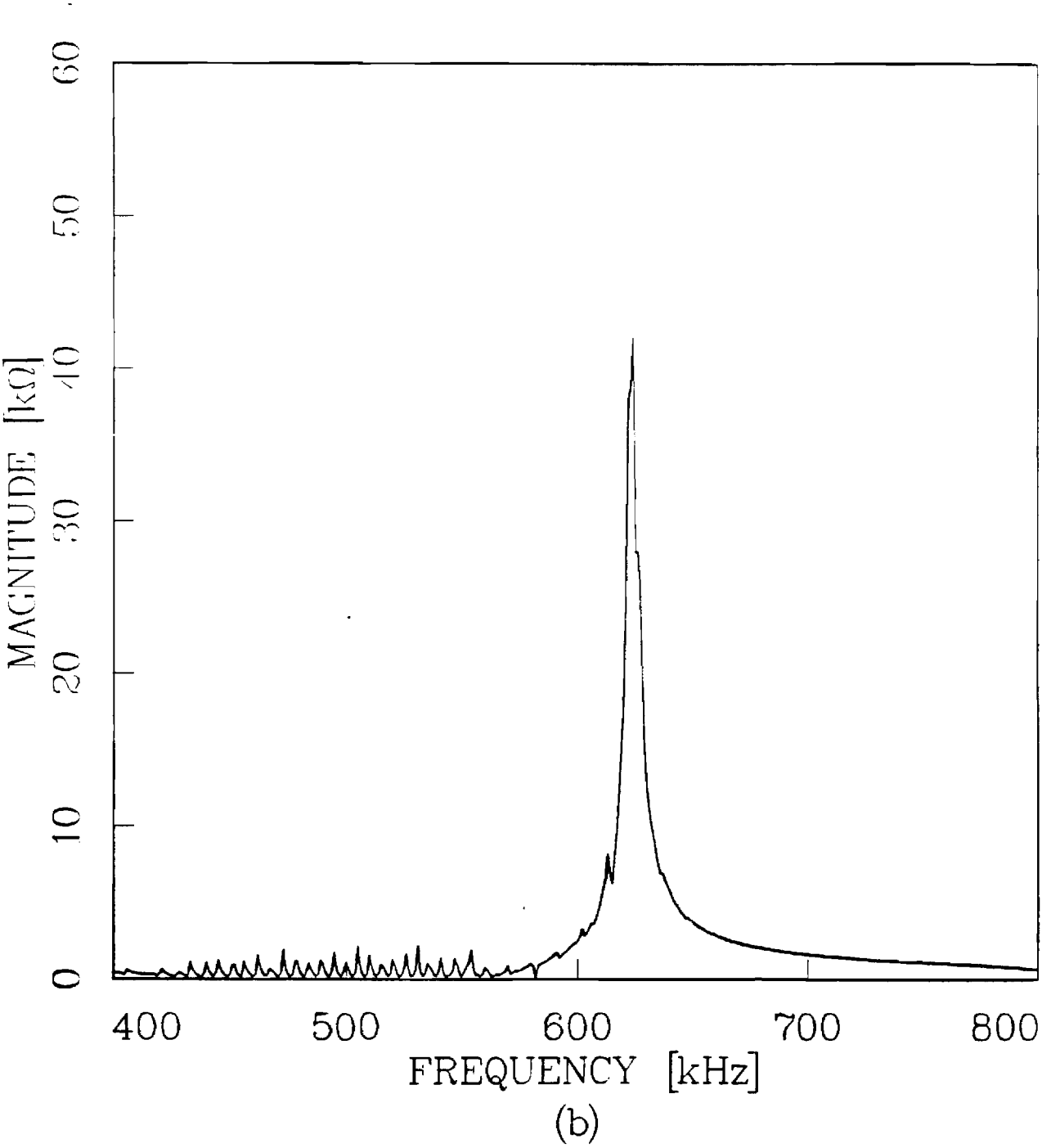
MAGNITUDE [kΩ]
0
10
20
30
40
50
60
400
500
600
700
800
FREQUENCY [kHz]

(b)

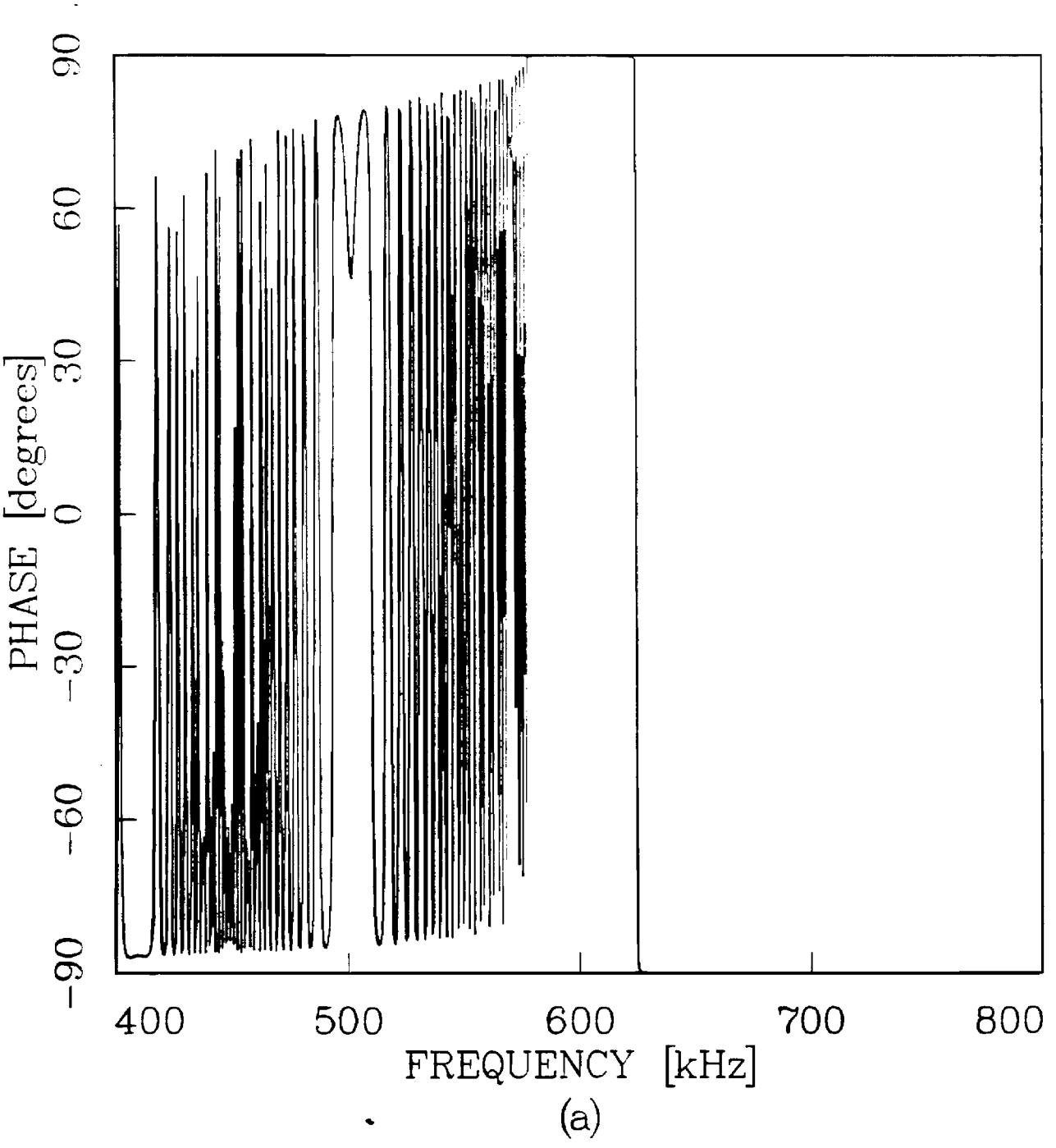
PHASE [degrees]
90
60
30
0
-30
-60
-90
400
500
600
700
800
FREQUENCY [kHz]

(a)

Fig. 6(b).

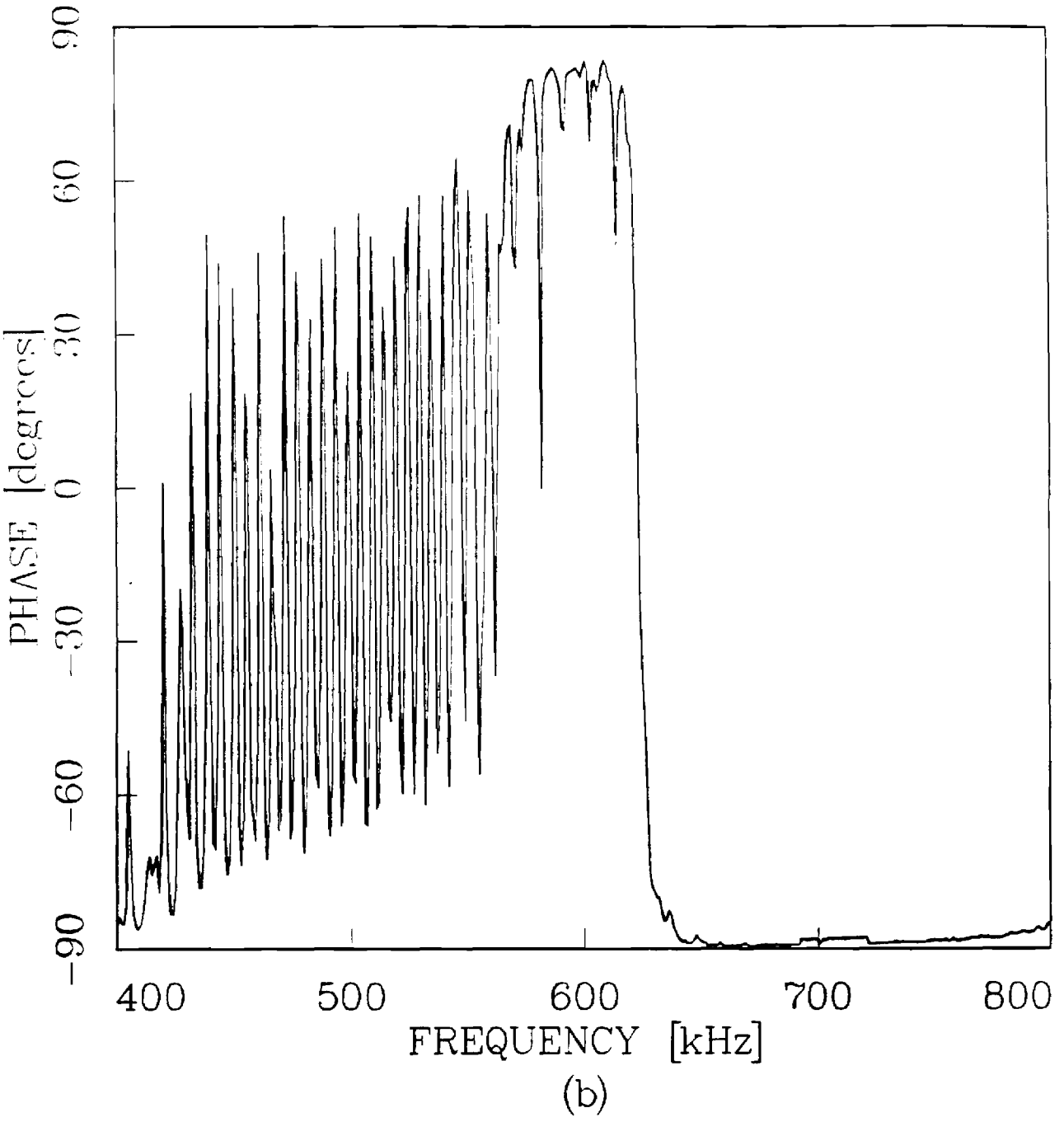
PHASE [degrees]
90
60
30
0
−30
−60
−90
400
500
600
700
800
FREQUENCY [kHz]

(b)

Fig. 7(a).

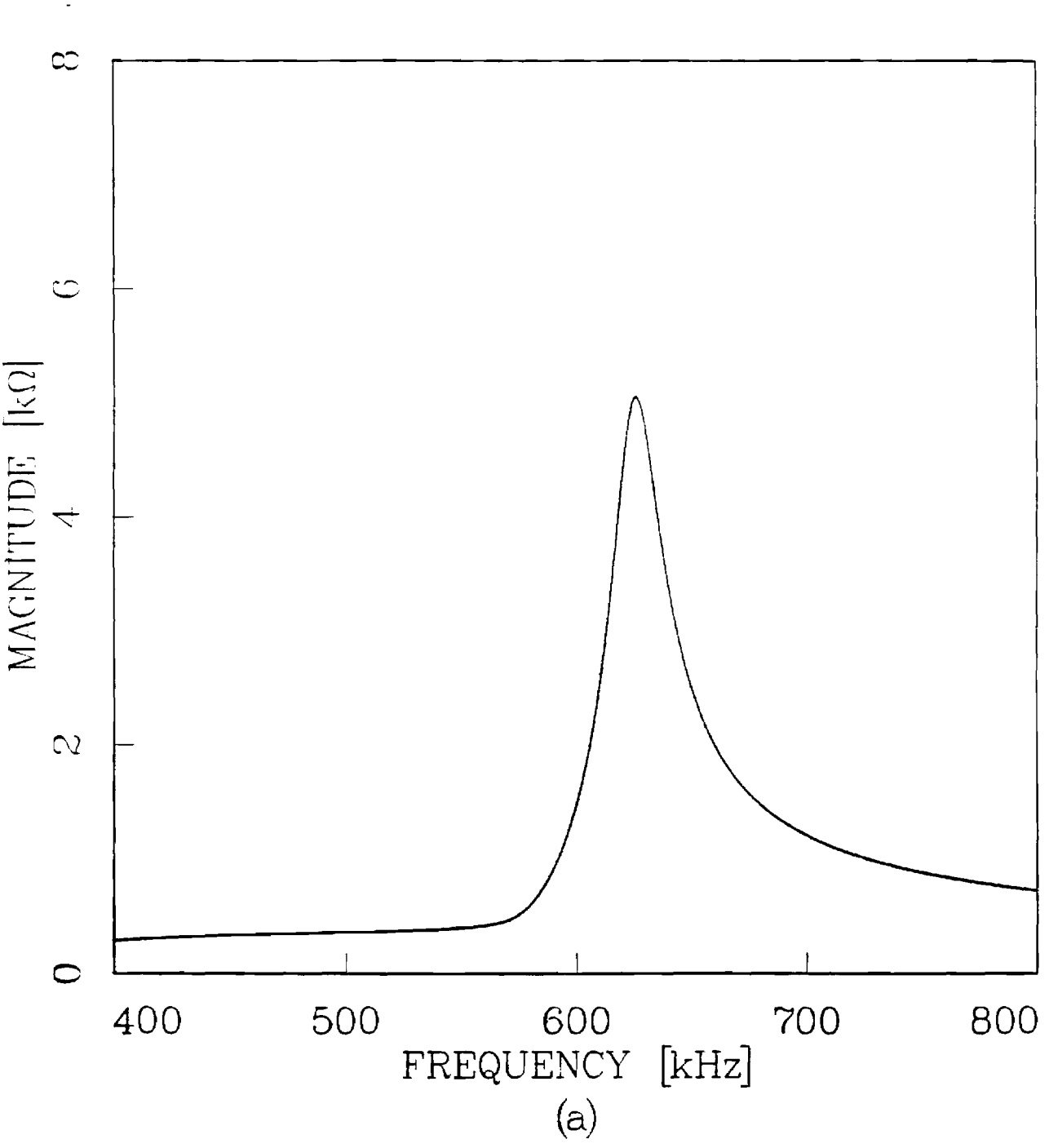

Fig. 7(b)

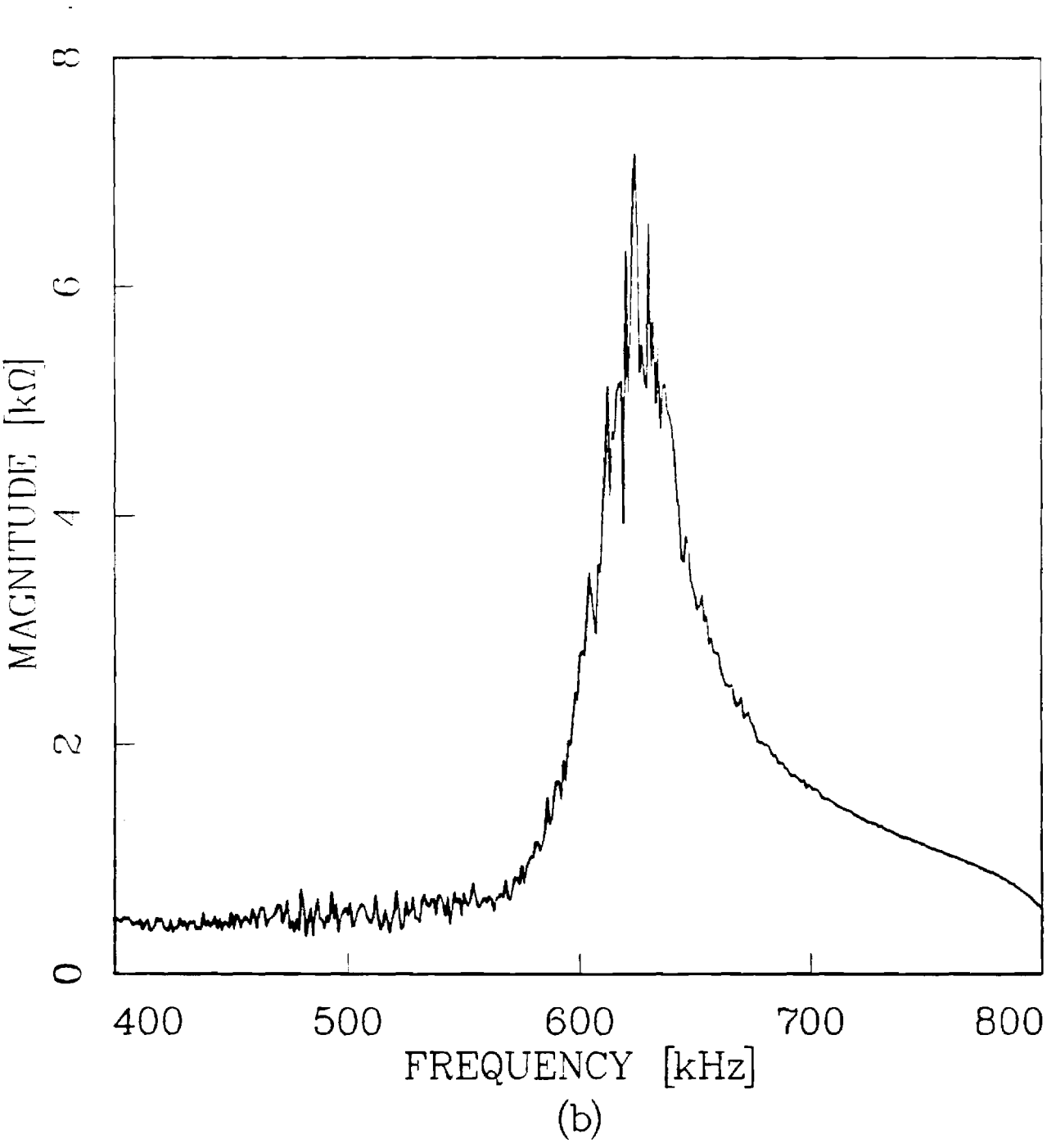

(b)

Fig. E...

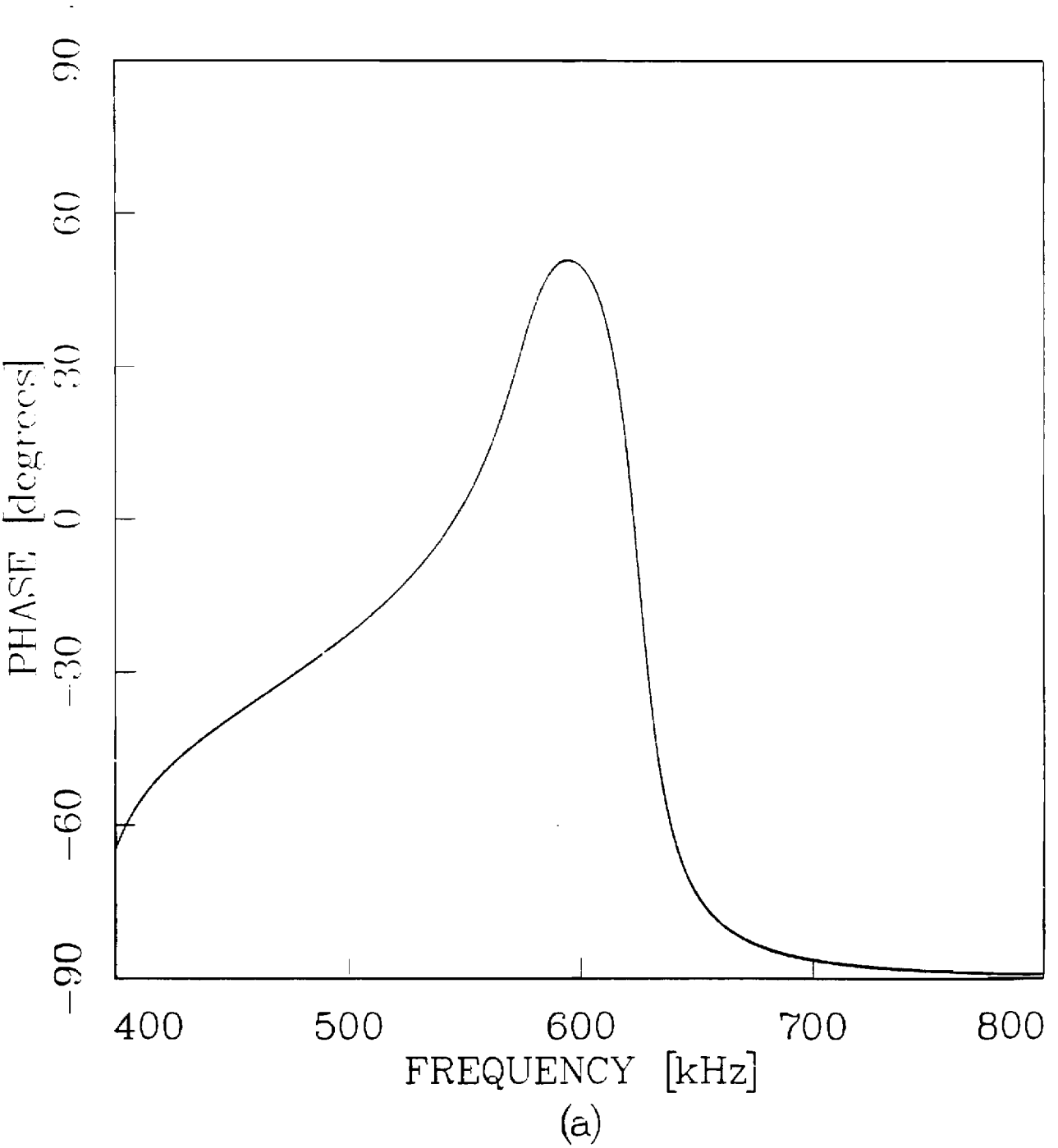
PHASE [degrees]
90
60
30
0
−30
−60
−90
400
500
600
700
800
FREQUENCY [kHz]

(a)

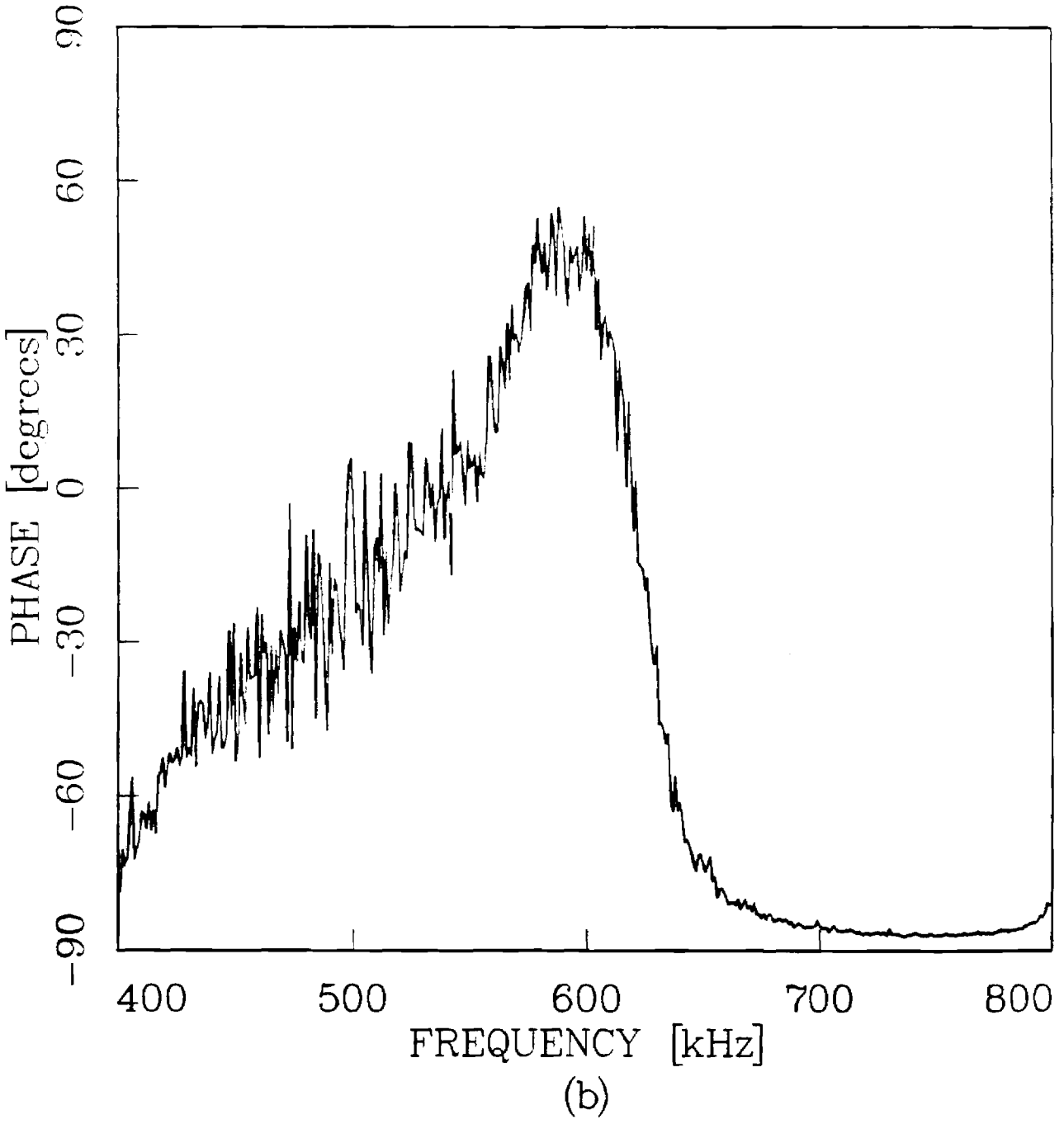
PHASE [degrees]
90
60
30
0
−30
−60
−90
400
500
600
700
800
FREQUENCY [kHz]

(b)

Fig. 5.

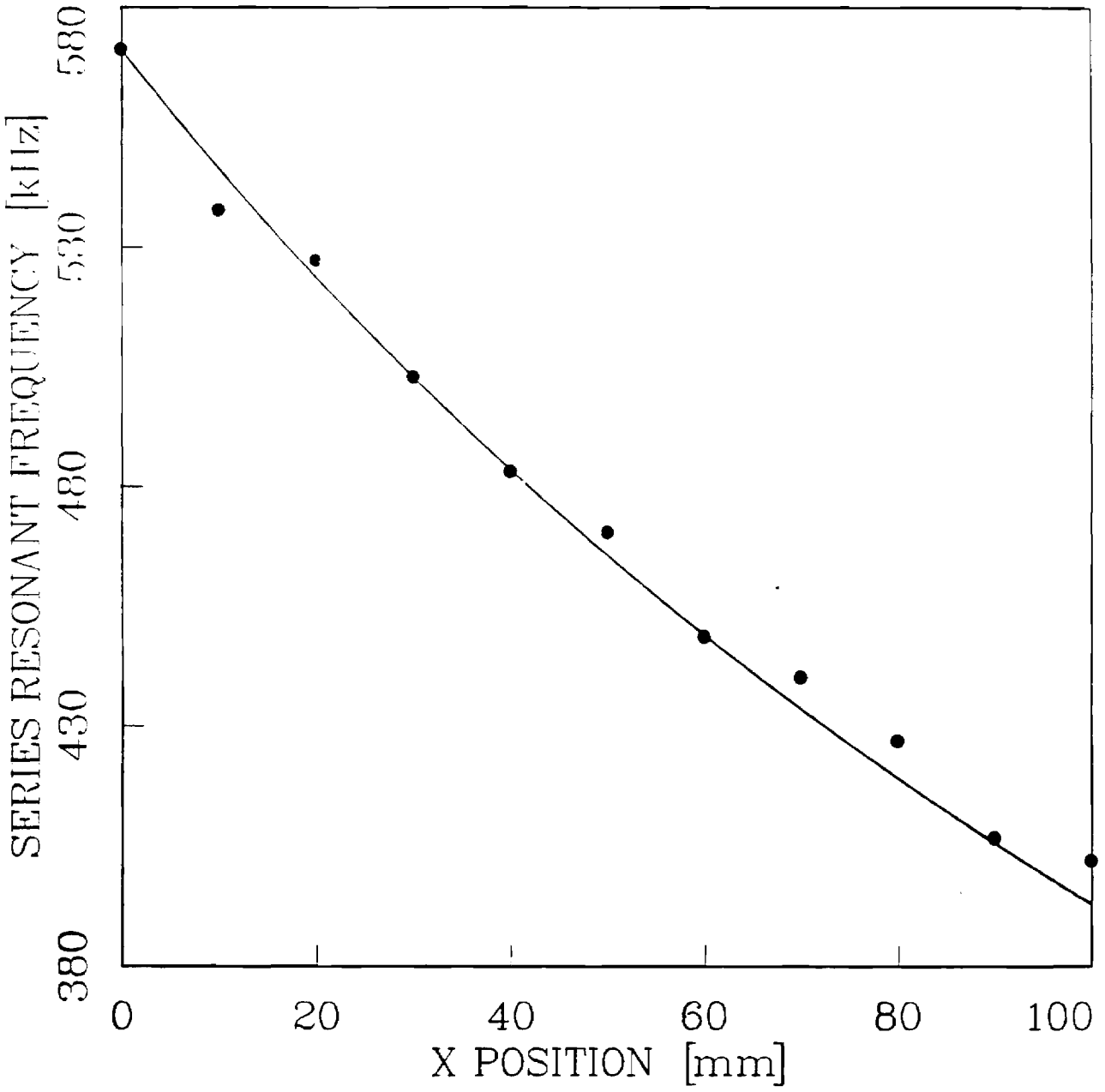
SERIES RESONANT FREQUENCY [kHz]
380
430
480
530
580
0
20
40
60
80
100
X POSITION [mm]

FIG. 10.

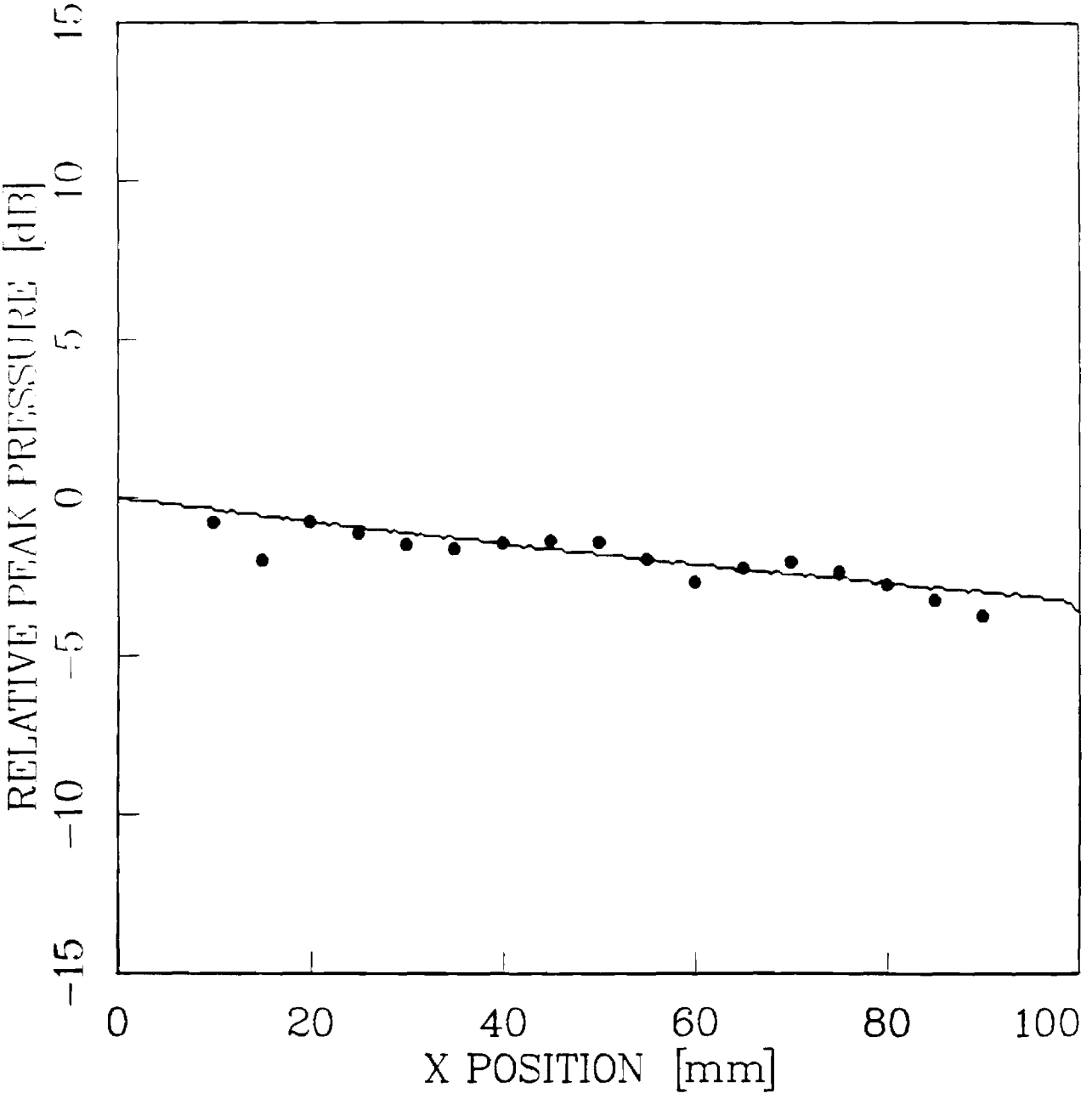
RELATIVE PEAK PRESSURE [dB]
15
10
5
0
−5
−10
−15
0
20
40
60
80
100
X POSITION [mm]

Fig. 11.

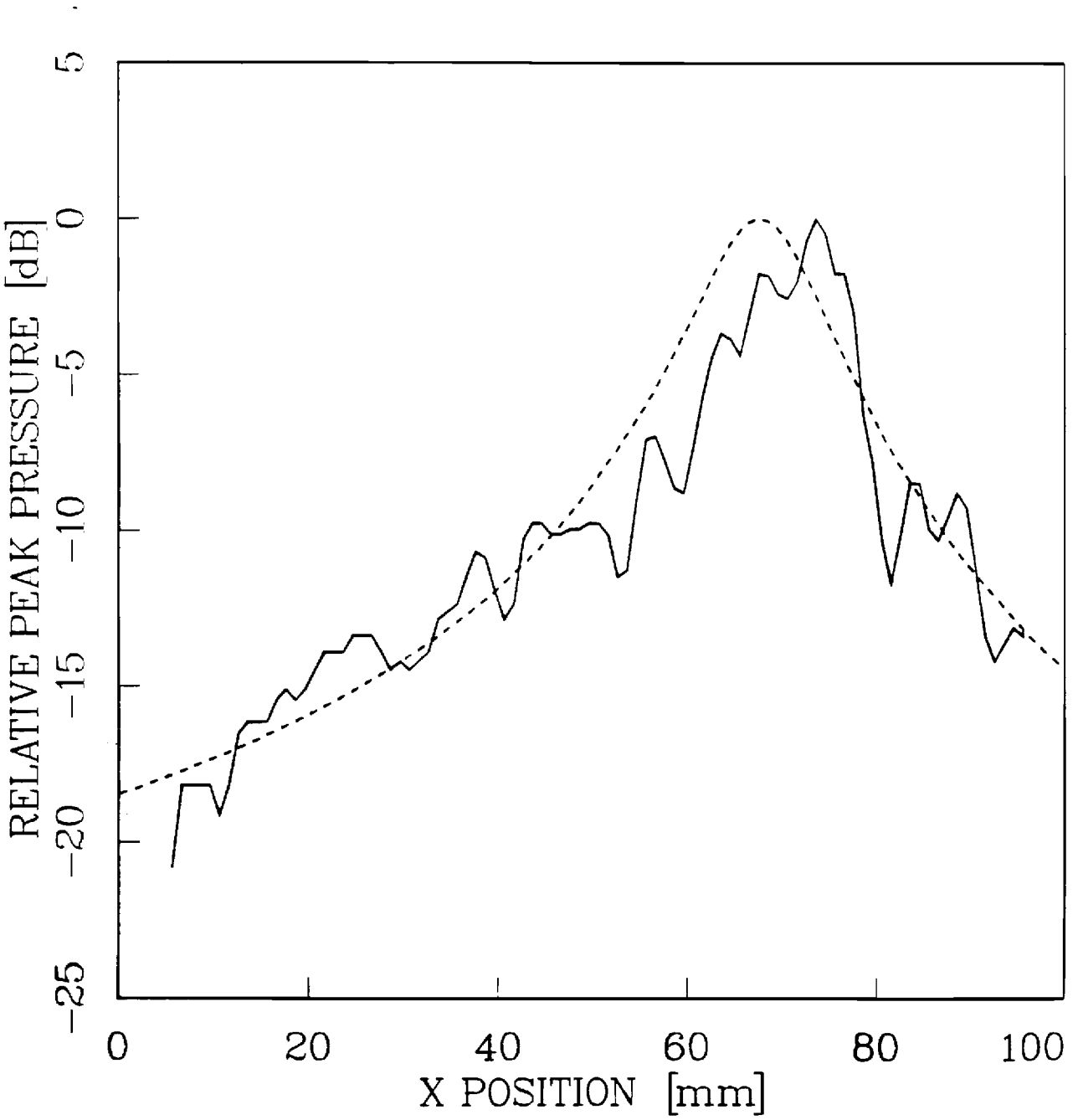
RELATIVE PEAK PRESSURE [dB]
5
0
−5
−10
−15
−20
−25
0
20
40
60
80
100
X POSITION [mm]